UNCLASSIFIED

AD NUMBER
ADC023527
CLASSIFICATION CHANGES
TO: unclassified
FROM: confidential
LIMITATION CHANGES
TO: Approved for public release, distribution unlimited
FROM: Controlling DoD Organization. Naval Ocean Research and Development Activity, Stennis Space Center, MS.
AUTHORITY
ONR ltr, 31 Jan 2006; ONR ltr, 31 Jan 2006

THIS PAGE IS UNCLASSIFIED

CONFIDENTIAL

Naval Ocean Research
and Development Activity
NSTL Station, Mississippi 39529

NORDA Technical Note N80C
Copy No. of 000

Surveillance Environmental Acoustic Support Project

ACOUSTIC SIGNAL CHARACTERISTICS MEASURED WITH THE LAMBDA III DURING CHURCH STROKE III (U)

AD C023527

DTIC ELECTE DEC 1 2 1980 A

DDC FILE COPY

15 September 1980

"NATIONAL SECURITY INFORMATION"

"Unauthorized Disclosure Subject to Criminal Sanctions"

Classified by: OPNAVINST S5513.5
Encl. 42, dated 31 August 1960
Review on 15 September 2000

Ocean Programs Management Office

80 12 12 515

CONFIDENTIAL

TRW

CONFIDENTIAL

November 26, 1980

From: I. B. Gereben
To: Distribution

Subject: CHURCH STROKE III Cruise 1; forwarding of report

Enclosure: (1) (C) "Acoustic Signal Characteristics Measured with LAMBDA III During CHURCH STROKE III" (U)

1. (U) The Surveillance Environmental Acoustic Support Project (SEAS) of the Naval Ocean Research and Development Activity (NORDA) sponsored a field exercise to obtain environmental and acoustic measurements during the month of July 1979. This effort included the measurement of long range propagation loss, the determination of the effects of bathymetry in transmission loss and evaluation of array performance parameters.

2. (U) Enclosure (1) is a report of the analysis of the signal related data acquired during the CHURCH STROKE III Cruise 1 exercise. As authorized by the Director, SEAS, enclosure (1) is forwarded for your information and retention.

Distribution: As specified in Enclosure(1)

Sincerely,

Istvan B. Gereben
Member of the Technical Staff

IBG:ss

Enclosure

Unclassified upon removal of enclosure

CONFIDENTIAL

DEFENSE AND SPACE SYSTEMS GROUP OF TRW INC.
WASHINGTON OPERATIONS • WESTGATE PARK • 7600 COLSHIRE DRIVE, McLEAN, VIRGINIA 22101 • (703) 893-2000

CONFIDENTIAL

Naval Ocean Research
and Development Activity
NSTL Station, Mississippi 39529

(9) NORDA Technical Note N80C
Copy No. of

(14) NORDA-TN-N80C

(21) Report on
Surveillance Environmental Acoustic Support Project,

(12) 156

(6) ACOUSTIC SIGNAL CHARACTERISTICS MEASURED WITH THE LAMBDA III DURING CHURCH STROKE III (U) (8)

15 September 1980

PREPARED BY:

(10) ISTVAN B. GEREBEN (TRW)
WILLIAM M. CAREY (B.K.D.)
RICHARD D. DOOLITTLE
(CONSULTANT TO B.K.D.)

Classified by: OPNAVINST S5513.5
Encl. 42, dated 31 August 1960
Review on 15 September 2000

Ocean Programs Management Office

392 113

FOREWORD

(C) The CHURCH STROKE III Cruise 1 Exercise was designed to provide measured acoustic and environmental data in the Florida Channel for theoretical and analytical studies of acoustic phenomena, assessment of surveillance system performance, acoustic model development and validation. The overall objective of the Exercise was to provide an assessment of the undersea acoustic surveillance alternatives at the entrance to the Gulf of Mexico. This report contains the acquired experimental results and an analysis which pertains to transmission loss and array performance necessary for the surveillance assessment.

(U) The Exercise was sponsored by the Chief of Naval Operations and conducted under the direction of Commander in Chief, U.S. Atlantic Fleet (ANCLANTFLT) and was under the general technical direction of the Surveillance Environmental Acoustic Support Project Office (SEAS, NORDA Code 520). Mr. Jimmy Gottwald of TRACOR Inc. served as Chief Scientist. Mr. Istvan B. Gereben of TRW, Inc. served as Principal Investigator for transmission loss and array performance measurements and data analysis. Dr. William M. Carey and Dr. Richard Doolittle participated in various stages of acquisition, processing and analysis of the information reported herein. Drs. Carey, Doolittle and Mr. Gereben are the authors of this report.

(U) This report: Acoustic Signal Characteristics Measured with the LAMBDA III During CHURCH STROKE III, presents findings and conclusions based on at-sea measurements during the CHURCH STROKE Cruise 1 Exercise. Although the data reduction and analysis have been extensive, as well as comprehensive there remain segments of data that may merit further processing and analysis. The data base obtained in this exercise is stored and can be obtained through the SEAS Project Office (NORDA Code 520).

Charles E. Stuart

Acting Manager, Measurements Program
Surveillance Environmental Acoustic Support Project

Accession For
NTIS GRA&I
DTIC TAB
Unannounced
Justification
By
Distribution/
Availability Codes
Dist Avail and/or Special
A-1

ACKNOWLEDGEMENTS (U)

(U) This work represents the joint effort of individuals from two organizations, TRW and BK Dynamics. Dr. Roy Gaul, former Director of the Long Range Acoustic Propagation Project (LRAPP), NORDA Code 600, and Charles Stuart, SEAS, NORDA Code 520 were responsible for the support and the encouragement essential to the completion of this study.

(U) Any investigation of this magnitude requires the coordinated effort and hard work of many individuals. In particular the support, participation and interest of Jim Gottwald (Tracor), Gus Wittenborn (Tracor), Robert Urick (TRW) and Paul Bucca (NORDA) is acknowledged by the authors. The Lloyd Mirror data were obtained by Bill Muellenhoff (formerly of U.R.C.) and analyzed by Jean-Pierre Feuillet (BK Dynamics). Stephen Koch (BK Dynamics) provided analysis support in the area of Array Performance. Dave DeLeeuw and Jim Aitkenhead (NOSC) supplied invaluable support with their knowledge of the Hewlett-Packard Batch Processor and their willingness to assist us in its utilization. Irby Fogleman (TRW) provided able assistance in the data analysis.

(U) The contribution of the Texas Instruments technical crew under the leadership of Bob Dunbar and Bruce Toal is also acknowledged, as is the contribution of the crew of the INDIAN SEAL led by Captain Kitzmiller.

TABLE OF CONTENTS

	Page
FOREWORD	i
ACKNOWLEDGEMENTS	ii
EXECUTIVE SUMMARY	ES-1
1. INTRODUCTION	1
1.1 Objectives	1
1.2 Approach	3
1.3 Assets	3
2. MEASUREMENT SYSTEM	5
2.1 LAMBDA System Description	5
2.1.1 Subsystem Descriptions	6
2.1.2 System Operation	8
2.1.3 Array	9
2.1.4 The LAMBDA III Data Acquisition and Processing System	12
2.1.5 Data Processing Techniques	15
2.1.6 System Calibration	19
2.2 Moored Source	28
2.3 Towed Source	31
3. DESCRIPTION OF THE EXERCISE	35
3.1 Command, Control and Communications	35
3.2 Area Description	37
3.2.1 Area Covered	37
3.2.2 Currents	39
3.2.3 Sound Velocity Profiles	39
3.2.4 Sound Propagation	42
3.2.5 Ambient Noise	49

UNCLASSIFIED

TABLE OF CONTENTS CON'T

	Page
4. EXPERIMENTAL RESULTS	51
4.1 Transmission Loss as a Function of Range	51
4.1.1 Measurement Techniques	52
4.1.2 Summary of Transmission Loss Data	58
4.1.3 Transmission Loss Characteristics	70
4.1.3.1 Leg E-F	72
4.1.3.2 Leg E-G	83
4.1.3.3 Leg G-E	83
4.2 Received Signal Characteristics	84
4.2.1 Measured Spectral Values	90
4.2.2 Measured Spatial Characteristics	96
4.3 Fluctuations	101
4.3.1 Short-Term Fluctuations	101
4.3.2 Long-Term Fluctuations	106
4.3.3 Array Gain Fluctuations	113
5. SUMMARY OF MEASUREMENTS AND EXPERIMENTAL RESULTS	121
5.1 Summary of the Measurements	123
5.2 Discussion of Transmission Loss Data	126
5.3 Discussion of Array Performance Results	133
6. CONCLUSIONS AND RECOMMENDATIONS	135
6.1 Conclusions	135
6.2 Recommendations	137
7. REFERENCES	139
8. DISTRIBUTION LIST	141

UNCLASSIFIED

LIST OF FIGURES

FIGURE		TITLE	PAGE
1-1	(C)	Operations Area CHURCH STROKE III, CRUISE I (U)	2
2-1	(U)	LAMBDA III Array Configuration	11
2-2a	(U)	LAMBDA/TAP III Data Acquisition and Processing System (U)	13
2-2b	(U)	LAMBDA/TAP III Batch Processing Scheme (U)	13
2-3	(U)	Lloyd Mirror Geometry (U)	22
2-4	(U)	Time Versus Range During the Lloyd Mirror Calibration Run (U)	23
2-5	(U)	Estimated Ranges for Lloyd Mirror Calibration Measurements (U)	24
2-6	(U)	WEBB Sound Source Deployed During CHURCH STROKE III CRUISE 1 (U)	30
2-7	(U)	Acoustic Source System Installed on USNS DESTEIGUER for CHURCH STROKE III CRUISE 1 (U)	33
3-1	(U)	Physiographic Provinces of the Gulf of Mexico, CHURCH STROKE III, CRUISE 1 (U) Ref. 2	36
3-2	(U)	July-September Current Patterns in the Gulf of Mexico CHURCH STROKE III, CRUISE 1 (U) Ref. 2	38
3-3	(C)	Reference Sites for CHURCH STROKE III, CRUISE I Operational Area (U)	40
3-4	(U)	Isovelocity Contours and Bathymetric Profile Along the CHURCH STROKE III, CRUISE 1 Exercise Baseline (U)	41
3-5	(U)	Selected Measured Sound Velocity Profiles Along the CHURCH STROKE III, CRUISE 1 Exercise Baseline (U)	43
3-6	(U)	Composite Speed Profiles for CHURCH STROKE III, CRUISE 1 (U)	44

LIST OF FIGURES CON'T

FIGURE		TITLE	PAGE
3-7	(U)	Negative Depth Excess for Gulf of Mexico (U)	45
3-8	(U)	Bottom Loss Estimates for Mississippi Fan (U)	47
3-9	(U)	Sound Attenuation Coefficient in Gulf of Mexico KIWI ONE Results (U)	48
4-1	(C)	Tabular Values of Received Levels and their Variances in the 0.08 Hz Processing Bands (C)	53
4-2	(C)	Plotted Values of Received Levels and their Variances in the 0.08 Hz Processing Bands (C)	54
4-3	(C)	Spatial Characteristics of Averaged Recieved Signals as Function of Hydrophone Group Location (U)	55
4-4	(C)	Typical Characteristics of Received 67 Hz Signal Levels for One Hydrophone Group as Function of Time (U)	56
4-5	(C)	Typical Characteristics of Received 173 Hz Signal Levels for One Hydrophone Group as Function of Time (U)	57
4-6	(U)	Measured Transmission Loss as a Function of Range and Bathymetry for Leg E-G (U)	67
4-7	(U)	Measured Transmission Loss as a Function of Range and Bathymetry for Leg G-E (U)	68
4-8	(U)	Measured Transmission Loss as a Function of Range and Bathymetry for Leg E-F (U)	69
4-9	(U)	Ranges for Limiting Ray Propagation (U)	75
4-10	(U)	Measured Transmission Loss and Bottom Loss Estimates Along Leg E-F for Towed Source at 67 Hz (U)	80
4-11	(U)	Measured Transmission Loss and Bottom Loss Estimates Along Leg E-F for Towed Source at 173 Hz (U)	82

LIST OF FIGURES CON'T

FIGURE		TITLE	PAGE
4-12	(C)	Beam Band Levels of the 173 Hz Signal as a Function of Beam Number and Relative Bearing (U)	85
4-13	(C)	Beam Band Levels of the 67 Hz Signal as a Function of Beam Number and Relative Bearing (U)	86
4-14	(C)	Beam Band Levels of the 175 Hz Signal as a Function of Beam Number and Relative Bearing (U)	87
4-15	(C)	The LAMBDA III HF Beam Response (U)	89
4-16	(C)	Band Level Spectra in the 67 Hz, 173 Hz and 175 Hz Filter Bands (U)	91
4-17	(C)	Mean Band Level Spectra with Minus and Plus Variance for 60 Hydrophones, 24 Ensembles in Three Filter Bands (U)	92
4-18	(C)	Beam and Hydrophone Band Levels (U)	93
4-19	(U)	Illumination Plots for the 67 Hz, 173 Hz and 175 Hz Signal (U)	97
4-20	(U)	MSC, Phase and Crosspower Versus Frequency (U)	99
4-21	(U)	MSC Versus Hydrophone Number (U)	100
4-22	(U)	S/N Versus Hydrophone Number (U)	100
4-23a	(U)	Probability Density Distribution for 48 Hydrophones at a Frequency of 172.92 Hz for the LAMBDA III, HF Array (U)	103
4-23b	(U)	Probability Density Distribution for 48 Hydrophones at a Frequency of 172.92 Hz for the LAMBDA III, HF Array (U)	103
4-23c	(U)	Probability Density Distribution for 48 Hydrophones at 172.97 Hz for the LAMBDA III, HF Array (U)	104
4-24a	(U)	Cumulative Probability Distribution for 194:20:28:04, The LAMBDA III, HF Array, Aft 24 Hydrophones (U)	105

LIST OF FIGURES CON'T

FIGURE		TITLE	PAGE
4-24b	(U)	Cumulative Probability Distribution for 194:20:28:04, The LAMBDA III, HF Array, Aft 24 Hydrophones (U)	105
4-25	(U)	Time Series for Signal Loss: Leg E-F (U)	107
4-26	(U)	"Windowed" Correlation for Time Series of Fig. 4-25 (200 Min. Window) (U)	109
4-27	(U)	Ranges and Depths for Sources and Receivers (U)	110
4-28	(U)	Ray Trace for Leg E-F (400 m Receiver Depth) (U)	111
4-29	(U)	Time Interval Comparisons for High Correlations Between Towed and Moored Source Signals (U)	112
4-30	(C)	Array Performance Statistics for 66.92 Hz (U)	114
4-31	(C)	Array Performance Statistics for 172.94 Hz (U)	115
4-32	(C)	Cumulative Probability for Array Signal Gain for the 173 Hz and 175 Hz Data (U)	116
4-33a	(C)	Towed Source, ANG, ASG, AG Versus Range (U)	118
4-33b	(C)	Towed Source, ANG, ASG, AG Cumulative Probability Distributions (U)	118
4-34a	(C)	Moored Source, ANG, ASG, AG Versus Time (U)	119
4-34b	(C)	Moored Source, ANG, ASG, AG Cumulative Probability Distributions (U)	119
5-1	(U)	Comparison of FACT Predicted and Measured Transmission Loss Values at 67 Hz as Function of Range for Leg E-F (U)	129
5-2	(U)	Comparison of FACT Predicted and Measured Transmission Loss Values at 173 Hz as Function of Range for Leg E-F (U)	130

LIST OF TABLES

TABLE		TITLE	PAGE
2-1	(U)	Measured Band Levels (dB) (FORELEG) with TAP III System (U)	26
2-2	(U)	Comparison Between Computed and Measured Pressures (U)	27
2-3	(U)	Technical and Operational Parameters of the Moored Webb Sound Source Deployed During the CHURCH STROKE III CRUISE I Exercise (U)	29
2-4	(U)	Technical and Operational Parameters of the HX-231F Sound Projector Deployed During the CHURCH STROKE III CRUISE I Exercise (U)	32
3-1	(U)	Geographical Locations of CHURCH STROKE III, CRUISE I Reference Sites (U)	39
4-1	(C)	Transmission Loss and Related Parameters for Leg F-E (U)	59
4-2	(C)	Transmission Loss and Related Parameters for Leg E-F (U)	60
4-3	(C)	Transmission Loss and Related Parameters for Leg E-G (U)	63
4-4	(C)	Transmission Loss and Related Parameters for Leg G-E (U)	64
4-5	(U)	Sound Velocity Profile for Ray Tracing Analysis (U)	76
4-6	(U)	Bottom Bounce Estimates from Ray Tracing (U)	78
4-7	(U)	Computations of Transmission Loss at 67 Hz Based on Eq. 4-4	79

EXECUTIVE SUMMARY

(C) Exercise CHURCH STROKE III, CRUISE I, sponsored by the Chief of Naval Operations (OP-95), was designed to update the understanding of ocean acoustic parameters and their effects on passive acoustic surveillance systems in the Florida Channel of the Straits of Florida, the northern end of the Yucatan Channel and the Eastern Gulf of Mexico.

(C) Data acquisition for the determination of signal characteristics was accomplished with the Large Aperture Marine Basic Data Array III (LAMBDA III), during July 1979.

(C) The analysis of the signal data and supporting information produced the following major results:

- When the influence of the slope was absent measured transmission loss showed good agreement with the FACT Model employing medium to low bottom loss curves, developed for this area by ARL.
- Slope enhancement effect was observed when the source, proceeding from deep water towards the slope, reached the location of the initiation of the slope. This effect was recognized by a change in the TL data trend.
- Short term TL fluctuation data (12-24 minutes) and related statistics were acquired. Standard deviation determined from power averaging were found to be between 3 and 5 dB in the band of the signal.
- Array signal gain ranged from 15 dB to 34 dB. It was determined that in this multipath environment towed array performance is affected by array signal gain and its fluctuations.
- Statistical distribution of ASG was found to be Log Normal Distribution when the multipath environments were not changing rapidly.
- Half power beam width was determined as $1.73^{\circ} \pm 0.35^{\circ}$ deg
- Side lobe levels near the signal beam were determined as -9 dB for the first lobe and -17 dB for the second lobe.
- Beam Width and side lobe levels were comparable to theoretical values for the prevailing operational condition of the array, and
- Signal coherence over the array aperture was established for high signal to noise ratio cases. The average MSC value was approximately 70%.

(U) It is recommended that the slope enhancement effects observed in this experiment as well as other measurements be the subject of more theoretical and experimental investigation. The obtained data base represents a rare case of absolute calibrated acoustic data under known environmental conditions.

1. INTRODUCTION (U)

(C) Exercise CHURCH STROKE III, CRUISE 1 was designed to update the understanding of ocean acoustics parameters and their effects on passive acoustic surveillance systems in the Florida Channel of the Straits of Florida, the northern end of the Yucatan Channel and the Eastern Gulf of Mexico. The area of interest is illustrated in Figure 1-1.

(U) The exercise sponsored by the Chief of Naval Operations (OP-095) and conducted under the direction of Commander in Chief, U.S. Atlantic Fleet (CINCLANTFLT), was under the general technical direction of LRAPP (NORDA Code 600). The participants were directed from an Exercise Control Center (EXCON) located at CINCLANTFLT, Norfolk, Virginia in accordance with the Exercise Plan and with CINCLANTFLT Letters of Instruction (References 1-3).

(U) The Exercise Plan was developed by using the results of the preassessment of the region of interest conducted by NORDA (CODE 600) (Ref. 4).

(U) Preliminary results of the "quick look" analysis of the data relating to the above objectives was published as part of Ref. 5.

(U) This report contains the results of the detailed analysis of data acquired during the CHURCH STROKE III, CRUISE 1 Exercise and pertaining to transmission loss and array performance.

1.1 OBJECTIVES (U)

(C) The overall objective of the exercise - as defined in the Exercise Plan (Ref. 2) - was to provide data to assess the undersea acoustic surveillance alternatives at the entrance to the Gulf of Mexico. Specific acoustic objectives addressed by this report are:

a. Measure long range propagation loss as function of frequency, range and receiver/source depth.

b. Determine the effects of bathymetry on transmission loss.

c. Determine array performance parameters using a high level towed source.

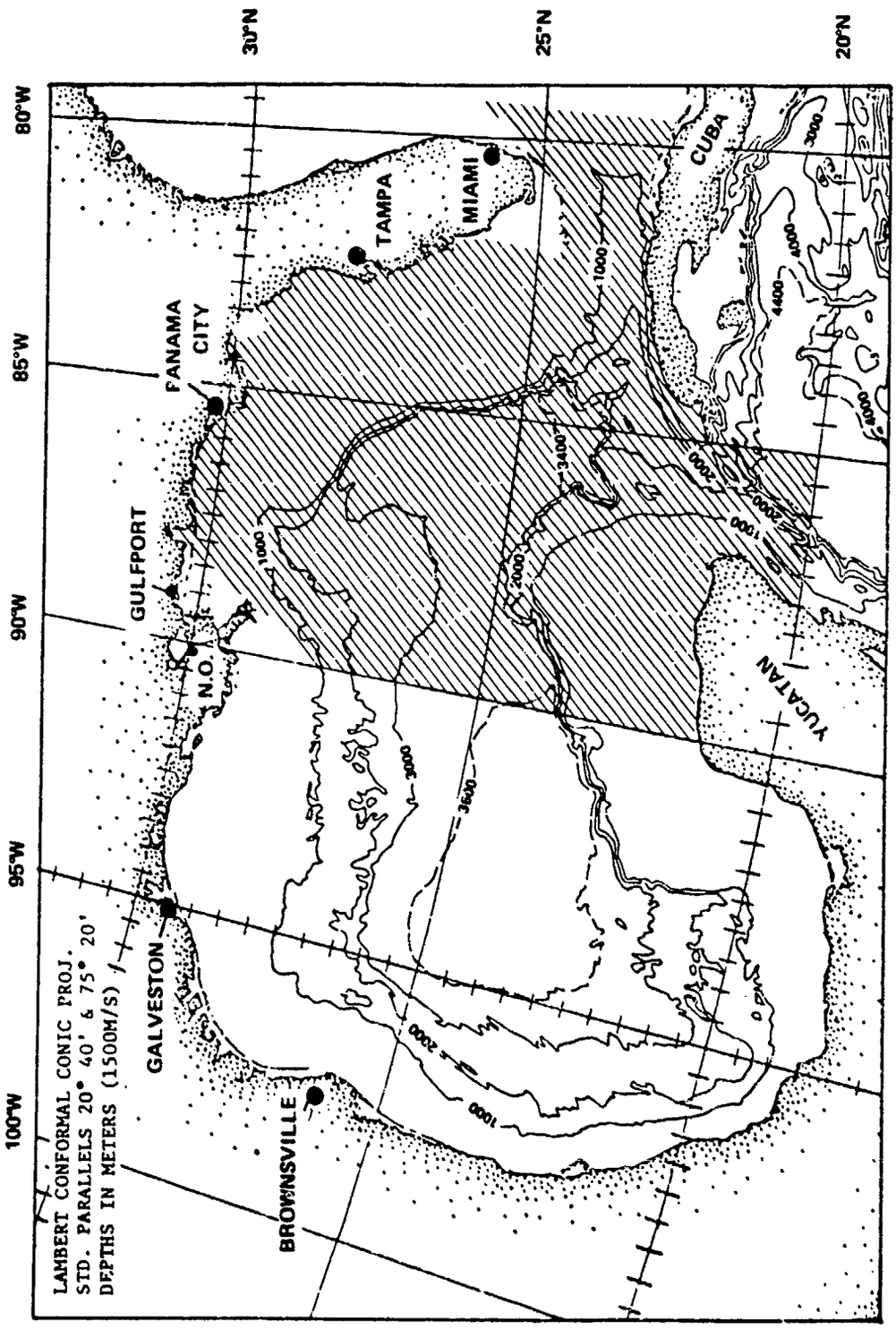

Figure 1-1. (C) Operations Area CHURCH STROKE THREE, CRUISE ONE (U)

1.2 Approach

(C) The objectives were met by measuring signal parameters to describe transmission loss and array performance. These measurements were made with the Large Aperture Marine Basic Data Array (LAMBDA).

(C) Received signal levels of the individual hydrophone groups of one of the three arrays of the LAMBDA system were used for transmission loss investigation. Received signal levels were averaged for the 64 hydrophones and for a selected period of time and selected frequencies. These values provide the base for transmission loss determination.

(C) Array performance was calculated from the signal gain and noise gain values measured through one of the three arrays of the LAMBDA System for selected time periods and signal frequencies.

(U) Other signal characteristics - i.e., signal level distribution as a function of space and time - were also measured to support the transmission loss and array performance analysis.

1.3 Assets

(C) The following assets were employed during the signal investigation portions of the Exercise:

- R/V INDIAN SEAL
  - LAMBDA System
    1) LF, MF, HF towed arrays each consisting of 64 hydrophones.
    2) Non-Acoustic Data Sensors and their recording system.
    3) Signal Conditioning Units.
    4) TAP III signal processor and beamformer.
    5) BATCH signal processor.
    6) HDDR recording system.
    7) NATOB system.
    8) AN/BQR-23 signal processor and display system.
  - Navigation System

- Environmental Measurements Systems
  1) XBT.
  2) Wind direction and speed.
  3) Other sensors.

- USNS DESTEIGUER
  - HX-231 sound source radiating at 67 Hz and 173 Hz with nominal source levels of 179.3 dB and 183.4 dB, respectively.
  - Navigation System.
  - SVTD System.

- Moored Source
  - The Webb Sound Source built by Woods Hole Oceanographic Institute was moored at a depth of 988 m in 3416 m of water and transmitted at a frequency of 174.89 Hz with a source level of 171 dB relative to 1μPa.

2. MEASUREMENT SYSTEM

(U) The Large Aperture Marine Basic Data Array (LAMBDA) System is a unique tool of underwater acoustics. Originally developed under the auspices of the Defense Applied Research Projects Agency (DARPA), it provided a flexible system to investigate highly specialized areas of ocean acoustics and to evaluate the feasibility of sophisticated ASW equipment designs. Later, when the System was turned over to the Navy, a second generation system was used to aid in the assessment of operational performance of long towed arrays. Along with basic ocean acoustics measurements the array has also been employed in Fleet exercises augmenting ASW assets.

(U) In 1979, a third generation LAMBDA System was developed; this was the system employed during the CHURCH STROKE III Exercise.

(U) The LAMBDA System was supported by other measurement systems providing CW tonal signals at different frequencies and that acquired environmental information necessary for the determination of acoustic parameters under investigation.

(U) A towed source, the HX-231F, was towed by the USNS DESTEIGEUR which also acquired bathymetric and oceanographic parameters.

(U) The Webb Sound Source was moored in the exercise area and provided an acoustic benchmark for the measurements.

2.1 LAMBDA SYSTEM DESCRIPTION

(U) The LAMBDA system was designed as a research tool to evaluate the physical and operational characteristics of a towed passive acoustic antenna system in a deep ocean basin environment. Maximum reconstruction ability in post-exercise data processing through redundant data recording was a characteristic of the system. Reliability requirements for data safety and human factor requirements were incorporated to minimize personnel-system interaction and to provide fault isolation capabilities. The LAMBDA system was designed with as much redundancy as could be generated for limited crew operation, with multiple paths for recording purposes, and with extensive display capability for scientific experimentation.

2.1.1 Subsystem Descriptions.

(C) The LAMBDA system was divided into subsystems with individual performance requirements and operational goals.

- Array - Primary sensing device for acoustic data and for water column non-acoustic data. The basic acoustic configuration had three performance apertures: 6 Hz to 26 Hz (Low Frequency,2400 m long); 6 Hz to 54 Hz (Medium Frequency, 806 m long), and 20 Hz to 160 Hz (High Frequency, 300 m long).

  Each aperture was composed of 64 equally spaced hydrophones (38.1 m for LF; 12.8 m for MF and 4.75 m for HF). The LF and MF apertures were interleaved.

  The engineering sensor packages were interspersed throughout the acoustic array, providing heading, depth, temperature and tension data for performance monitoring and recording.

- Array Acoustic Front-End Electronics - Provided acoustic signal conditioning, monitoring and switching capability.

- TAP III (Beamformer) - The frequency and time domain beamformers provided processing, recording and display of the acoustic signals. The frequency domain beamformer was capable of forming all 64 beams simultaneously. The time domain beamformer provided only 16 adjacent beams simultaneously.

- High Density Digital Recorder - This was the primary recorder for "raw" acoustic data.

- Array Non-Acoustic Front-End Electronics - This was the processing interface between the array non-acoustic data and the batch processing and recording system having data display capability.

- Integrated Navigation System - Gave the course and position information utilizing a number of independent measurement methods.

Displayed this information both on the bridge and in the instrument room.

Inputed the data to the Batch Processor.

- Non-Acoustic Data System - Provided system status, ship's velocity and ocean environment information.
- Synchronous Time Code - Synchronizing connection between rubidium clock in the Integrated Navigation System to the High Density Digital Recorder time code generator and the TAP III time code generator.
- Analog Tape Recorder - Recorded the output of the time domain beamformer.
- Batch Processor and Recorder - Assembled all non-acoustic data and periodically transmitted these data to the beamformer system for simultaneous recording with the beamformer data.

  Provided off-line data analysis capability.
- AN/BQR-23 Analyzer with hard copy writer - Provided analysis of 16 selectable beams.

  Provided output of 16 selected and analyzed beams for tape recording.

  Provided hard copy of 1 selected beam.

(U) There were a number of other systems that provided support to the LAMBDA system:

- Array Deployment/Retrieval - The array was stored on a spool at the stern of the ship with array deployment/retrieval being controlled from a monitor house sitting above the spool.
- Communications - The communications system utilized Marisat for primary encrypted/unclassified ship-to-shore communications

with CRATT and bridge HF as back-ups. Ship-to-ship communication was handled through additional VHF and UHF radios.

- Power Generation - There were three power systems on board: ship, instrumentation and uninterruptible. Most equipment drew from the ship power system. The instrumentation power was designed to provide an electrically quiet ground for the instrument room. The uninterruptible power system provided a limited battery back-up capability to permit selected equipment to perform shut-down functions in the event of power failure.

(U) The system was installed on-board R/V INDIAN SEAL, a 205 foot long supply vessel with a beam of 40 feet. The ship had two main engines each providing 2,000 shaft horsepower, and was equipped with two variable pitch propellers. The vessel had a 10 knot cruising speed. Minimum low speed was a nominal 0.75 knots.

2.1.2 System Operation

(U) The system was operated to serve two purposes: data collection and realtime data processing. Data collection consisted of recording raw acoustic data from the 64 individual hydrophones of one of three arrays (LF, MF, or HF) on the high density digital recorder. This recording enabled post-analysis processing of sectors which were not searched in realtime and the application of different processing parameters to the data. The array selected for recording presents the only limitation in the application of these parameters. Realtime data processing uses either the time domain or the frequency domain beamformer. The time domain data are stored on analog magnetic tape and are simultaneously processed and displayed in real time by the BQR-23 spectrum analyzer. The output from the frequency domain beamformer is stored on digital magnetic tape for further processing in the batch computer.

(U) The time domain beamformer provides time-frequency information for 16 adjacent beams. The search sector width depends upon the relative steering angle and the array selected. (At broadside, the sector width is 48^{o} for the MF array.) Four selectable adjacent beams are presented on the CRT of the BQR-23 spectrum analyzer. The longest time history of this display is approximately 13 minutes. This limitation affects the ability of the analysts to compare displayed acoustic data with previously observed acoustic events. The BQR-23 also provides a hard copy of any one of the 16 processed beams. The output of 12 of the 16 beams can be recorded on the analog tape recorder for post-event analysis at sea and post-exercise analysis ashore.

2.1.3 ARRAY

(C) The LAMBDA III array consisted of three different acoustic arrays: the low frequency array (LF), the mid-frequency array (MF), and the high frequency array (HF). In addition, the array had six depth, temperature and heading modules; fore and aft vibration isolation modules (VIMS) and parachute tail drogues. The LAMBDA III array was a geophysical type hard-wired array. The tow cable was a torque balanced, 5.125 cm diameter armored cable with an overall length of 1485 m. This cable was configured to tow the array at cable scopes between 200 and 1200 m with 450 m of "zip on" flag fairing. The cable consisted of 216 twisted pairs and 7 shielded twisted pairs. The lower end of the tow cable had an optional additional mass (543 kg) in the form of 11.4 cm diameter lead cylinders, which were band-strapped to the cable.

(C) The LAMBDA III array was used in several different configurations. Generally the fore end of the array had 600 m of VIMS while the aft end had 300 m of VIMS preceding the tension producing parachute or rope drogues. The HF array preceded the MF and LF arrays.

(C) These three acoustic arrays had 64 hydrophone groups each. The HF array hydrophone groups were center spaced at 4.75 m. Each HF group had seven series-connected Benthos AQ-1 hydrophones. Both the MF and LF hydrophone groups consisted of two of these seven series-connected groups connected in parallel. The MF array which was nested in the LF array consisted of 64 groups of hydrophones center spaced at 12.8 m. The LF

array consisted of 64 hydrophones with a center spacing of 38.1 m. This resulted in a HF array of 300 m , an MF array of 806 m and an LF array of 2,400 m acoustic aperture (Figure 2-1).

(C) The Benthos AQ-1 hydrophone (Ref. 6) had a nominal free field sensitivity of -203 dB reV/Pa over the 5 Hz to 1000 Hz band. This hydrophone was designed to operate at ambient pressures of up to 21 MPa and in the temperature range of $-2^{o}C$ and $30^{o}C$. The nominal capacitance of this special lead zirconate/lead titanate hydrophone was 120,000 pf. The hydrophone itself weighed 17 grams and was 5 cm long. This hydrophone was air backed and was mounted in an open cell urethane plug within a stainless steel jacket. This jacket was mounted in a spider mount fastened to the array strength members. This hydrophone was observed to have a sensitivity that changed less than 1 dB over the pressure range 0 to 21 MPa and a sensitivity change with temperature less than 0.3 dB over the range from $-2^{o}C$ to $30^{o}C$.

(C) Each hydrophone was connected to a .1μf capacitive coupled differential amplifier. The input to this amplifier wasprotected by a diode clipping circuit. The amplifier had a gain of 30 dB and a +.02 dB gain stability in the $-20^{o}C$ to $+22^{o}C$ temperature range. The amplitude response was down by 3 dB at 4.5 and 500 Hz. The roll-off at the low frequency end was 4 dB per octave while the high frequency roll-off was 3 dB per octave. The noise value for this preamplifier was -145.6 dB re 1V @10 Hz (0.4 db re 1μPa equivalent) and -152.6 dB re 1V @300 Hz. The differential input was maintained balanced to a virtual ground to provide a common mode rejection of greater than 70 dB. The amplifier had a dynamic range of 115 dB.

(C) The signals from all the hydrophones were conditioncd at the tow ship by the use of differential signal conditioning amplifiers. These signal conditioning amplifiers had selectable gain and pre-emphasis. The amplifier response had a low frequency cutoff (3 dB down) point of 4.9 Hz and rolled off at 12 dB/octave below that frequency. Without pre-emphasis, these amplifiers were flat out to 300 Hz with a high frequency 3 dB down point of 305 Hz. With pre-emphasis, the characteristic increased beginning at 50 Hz with a slope of 5 dB/octave to 300 Hz.

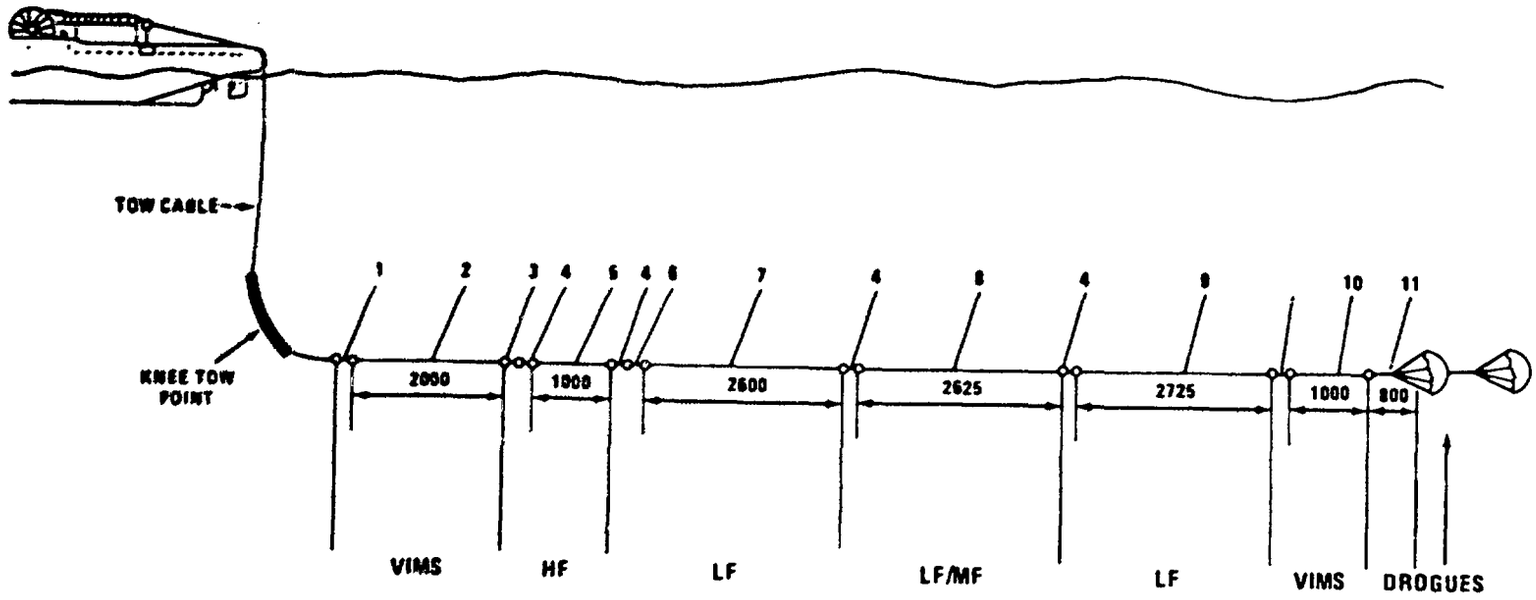

NOTES

1. SENSOR SECTION - ACCELERATION, TENSION & DEPTH
2. FORWARD VIMS - 10 SECTIONS AT 200 EACH (SECTION 10 CONTAINS ACCLEROMETER)
3. HF POWER REGULATOR SECTION
4. SENSOR SECTION - DEPTH, TEMPERATURE, HEADING
5. HF ARRAY - 8 SECTIONS AT 125 EACH
6. LF MF POWER REGULATOR SECTION
7. FORWARD LF ARRAY - 20 SECTIONS AT 125 EACH. 1 SECTION AT 75
8. MF ARRAY - 21 SECTIONS AT 125 EACH
9. AFT LF ARRAY - 20 SECTIONS AT 125 EACH. 1 SECTION AT 75
10. AFT VIMS - 5 SECTIONS AT 200
11. DROGUE

Figure 2-1. (U) LAMBDA III ARRAY CONFIGURATION (U)

UNCLASSIFIED

2.1.4 The LAMBDA III Data Acquisition and Processing System

(U) The LAMBDA III Acoustic Data Acquisition and Processing System is illustrated in Figure 2-2. This system was complemented by a Nonacoustic Data Acquisition System (NADS). The Acoustic System consists of signal conditioning amplifiers, 15 bit A/D converters, a high density digital tape recorder subsystem and a TAP III processor. The acoustic and nonacoustic data were processed on the off-line 21MX batch processor. The NADS system sampled all nonacoustic data such as array heading, ship heading, ships speed, latitude, longitude, wind speed, array depth and array temperature. A synchronous line code was utilized between the rubidium clock in the integrated navigation system and high density digital recorder time code generator. This integrated navigation system determines the positional data using both satellite updates and ship course and speed data. The NADS system which is continually running in the background of the HP21MX batch processor maintains a time-indexed file of all these data. The 21MX processor had two video displays, one high speed plotter printer, a 25-megabyte disk and a graphics terminal. This allowed a graphically displayed set of NADS data for specified parameters.

(U) Sixty-four channels of acoustic data were selected from either the high frequency (HF), mid frequency (MF) or low frequency (LF) arrays. After signal conditioning amplifiers and anti-aliasing filters these sixty-four signals were digitized by a fifteen bit analog/digital (A/D) system with a 1 KHz sampling rate. A selectable channel was converted back to analog for analysis on the SD301 analyzer. The high density digital recorder (HDDR) takes the output of the digitizers and uses a "sample and hold" amplifier for simultaneous signal processing. The system samples one thousand times per second per channel through an independent multiplexer. A flexible input/output capability was built into the unit to drive the Hiller code encoder or read the output of the decoder. The basic tape drive was a modified 14 track analog recorder. Twelve of the 14 tracks were used for data, and track 13 was reserved for an IRIG B

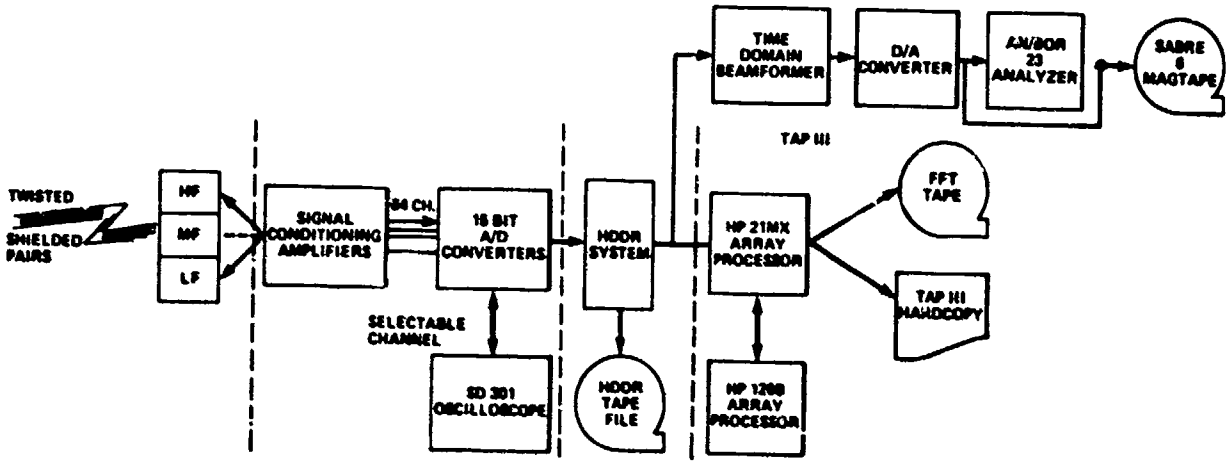

Figure 2-2a. (U) LAMBDA/TAP III Data Acquisition and Processing System (U)

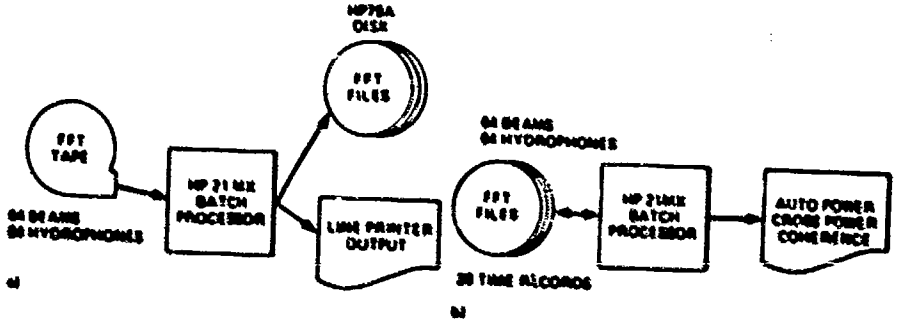

Figure 2-2b. (U) LAMBDA/TAP III Batch Processing Scheme (U)

time code. The frame consisted of 82 words. The HDDR system had simultaneous recording and playback capabilities which aided in monitoring the output. The HDDR system was used to record the output of the LAMBDA array whenever the array was operational. This included all measurement periods, all turns, and all array stabilization periods.

(U) The Three-Array Processor, central to all shipboard data processing, performs beamforming and spectral analysis for signals received by the LAMBDA array by means of successive Fourier transforms. TAP III frequency domain beamformer hardware consisted of a Hewlett Packard 21MX computer, a Floating Point System HP-120B high-speed array processor, a magnetic disk HP7970A, IBM-compatible magnetic tape decks, and an interactive CRT keyboard display terminal. The combination of this hardware and special software results in an extremely flexible system. Figure 2-2a contains a block diagram of the TAP III Processor. A detailed description of the processor is presented in References 7, 8 and 9 (Appendix A of this report).

(U) The frequency domain beamformer provides a 0.08124 Hz frequency resolution in three selectable 4 Hz bands anywhere within the total passband from 3 to 305 Hz. The system operates at a fixed sample rate of 914.91 samples in 1 sec. In this experiment, the system was used to determine the fast Fourier transform coefficients of sixty-four hydrophones and sixty-four beams. These complex coefficients were written on a nine track magnetic tape. The system response was 12.5 seconds of data every 62.5 seconds for all 128 channels. Both tabular and graphical displays of the beam response functions and hydrophone illumination functions were obtained from this processor in addition to the magnetic tape record. The details of this processor are discussed by Rennie (Ref. 8).

(U) In addition to FDB, we had a time domain Beamformer (TDB) which operated in parallel with the FDR to form 16 beams in real time. These sixteen beams were also recorded on a Sabre 6 tape recorder.

(U) The spectral data discussed in this paper were obtained with the .08124 Hz resolution and the complex coefficients of the FFT of 64 hydrophones and beams written on the HP21MX 9 track magnetic tape. This digital magnetic tape enabled onboard analysis of the data with the HP21MX batch processor shown in Figure 2-2b. The basic off line processing scheme was to load

64 beams, 64 hydrophones and 25 time ensembles onto a data file on the HP 79A disk.

(U) The basic processing was accomplished with this large disk file and the software resident on the batch processor.

2.1.5 Data Processing Techniques

(U) The TAP III processor has been described in Section 2.1.3 The band levels for the sixty four beams and hydrophones in the three selectable band-pass filter ranges processed by the TAP III were outputed on a line printer and displayed on a CRT display. In addition these outputs were recorded on magnetic tape. The output could be specified as the Fast Fourier Transform (FFT) complex coefficients or the band levels for the hydrophones and beams. In the CHURCH STROKE III Cruise I experiments the output was the complex coefficients of the FFT's. The primary reason for this type of output was the preservation of signal amplitude and phase. The duty cycle for this type of data acquisition was 12.5 secs. of data and approximately 40 secs. of processing. Backup files of all processed data were recorded on HDDR and are maintained for further processing.

(U) The discrete Fourier Transform may be written as:

$$X_i^{(p)}(m\Delta f) = h \cdot \sum_{n=0}^{N-1} x_i^{(p)}(nh) \cdot e^{-j2\pi mn/N}$$

where

N	The number of samples
i	The hydrophone channel
p	The p^{th} ensemble
f_s	The sampling frequency
h	$1/f_s$, reciprocal of sampling frequency
m	The frequency bin number
Δf	The frequency resolution

$$x_i^{(p)}(nh) = 0 \qquad \text{for } n \leq 0 \text{ 'or' } n \geq N-1$$

(U) The power spectral density can be determined by the mean squared pressure in a Δf Hz band. We assume $x_i(p)(nh)$ has the units of pressure; i.e., all system calibration factors have been applied. It follows that the mean squared pressure for the p^{th} ensemble h sec long is:

$$P_i^{(p)}(m\Delta f) = \chi_i^{(p)}(m\Delta f) \cdot [\chi_i^{(p)}(m\Delta f)]^*$$

(U) $P_i^{(p)}(m\Delta f)$ represents the estimate of the squared pressure in the m^{th} frequency bin which is Δf Hz wide for the p^{th} ensemble h sec. long.

(U) The number of degrees of freedom (Ref. 9.a) for this estimate is $2\Delta fh$. In our case we have $2\Delta fh = 2\ (.08124)(12.5\ sec.) = 2$. We wish to obtain an estimate of the true mean spectral density, in this case, proportional to the true mean square pressure. We must average or smooth the data. We require the total averaging time to be short enough that the process can be considered stationary. We also require $2\Delta fhM$ be large enough for a true estimate of the mean. For M = 12, 24, we have the following

% of data within spread	spread dB 12 ensemble	spread dB 24 ensemble
40%	1.25	.88
60%	2.08	1.50
80%	3.33	2.33
90%	4.17	2.92

These estimates are based on a white noise distribution of energy. When we have a single peak in the spectrum of data with high signal to noise ratio then we can use K = 2 degrees of freedom provided that 1/h is not small compared to the width of the line. To insure a higher degree of confidence averaging was employed. The average mean squared pressure was thus determined.

$$\bar{P}_i(m\Delta f) = \sum_{p=1}^{M_e} \frac{P_i^{(p)}(m\Delta f)}{M_e}$$

where M_e is the number of ensembles and the variance

$$\sigma_i^2(m\Delta f) = \sum_{p=1}^{M_e} \frac{(\overline{P}_i - \overline{P}_i^{(p)})^2}{M_e - 1} \quad .$$

(U) When spatial averages were employed we have

$$\overline{P}(m\Delta\overline{f}) = \frac{1}{N_s} \cdot \sum_{i=1}^{N_s} \overline{P}_i(m\Delta f) = \frac{1}{N_s M_e} \sum_{i=1}^{N_s} \sum_{p=1}^{M_e} P_i^{(p)}(m\Delta f)$$

where N_s is the number of sensors.

$$\sigma^2(m\Delta f) = \frac{1}{(N_s - 1) \cdot (M_e - 1)} \cdot \sum_{i=1}^{N_s} \sum_{p=1}^{M_e} (\overline{P}_i - P_i^{(p)})^2$$

(U) In addition to the estimates of mean square pressure and its band level, we can also estimate the cross power spectral density, the magnitude squared coherence and the phase coherence. The cross product is defined as:

$$P_i^{(p)}(m\Delta f) = \chi_i^{(p)}(m\Delta f) \cdot [\chi_j^{(p)}(m\Delta f)]^*$$

$$= \left| \chi_i^{(p)}(m\Delta f) \cdot \chi_j^{(p)*}(m\Delta f) \right| \cdot \exp(i\phi)$$

where the cross power is proportional to the magnitude and the phase is in the argument of the exponential in the above expression.

(U) The magnitude squared coherence is defined as

$$\text{MSC} = \gamma_{ij}^{(p)2} = \frac{\left| \chi_i^{(p)} \cdot \chi_j^{(p)*} \right|^2}{P_i^{(p)} \cdot P_j^{(p)}} \quad .$$

Averaging is performed on the ensemble number p and statistical considerations apply as before.

(U) These values all represent band level estimates of the mean squared pressure. For plane waves we then have that the intensity ($\bar{I}$) is proportional to the mean squared pressure times the sonic velocity (C) and density (ρ).

$$\bar{I} = \frac{\bar{p}^2}{\rho c}$$

a reference pressure is taken as 1μPa and all quantities are converted to band levels

$$\text{Band level dB re } 1\mu\text{Pa} = 10 \text{ Log} \left[\bar{p}^2 / \bar{p}_r^2 \right]$$

For cases of white noise one can apply a bandwidth correction:

$$\text{Spectrum level dB re } (1\mu\text{Pa})^2/\text{Hz} = 10 \text{ Log} \left[\bar{p}^2 / \bar{p}_r^2 \right] - 10 \text{ Log}(\Delta f)$$

for the $\Delta f = .08124$, the correction is +10.9 dB. We have not applied this bandwidth correction to the estimate of the narrowband signal level.

2.1.6 System Calibration

(U) Acoustic data obtained in this experiment were referenced to absolute values through several calibrations. The individual hydrophones were carefully selected on a "binning" technique described by Doolittle (Reference 6) to ensure reliable and consistent sensitivities. CAVAC tests were performed at Benthos to provide a secondary calibration of each hydrophone to a reference standard. Test of the acoustic sensitivity, capacitance, resistance, and other parameters were performed at NRL/USRD, Orlando, Florida, on a sample batch of thirty-seven AQ-1 hydrophones drawn from the production line as procured and accepted by Texas Instruments for use in the LAMBDA III array. Individual array modules were CAVAC calibrated by George Pickens of NOSC to ensure that a secondary calibration on all hydrophone groups was available. Electronic calibration of the system was accomplished by use of two techniques. The first was the built-in system calibration which used square wave signal injected into the hydrophone preamplifier providing a calibration in amplitude and phase for the entire system. The second technique using the NOSC-developed inverse beamformer allows use of signal plus noise as a calibration tool at preselected steering angles. These calibrations were done on a routine basis to ensure the integrity of these absolute values.

(U) These calibration techniques were evaluated by R. Hecht (Ref. 10). This particular evaluation used a 57.2 Hz sine wave at a level of -14 dB re 1 Volt. The measurement from the input to the signal conditioning unit to the output of the TAP III calibration program revealed a 1 to 1 transfer function. Using a bandwidth of 0.08124 Hz the operating channels were found to have an amplitude standard deviation of 0.126 dB (all measurements within $\pm$ 0.68°. The calibration technique was employed to insure relative calibration of the channels during the course of these measurements.

(U) In addition to these experiments, a Lloyd mirror calibration was performed prior to these measurements. The purpose of the Lloyd mirror calibration was to provide an at sea verification of the absolute calibration factor. The Lloyd mirror calibration uses the interference pattern

from the surface reflected ray and direct ray of sound. This interference produces an easily recognized pattern of maxima and minima in the received signal and noise level as the range between the receiver and source is varied.

(U) The field of the source can be observed in three distinct regions, the near field, the interference field and the far field. The near field is that region where the effect of the surface reflection is negligible and the spreading is spherical. The interference field is the region dominated by the constructive and destructive interference between the surface reflected and direct paths. The far field is the region where the source and its image appears as a dipole and fourth power spreading is observed. The Lloyd Mirror calibration was conducted in the Interference field; that is distances greater than 2 $(d_s d_R)^{1/2}$. In the interference field the intensity is given by:

$$I = I_0 (1 + \mu^2 - 2\mu \cos (\omega_0 \tau))/R^2$$

where I_0 = intensity of direct arrival at one meter from the source

μ = the surface reflection coefficient

$\omega_0 = 2\pi f_0$ (Hz)

τ = time difference between the surface and direct arrivals

R = range separation between source and receiver

This equation clearly shows that four variables must be known: the source level, source frequency, the surface reflection coefficient and the source-receiver separation. The source level and frequency are independent calibrated values of 170 dB re 1μPa @ 1 m and 173.13 Hz.

(U) The surface reflection coefficient can be taken as unity for these frequencies. This term could represent a major contributor to the short term variation of the received signal. The reflection coefficient

pertains to the specular reflection of the sound wave at the pressure release surface. When the surface is flat or disturbances of the surface are small compared to a wavelength, the reflection coefficient is indeed unity. However when the surface is not flat, due to the existence of higher sea states, the reflection coefficient is less than unity and thus scattering may become important as surface disturbances approach the wavelength of the sound. In this calibration measurement a sea state less than 4 was observed and M=1 was used. That is to say, we did not have a fully developed sea but wind speeds up to 19 knots were observed.

(U) The last variable in the equation is the range separation between the source and receiver. Ideally we would require the knowledge of the range exactly in order that we could predict the exact range of the maxima. However in those cases where one does not have an exact knowledge of the range the intensity of the maxima is given by

$$I = 4\ I_o/R^2$$

We can identify the maxima from our experimental data and predict the measured intensity with the approximate range.

For the Lloyd mirror calibration relative range between the source and receiver was determined by precise knowledge of the location of the source and receiver at selected times. Between these reference locations a constant speed was assumed to estimate the range. As we were unable to maintain an exact time reference between the acoustic data files and the ship's position, the approximate ranges were estimated from the approximate lines and the range plot.

Referencing Figure 2-3 we see that the geometry chosen for the Lloyd mirror calibration was simply a straight tow track past a moored sound source with the closest point of approach (1650 m) well within the interference field ($>>$ 854 m for d_S = 911 m and d_R = 200 m). Figure 2-4 shows the true earth speed of the tow ship for this track while Figure 2-5 shows the measured acoustic band levels. These band levels were observed by use of an SD-301 (spectral dynamics analyzer) while the acoustic data was being obtained

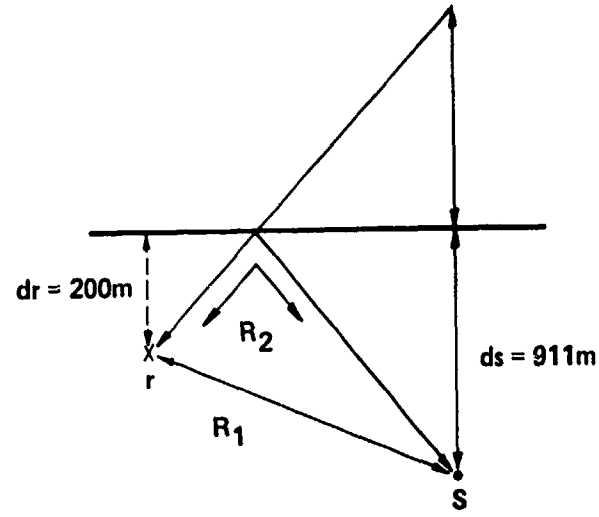

(BOTTOM DEPTH = 3170m)

THE LLOYD MIRROR GEOMETRY, Vertical

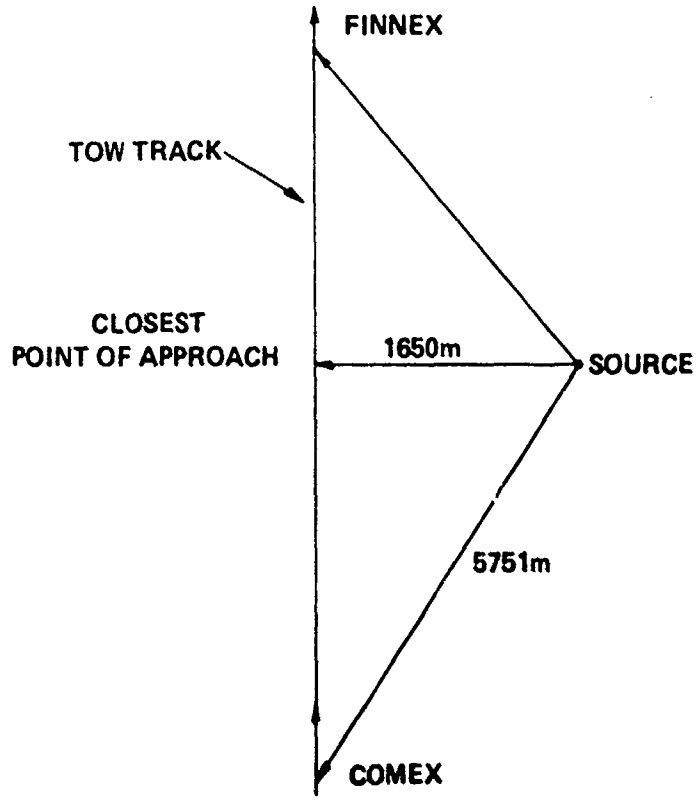

f_o = 175.13 Hz
S_L = 170 dB re 1μ Pa 1m.
C_S = 911m

THE LLOYD MIRROR GEOMETRY, Horizontal

Figure 2-3. (U) Lloyd Mirror Geometry (U)

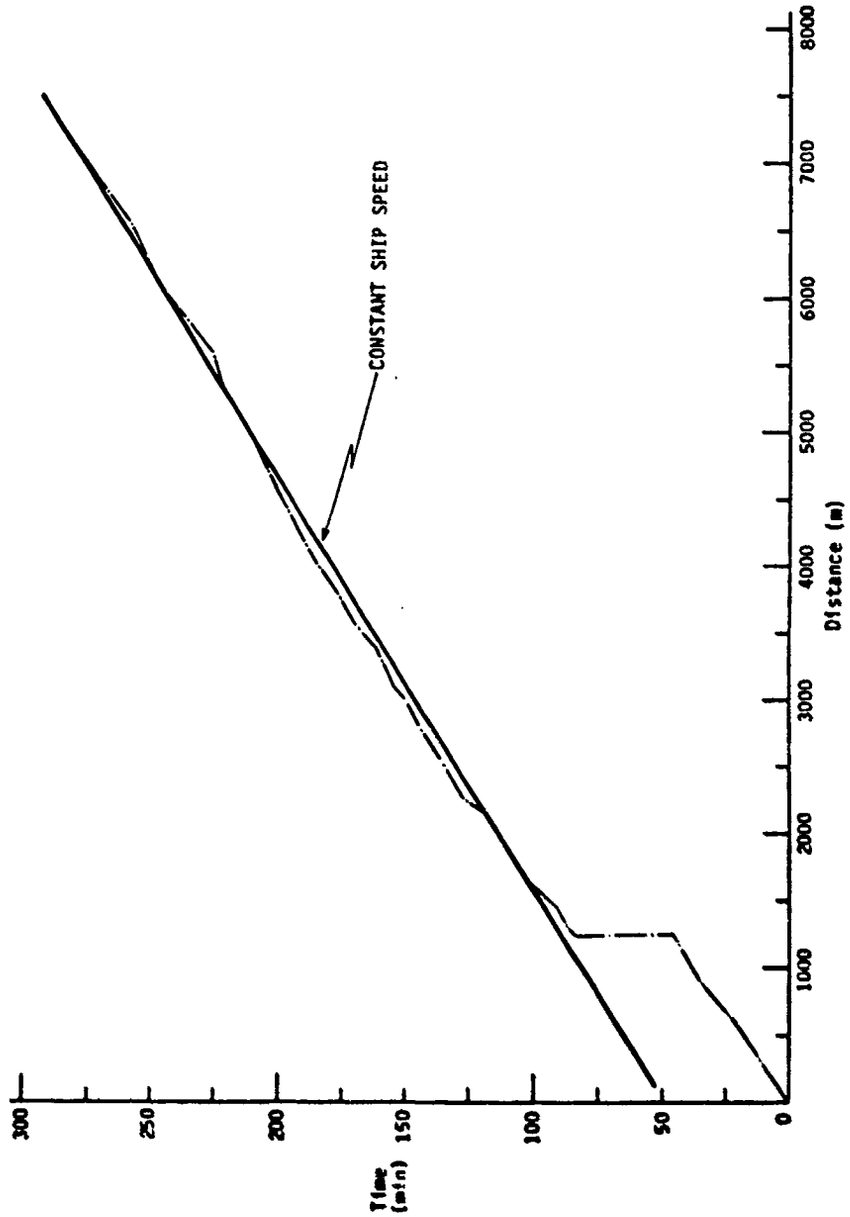

Figure 2-4. (U) Time Versus Range During the Lloyd Mirror Calibration Run (U)

UNCLASSIFIED

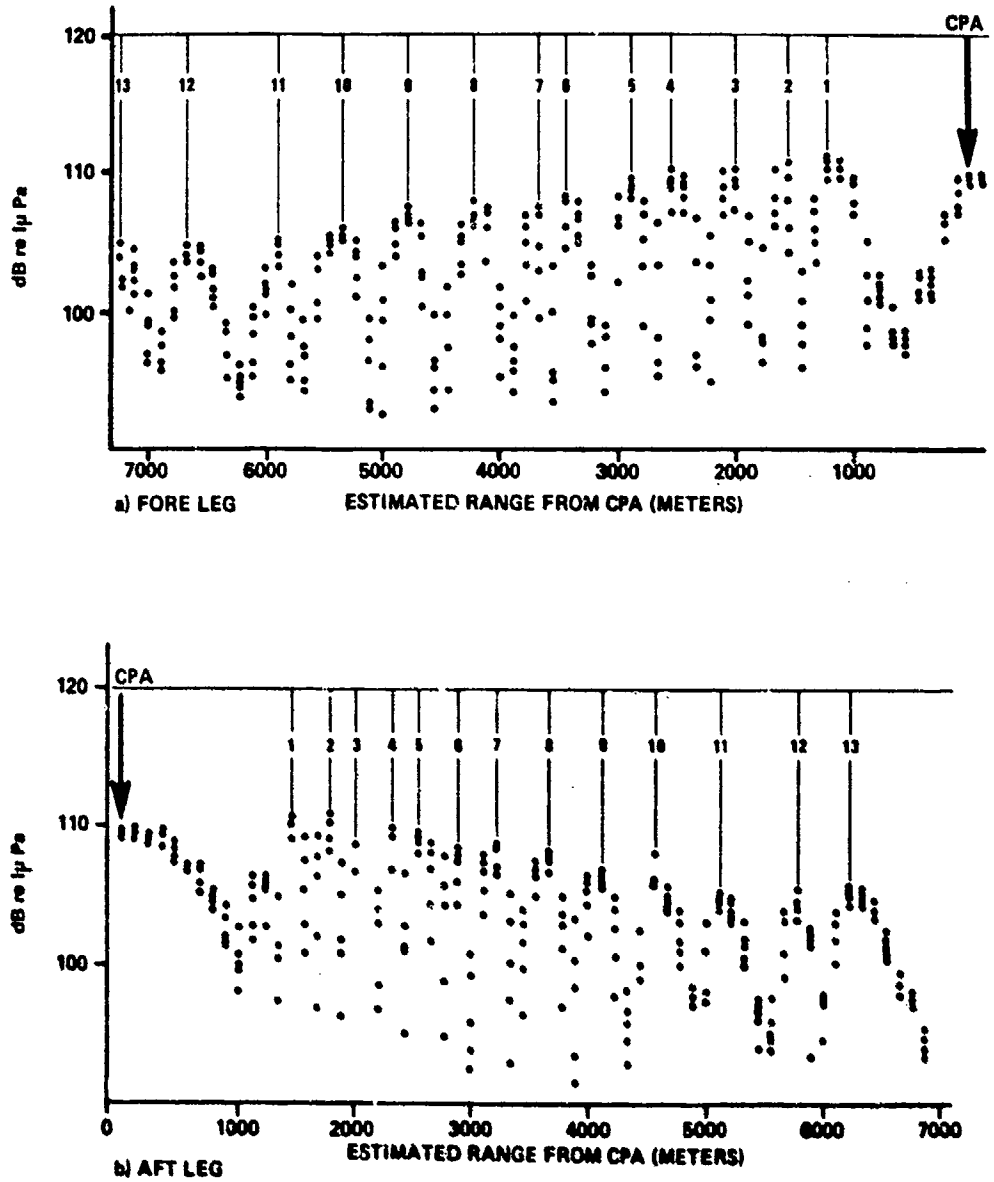

Figure 2-5. (U) Estimated Ranges for Lloyd Mirror Calibration Measurements (U)

UNCLASSIFIED

with the TAP III data acquisition system. This figure clearly shows the successive maxima which one would expect from the Lloyd mirror effect. The figure is labeled with the estimated range.

(U) Concurrent with the measurements performed with the SD-301, data were obtained with the TAP III system. These data were processed on the HP batch processor to yield band level versus time for all twenty-four hydrophone channels as shown in Table 2-1. These data are shown for several peaks. Of the twenty-four hydrophones three (#12, 17, 18) consistently were low. Mean levels were determined with and without these phones. The variances were also determined. With all phones the standard deviations ranged from 1.38 dB to 1.84 dB increasing with a decrease in the signal to noise ratio. Without the three low hydrophones these standard deviations were between 0.17 and 0.5 dB, very low values. The data in Table 2-1 clearly show that the relative calibration over all the hydrophone channels was quite good. The consistency of these results is probably a direct consequence of the calm state of the sea.

(U) A comparison of theoretical results with the values obtained with the SD-301 are tabulated in Table 2-2 and show that on the average our measurements agree with the prediction within a dB when we are close to the CPA and our range determination is more accurate. Farther away from the CPA our uncertainty increases as much as 1.4 dB. This disagreement with theory is most likely due to the uncertainty in our range estimates at these distances. The basic result of this at sea calibration is that in those instances (P# 3,4, 5) where the ranges were known, sea state calm and speed constant we were able to verify that we are within $\pm$ .7 dB of our system calibration factor of 186 dB re 1 Volt/μPa.

UNCLASSIFIED

Table 2-1. (U) Measured Band Levels (dB) (FORELEG) with TAP III System (U)

(Note: These data contain a downward bias due to filter width and doppler effect, and should be used only for this relative comparison)

PLANE \ BEAM	13	12	11	10	9	8	7	6	5	4	3
1	99.7	100.5	100.1	101.3	103.0	102.5	104.0	104.3	104.1	104.3	105.9
2	100.3	100.6	100.3	101.7	102.7	102.6	103.8	104.4	104.3	104.7	105.3
3	100.9	100.7	100.4	101.4	102.8	102.8	104.1	104.4	104.0	104.6	105.5
4	99.8	100.0	100.3	101.4	102.8	102.7	104.2	104.0	103.6	104.4	105.5
5	100.0	101.6	100.7	101.7	102.9	102.4	103.8	104.1	103.4	104.3	105.7
6	100.0	100.6	100.1	101.7	102.7	102.5	104.0	104.2	103.6	104.3	105.5
7	99.8	100.3	100.0	101.4	102.7	103.0	103.9	103.9	103.7	104.0	105.5
8	100.5	100.2	100.0	101.0	102.7	102.7	103.7	103.7	103.7	104.2	105.6
9	100.4	100.3	100.5	101.6	103.0	102.5	104.0	104.0	104.1	104.8	105.8
10	100.2	100.4	100.2	101.7	102.7	102.6	104.0	104.0	103.7	104.5	105.9
11	100.1	100.5	100.3	101.6	102.7	103.1	103.9	104.0	103.3	104.4	105.8
12	96.2	96.4	97.3	98.8	99.2	99.5	99.7	100.4	100.4	101.6	102.9
13	100.2	100.2	100.4	101.0	102.8	102.4	104.0	104.0	103.4	104.4	105.7
14	99.8	100.2	100.4	101.3	102.7	102.4	104.0	103.8	103.3	104.5	105.9
15	100.2	100.5	100.3	101.6	102.5	103.2	104.0	103.9	103.1	104.4	106.1
16	100.1	100.2	100.0	101.3	102.6	102.8	103.7	103.6	103.0	104.4	105.9
17	92.7	92.8	92.8	93.6	95.7	97.8	98.3	99.6	98.6	99.5	99.1
18	96.2	96.4	96.6	97.2	98.7	97.2	98.0	97.3	100.3	101.8	103.5
19	100.3	100.4	100.5	101.4	102.7	102.7	103.7	103.5	103.4	104.5	106.2
20	100.5	100.2	100.7	101.7	102.7	103.4	104.0	103.8	103.5	104.6	105.2
21	100.1	100.7	100.6	101.5	102.6	103.3	104.1	103.8	103.7	105.5	106.2
22	100.0	100.4	100.1	101.1	102.4	102.8	104.1	103.6	104.0	105.6	106.0
23	100.2	100.2	100.7	101.2	102.6	103.0	104.2	103.6	103.9	105.8	106.0
24	99.8	100.0	100.5	101.5	102.3	102.7	103.9	102.9	103.7	105.5	105.8
Mean	99.5	99.7	99.7	100.8	102.1	102.2	103.3	103.3	103.2	104.2	105.3
Variance	3.26	3.40	3.02	3.26	2.87	2.50	3.15	2.81	1.83	1.83	2.23
Std Dev	1.84	1.88	1.78	1.84	1.73	1.62	1.81	1.71	1.38	1.38	1.52
Mean	100.1	100.4	100.3	101.4	102.7	102.8	104.0	103.9	103.6	104.7	105.8
Variance	.08	.11	.05	.04	.03	.09	.02	.11	.11	.24	.07
Std Dev	.29	.34	.23	.23	.17	.30	.15	.34	.34	.50	.27

UNCLASSIFIED

Table 2-2. (U) Comparison Between Computed and Measured Pressures (U)

FORE LEG

PEAK #	DIRECT PATH RANGE $D_S - D_R$ (m)	REFLECTED PATH RANGE $D_{s_1(\bar{m})} D_R$	MEASURED PHONE LEVEL S_{D-301} SPECIAL ANALYZER (dB)	PREDICTED PHONE LEVEL (dB)	PREDICT-ML MEASURED (dB)
13	5110	5181	102.9	101.8	1.1
12	4632	4710	102.8	102.6	0.2
11	4212	4298	102.8	103.4	0.6
10	3931	4023	103.9	104.0	0.1
9	3474	3578	105.6	105.1	0.5
8	3165	3279	106.0	105.9	0.1
7	2910	3033	105.4	106.6	1.2
6	2924	2855	106.3	107.1	0.8
5	2440	2614	107.4	107.9	0.5
4	2298	2452	108.3	108.5	0.2
3	2153	2316	108.8	109.0	0.2
2	2017	2190	108.8	109.6	0.8
1	1910	2092	109.0	110.0	1.0

AFT LEG

1	1913	2096	109.6	110.0	0.4
2	2044	2216	108.6	109.5	0.9
3	2167	2329	109.1	109.0	0.1
4	2301	2455	108.5	108.5	0.0
5	2470	2612	108.0	107.9	0.1
6	2600	2737	107.6	107.5	0.1
7	2771	2899	106.5	107.0	0.5
8	2980	3100	106.7	106.4	0.3
9	3233	3344	106.2	105.7	0.5
10	3506	3608	105.0	105.0	0.0
11	3766	3861	104.0	104.4	0.4
12	4122	4204	103.2	103.6	0.4
13	4527	4606	103.7	102.8	1.1
14	3014	5086	103.4	102.0	1.4
				Standard Deviation	.67

UNCLASSIFIED

2.2 MOORED SOURCE

(U) Acoustic benchmark for the exercise was provided by a Webb Sound Source moored at the approximate depth of the sound channel nominally 100 miles from the LAMBDA operational area on the track of the towed source.

(U) The Webb Sound Source developed and manufactured by Woods Hole Oceanographic Institution is an organ pipe type source made of 12" diameter 6061 aluminum cylinder with a wall thickness of ¼". At one end of the cylinder a ceramic bender transducer is mounted, the other end is open. Two such organ pipes are attached onto a longer cylinder of the same material and diameter that contains the necessary batteries and electronics for driving the transducer. The electronics/battery housing gives inertia to the system so that the organ pipe cylinders are essentially stationary in the water.

(U) With the wavelength long compared to the radius, the bender acts like a piston in that only the zero order mode (plane wave) is generated in the tube cut to approximately \/4. This cutting is actually done to give maximum conductance to the driving amplifiers. Due to the standing wave effect or standing wave ratio, the open end acts as a source which is some 10^4 times stronger than that produced at the other end.

(U) The diffraction of a scalar plane wave by an aperture in an infinite plane screen-- the basis for the operation of the Webb Sound Source-- is examined theoretically by Levine and Schwinger in Reference 11.

(U) The technical and operational parameters of the Webb Sound Source are summarized in Table 2-3. An outline drawing of the Source is presented in Figure 2-6. The source was calibrated by the Underwater Sound Reference Division of the Naval Research Laboratory before deployment.

Table 2-3. (U) Technical and Operational Parameters of the Moored Webb Sound Source Deployed During the Church Stroke III Cruise 1 Exercise (U)

Overall length	5.37 m
Length of organ pipes	2.13 m
Diameter of organ pipes	0.30 m
Weight in air	459.6kg
Maximum operating depth	2000 m
Carrier frequency nominal	175Hz
Frequency stability	±1ppm
Acoustic power output level	171dB//1μPa at 1 m
Modulation	Continuous wave
Endurance	3 weeks continuous
Position:	
Latitude	24° 41.1'N
Longitude	84° 29.8 W
Depth of source	988 meters
Depth of bottom	3416 meters
Date of deployment	06/2113Z July 1979
Date of recovery	19/1630Z July 1979
Optimum sound velocity for operations	1490 to 1494 m/sec.

UNCLASSIFIED

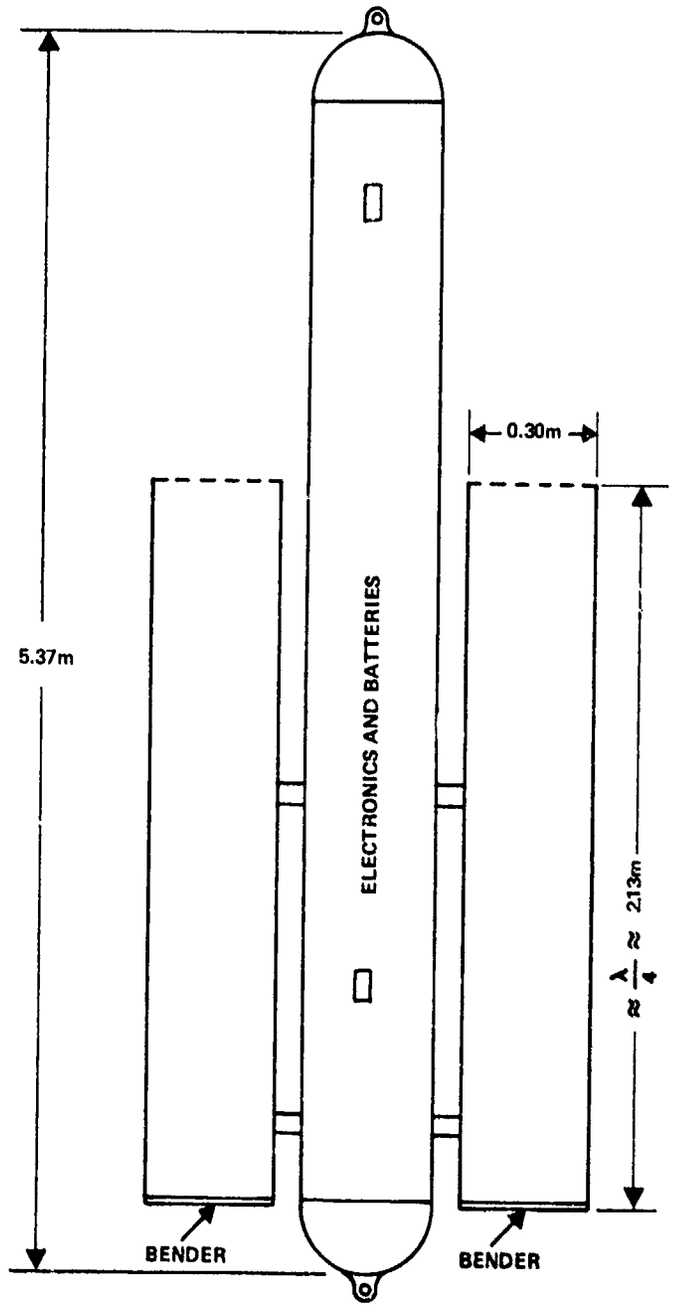

Figure 2-6. (U) WEBB Sound Source Deployed During CHURCH STROKE III CRUISE 1 (U)

UNCLASSIFIED

2.3 TOWED SOURCE

(U) A source, emitting high level CW signals for transmission loss and array performance measurements,was installed on the USNS DESTEIGUER. The source built by Honeywell was operated by personnel from the Naval Ocean System Center (NOSC).

(U) The Honeywell HX-231F projector is an omnidirectional sound source. It consists of four sections formed from a lead zirconate titanate ceramic bender bar transducer, driven by a step-up auto transformer with a turns ratio of 1:3. Manufacturer's specifications are presented in Table 2-4.

(U) The HX-231F projector is enclosed in a tow body designed to provide protection during deck handling, reduce drag and provide stability while towing.

(U) For monitoring the output of the acoustic source the ITHACO Inc. Model 601 wideband hydrophone was used. A National Inc. absolute pressure transducer calibrated by NOSC was used as a depth sensor attached to the tow-body.

(U) A schematic of the Acoustic Source System is presented as Figure 2-7.

(U) The HX-231F source was calibrated acoustically at Lake Pend Oreille before installation on the USNS DESTIEIGUER.

(U) A detailed description of the HX-231F and its support systems is provided by Reference 12.

(U) The HX-231F was operated at two frequencies 67 Hz and 173 Hz with source levels of 179.3 and 183.4 dB respectively. Source levels are given relative to 1μPa at 1 meter.

Table 2-4 (U) Technical and Operational Parameters of the HX-231F Sound Projector Deployed During the Church Stroke III Cruise 1 Exercise (U)

Number of Modules	2
Number of bars	28
Weight in air	3700 pounds
Exterior envelope	
Length	80 inches
Diameter to contain unit	32 inches
Weight in air with tow body	4500 pounds
Resonant frequency	104 Hz
Maximum measured source level at f_r (re 1μPa)	192 dB
Calculated maximum source level possible at f_r	202 dB
Directivity at f_r	Omni
Transmitting efficiency at f_r	20 percent
Maximum operating depth	206 m

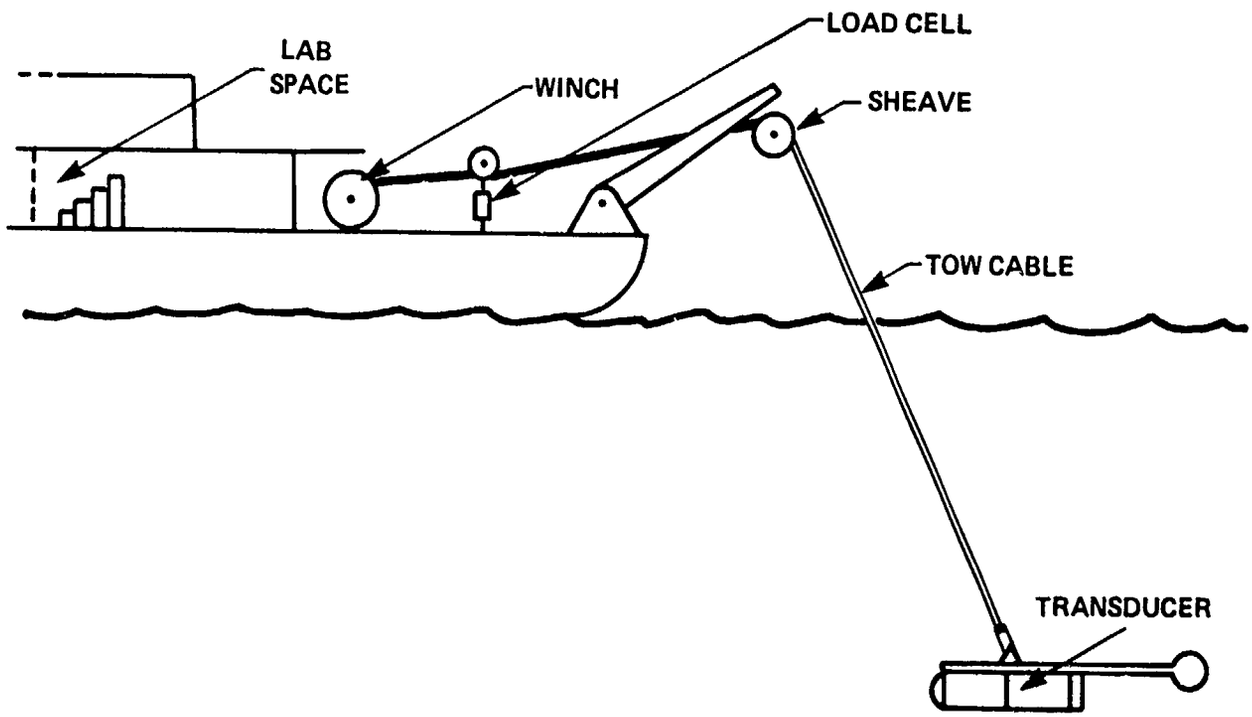

Figure 2-7. (U) Acoustic Source System Installed on USNS De Steiguer for CHURCH STROKE III CRUISE 1 (U)

3. DESCRIPTION OF THE EXERCISE

(C) The objective of CHURCH STROKE III was to obtain the data necessary for assessing passive acoustic surveillance alternatives at the entrance and approaches to the Gulf of Mexico. Particular emphasis was placed on the wide aperture towed array (LAMBDA). The objective was addressed through specific measurements of propagation loss, bottom interaction, array performance, and environmental factors.

(C) In response to recent CINCLANTFLT concern over understanding of operational performance of ASW systems in the Gulf of Mexico, the Director ASW and Ocean Surveillance Programs, OP-95 tasked the Director, LRAPP to investigate the environmental parameters necessary to consider long term solutions to the ASW problems of the Gulf of Mexico. Specifically, a measurement exercise was to be performed which would address the ocean acoustics aspects of knowledgeable assessment of surveillance alternatives at the approaches and the entrance of the Gulf of Mexico. The measurement exercise was accomplished and data permitting the evaluation of mobile and fixed ASW systems was obtained.

3.1 COMMAND, CONTROL AND COMMUNICATIONS

(C) The CHURCH STROKE III Cruise 1 Exercise took place in the entrance to the Gulf of Mexico between the Florida and Campeche Shelfs northwest of Cuba during the month of July 1979. The R/V INDIAN SEAL deployed the LAMBDA system in the Catoche longue at two operational depths of 800 m and 400 m. The USNS DESTRIGUER deployed the HX-231F towed acoustic projector providing CW signals at two frequencies (67 Hz and 173 Hz) for transmission loss and array performance investigations. The tow depth of the HX-231 was at 100 m throughout the exercise. The Webb Sound Source was moored at a strategic location of the exercise area and provided an acoustic benchmark emitting a 175 Hz CW signal during the duration of the Exercise.

PRECEDING PAGE BLANK-NOT FILMED

(U) The CHURCH STROKE III Cruise 1 Exercise was sponsored by the Chief of Naval Operations (OP-095) and, due to the involvement of Fleet assets in phases of the exercise other than that addressed by this report, was conducted under the direction of Commander in Chief, U.S. Atlantic Fleet (CINCLANTFLT). CAPT. N. E. Koehler, USN was assigned as the Officer in Charge of the Exercise (OCE)/Officer in Tactical Command (OTC) and CDR. T. A. Northam, USN was designated Project Officer by CINCLANTFLT. The Program Manager was Dr. R. D. Gaul, Director LRAPP; Dr. D. L. Bradley was designated Technical Manager. Subsequently Dr. Gaul was succeeded by Dr. Bradley as Program Manager and Mr. Charles E. Stuart replaced Dr. Bradley as Technical Manager. Mr. J. T. Gottwald, TRACOR, Inc. was assigned as chief Scientist of CHURCH STROKE III Cruise 1.

(U) The Chief Scientist was responsible for organization planning and implementation of the technical aspects of the exercise. Mr. V. Anderson, Underwater Research Corporation, served as Exercise Director and provided integration of operations.

(U) During at-sea phases of the exercise, the Exercise Director and the OTC/Project Officer were located at Exercise Control (EXCON), CINCLANTFLT Headquarters. The Exercise Director was responsible for coordinating at-sea operations and for liaison with Fleet Commands.

(U) The Chief Scientist aboard the R/V INDIAN SEAL directed at-sea scientific and technical operations. The Principal Investigators aboard the participating vessels conducted the data acquisition and analysis tasks of their specific areas of responsibility.

(U) Masters of the participating vessels were responsible for ship operations and movements in accordance with the Exercise Plan and for crew and ship safety.

(C) The primary communication link between R/V INDIAN SEAL and EXCON was via MARISAT using secure channels. Communications were in accordance with applicable Naval Telecommunications Procedures. Message releasing

authority was vested in the Chief Scientist for technical matters and in the ship's Master for matters concerning ship operations.

(U) Communications traffic were held to an absolute minimum.

(U) Participating fleet units communicated via the U.S. Naval Telecommunications System.

3.2 AREA DESCRIPTION

(U) The acoustic and environmental characteristics of the CHURCH STROKE III Cruise 1 Exercise area were assessed by pre-exercise efforts. The results are published in Reference 4. The following description of acoustic, physiographic and oceanographic parameters of the exercise area is partially based on these results, augmented by the measured and analyzed bathymetric and sound velocity characteristics.

(U) Parameters vital to the analysis of the acquired acoustic data but not measured during the exercise were derived from information established by preassessment efforts and published in Reference 4.

3.2.1 Area Covered

(C) The area included in CHURCH STROKE III, Cruise 1 is the eastern Gulf of Mexico, including the Straits of Florida. This area is roughly described in Figure 3-1 by the physiographic provinces identified as the Mississippi Cone plus the Straits of Florida. The exercise area extends over the slopes onto the shelves shown in Figure 3-1.

(U) The Gulf of Mexico is almost totally surrounded by the North American continent and Cuba. The exercise area of the Gulf bounded by the latitudes 22^{o}N and 30^{o}N is within the region that experiences tropical storms, particularly during the months of August, September and October.

(U) The entire exercise area is in a region that experiences strong and highly variable currents. Shown in Figure 3-2 entering the area from the south through the Yucatan Channel is the Yucatan Current which has been measured at four knots near its western edge. As the current enters the

CONFIDENTIAL

(This page is unclassified.)

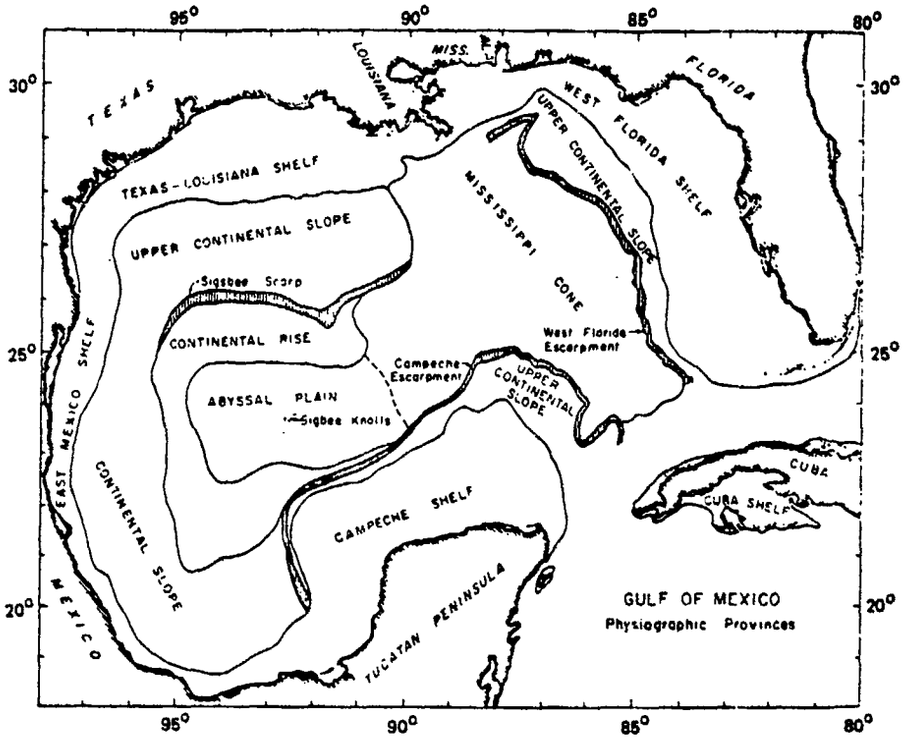

Figure 3-1. (U) Physiographic Provinces of the Gulf of Mexico, CHURCH STROKE THREE, CRUISE 1 (U) Ref 2.

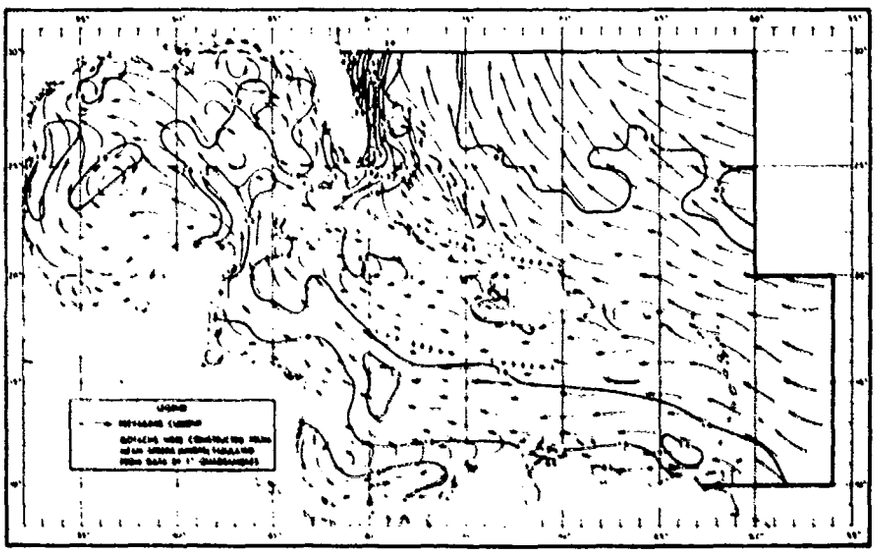

Figure 3-2. (U) July-September Current Patterns in the Gulf of Mexico. CHURCH STROKE THREE, CRUISE 1 (U) Ref 2.

Gulf of Mexico, part of it turns east and flows into the Straits of Florida, while part of it flows north to form the Loop Current of the Gulf of Mexico. The Loop Current and the anticyclonic gyres which separate from it are the major circulation features of the eastern Gulf of Mexico. The northern penetration of the Loop Current is reported to be cyclic with periods variously reported between six months and a year. At its northern extreme the Loop Current "loops" to the east then south southeast where it rejoins the flow from the Yucatan Current into the Straits of Florida.

(C) The locations of the exercise reference sites are shown in Figure 3-3 and tabulated in Table 3-1.

Table 3-1. (U) GEOGRAPHICAL LOCATIONS OF CHURCH STROKE III CRUISE 1 REFERENCE SITES (U)

Reference Site	Latitude (N)	Longitude (W)
Moored Source	24° 41.1'	84° 29.8'
E	23° 37'	86° 00
F	25° 22'	83° 30'
G	22° 40'	87° 19'

3.2.2 Currents

(U) Currents can be expected to influence relatively low speed ship operations in the area. One can expect to frequently encounter surface currents of at least one knot, diminishing with depth. Near-bottom currents may however, also be a non-negligible factor affecting measurement systems. Currents in the exercise area can influence the acoustic propagation conditions.

3.2.3 Sound Velocity Profiles

(U) The warm saline water flowing from the Staits of Yucatan into the cooler Gulf of Mexico produces a significant lateral change in sound speed structure as illustrated in Figure 3-4.

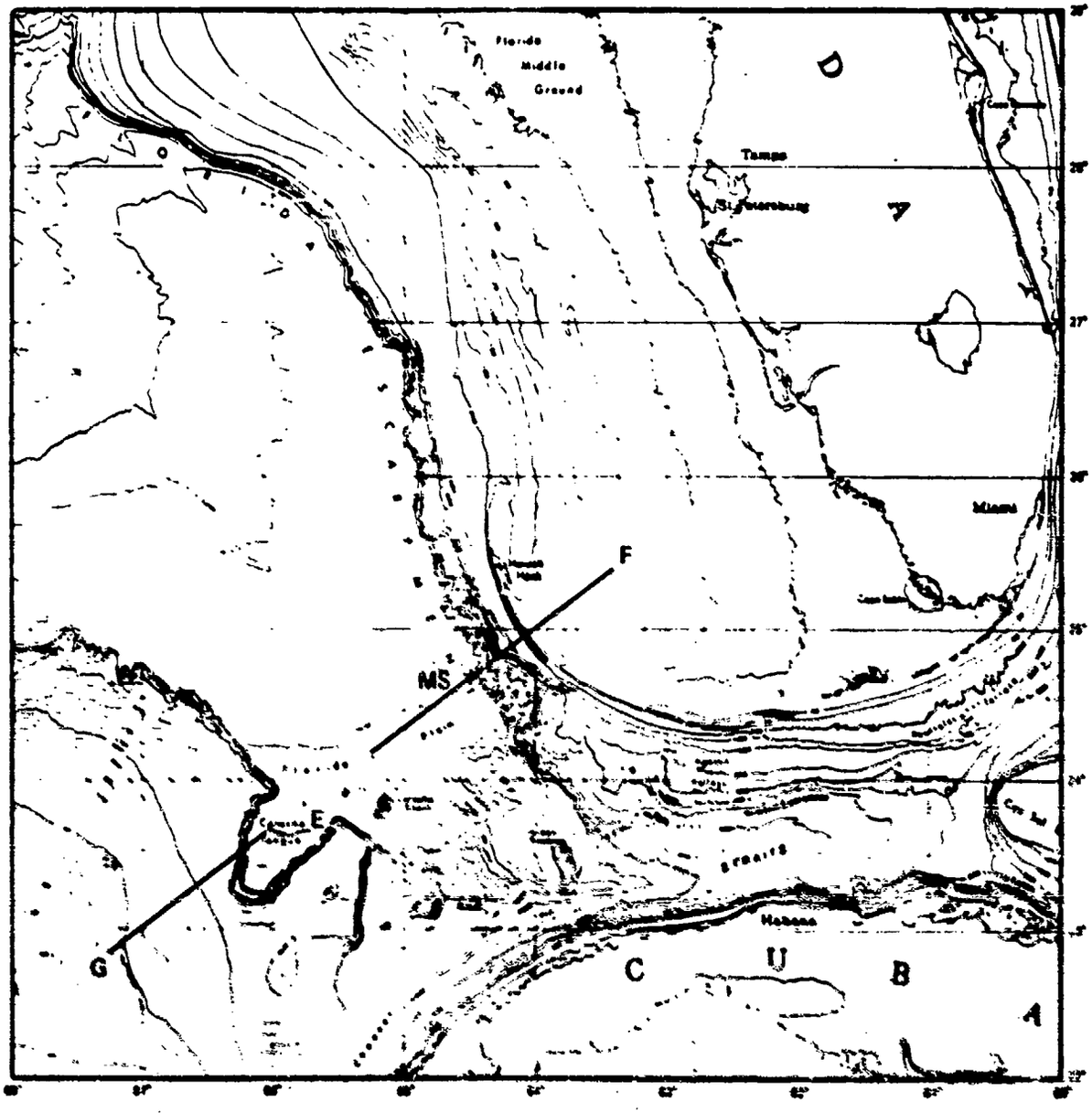

Figure 3-3. (C) Reference Sites for CHURCH STROKE III CRUISE 1 Operational Area (U)

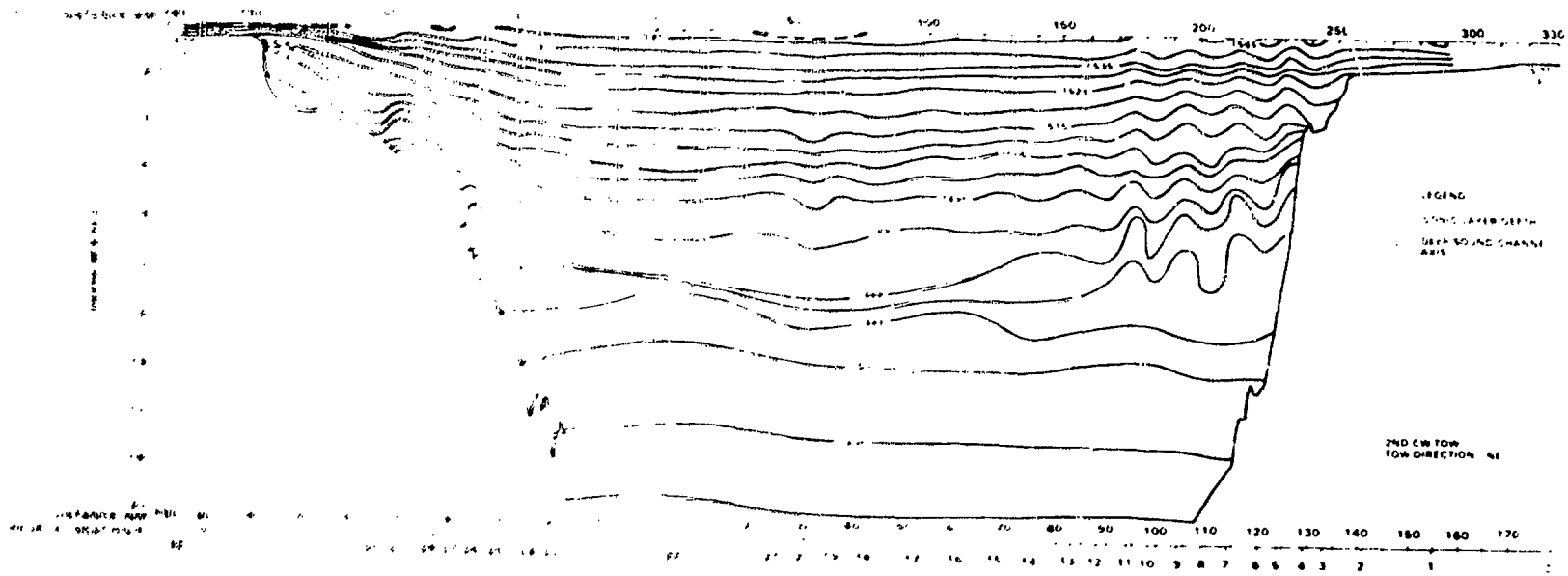

Figure 3-4. (U) Isovelocity Contours and Bathymetric Profile Along the CHURCH STROKE III CRUISE 1 Exercise Baseline (U) (Ref. 13)

(U) The isovelocity contours superimposed on the bathymetric profile along the Exercise Baseline (G-E-F) were derived from 32 selected sound velocity profiles. The location of these 32 sound velocity profiles are marked as function of range from Site E, the general vicinity of the receiver during the exercise.

(U) A marked shallowing of the isovelocity contours above the sound channel can be observed at a range of approximately 20 nm from Site E towards Site G. The effect of the Loop Current at the other end of the Exercise Baseline, towards Site F, is not so pronounced.

(U) Fifteen representative sound velocity profiles out of the 32 used in the derivation of the isovelocity contours presented in Figure 3-5 are superimposed on the bathymetric profile of the Exercise Baseline in Figure 3-4. Profile numbers used in Figure 3-4 do not correspond with those used in Figure 2.

(U) Figure 3-6 is a composite of sound velocity profiles along the Exercise Baseline. Profile numbers are related to the corresponding profile numbers used in Figures 3-4 and 3-5 by the code of Figure 3-6.

(U) The sound velocity profiles show a marked variation of sound speed as a function of location relative to the Loop Current. Profiles 1, 5 and 6 which show the most drastic anomaly from Profile 3 - the profile derived from temperature measurements taken in the middle of the Loop Current - were located either on the West Florida or the Campeche Shelf in shallow water thus having no effect on measured transmission loss at Site E. Profile 4 obtained 42 miles towards Site G from Site E on the slope may have affected transmission loss characteristics along legs E-G and G-E.

(U) The material used in this section is based on Ref. 13.

3.2.3 Sound Propagation

(U) The propagation of sound at long ranges in the Exercise Area is primarily limited by the ocean bottom due to the warm water near the surface and the shallow water depth relative to the critical depth. Figure 3-7 taken from Ref. 14 shows plotted contours of depth difference or "negative" depth excess for the summer season. These contours are the difference between

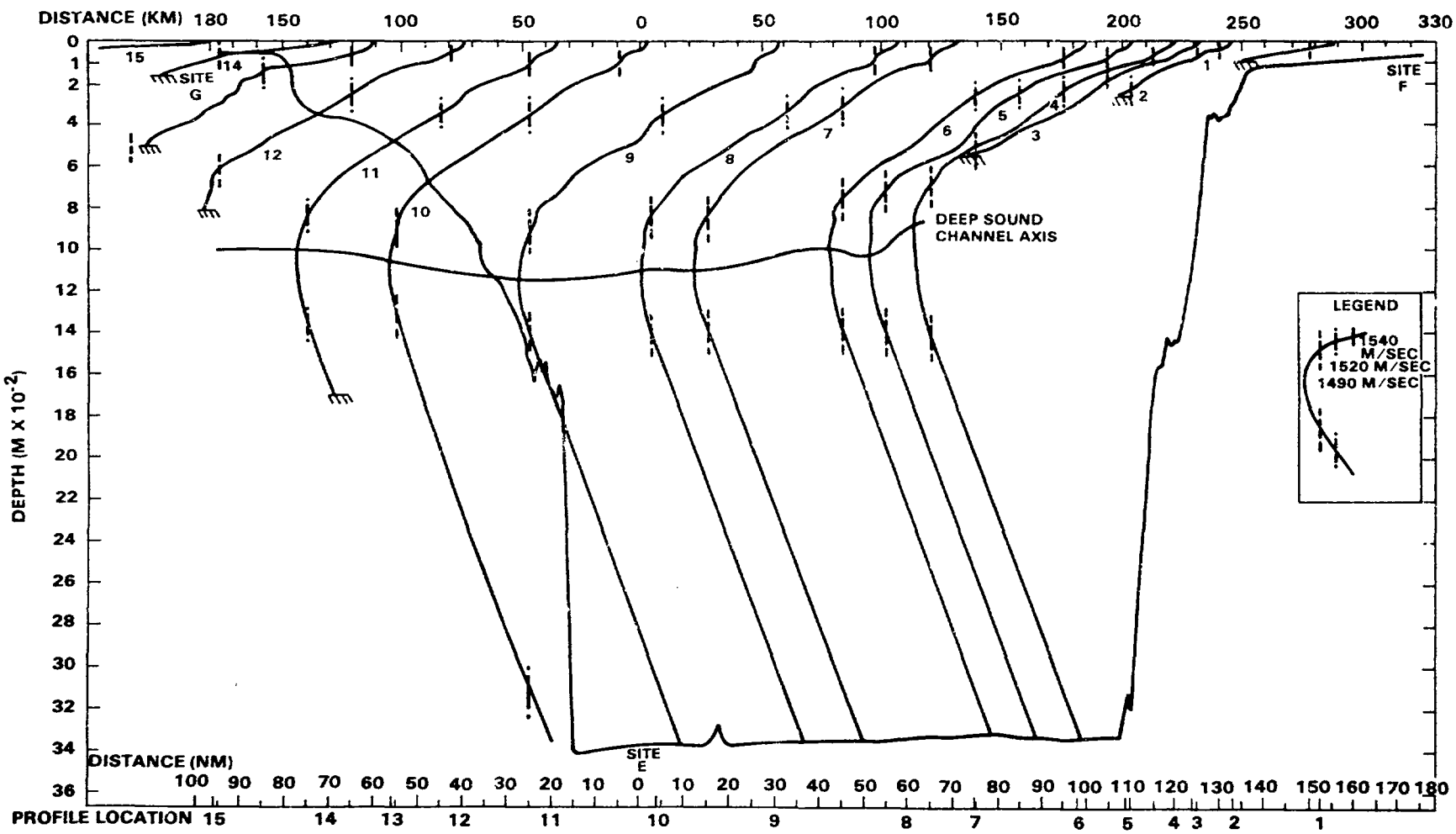

Figure 3-5. (U) Selected Measured Sound Velocity Profiles Along the CHURCH STROKE III CRUISE 1 Exercise Baseline (U) (Ref. 13)

UNCLASSIFIED
UNCLASSIFIED

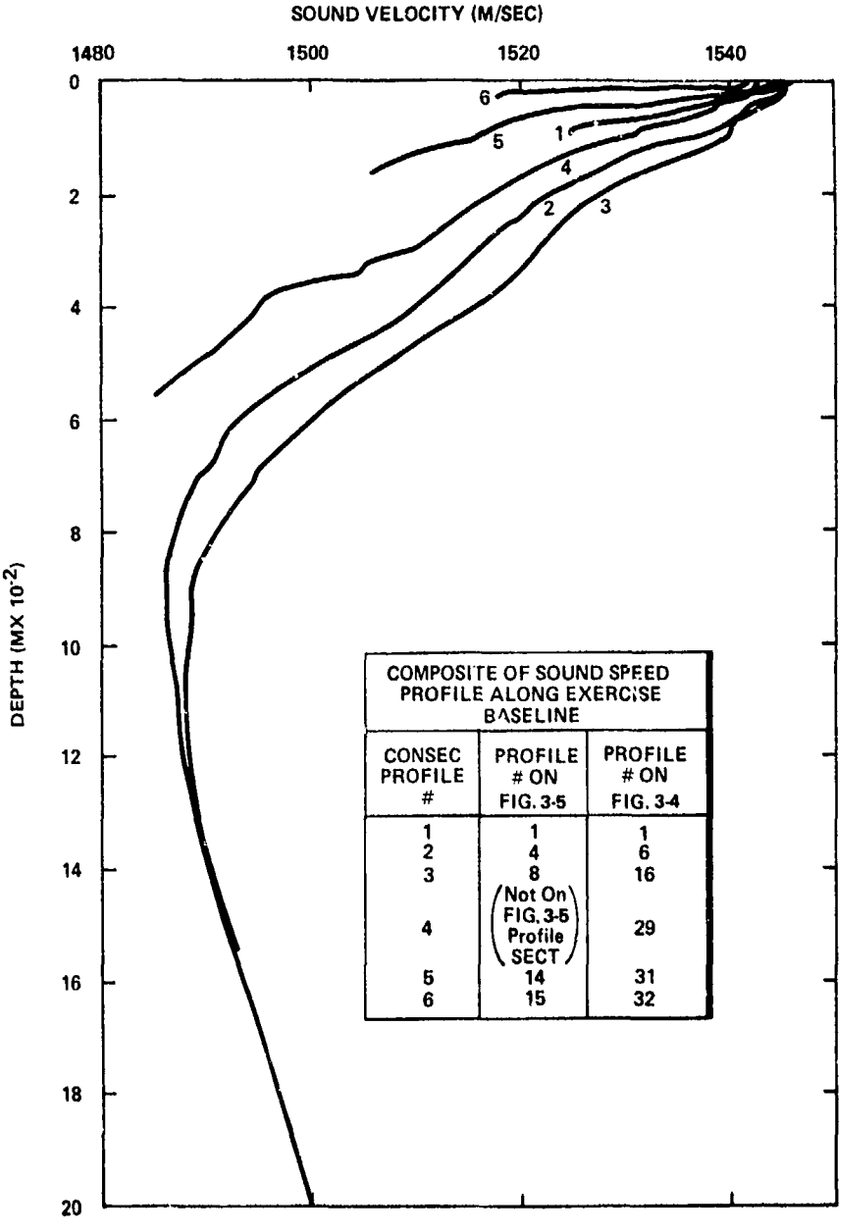

COMPOSITE OF SOUND SPEED PROFILE ALONG EXERCISE BASELINE

CONSEC PROFILE #	PROFILE # ON FIG. 3-5	PROFILE # ON FIG. 3-4
1	1	1
2	4	6
3	8	16
4	(Not On FIG. 3-5 Profile SECT)	29
5	14	31
6	15	32

Figure 3-6. (U) Composite Sound Speed Profiles for CHURCH STROKE III CRUISE 1 (U) (Ref. 13)

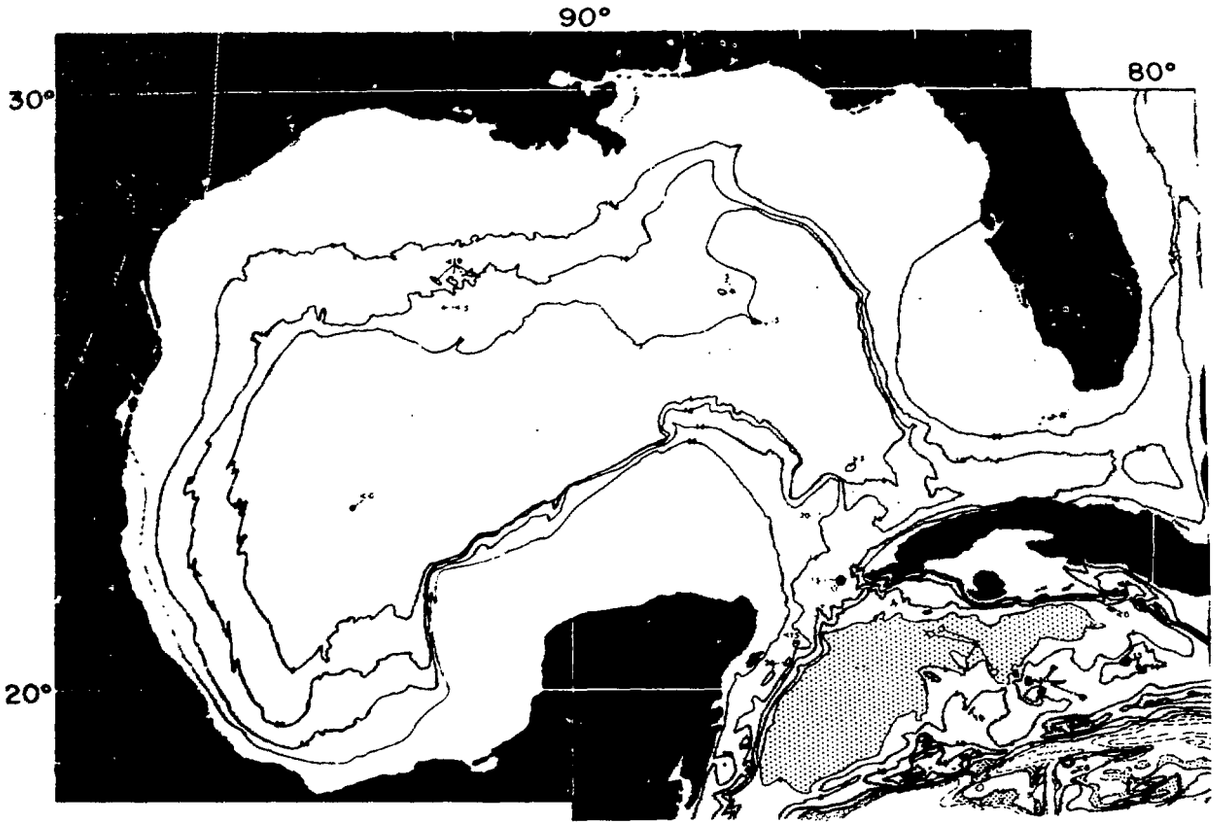

Figure 3-7. (U) Negative Depth Excess for Gulf of Mexico (U) (Ref. 14)

critical depth and local bottom depth in 100 fathom units. There are no data at any time of the year to indicate the presence of positive depth excess. Thus, bottom limited propagation is the rule in entrance to the Gulf of Mexico, the region covered by Church Stroke III, for shallow sources.

(U) An estimate of the minimum grazing angle, θ_m, for bottom limited rays can be obtained from the deep water sound velocity gradient, g, the depth difference d, and surface sound velocity, C_o

$$\theta_m = \text{Cos}^{-1} \left(1 + \frac{gd}{C_o}\right) \quad , g < 0$$

For the contours shown in Fig. 3-7, the values of θ_m for given values of d expressed in fathoms are as follows ($g = 0.0178$ sec^{-1}):

d (fathoms)	θ_m
500	8.3^o
1000	11.7^o

(U) Bottom loss in the Church Stroke III area was computed during pre-exercise estimates (Ref. 15) from a two-path model of bottom interaction, the first path being the reflection at bottom depth, and the second, the refracted path through the underlying sediment. The result is plotted for three classes of bottom as bottom loss/reflection versus grazing angle in Fig. 3-8 (ref. 14, fig. 6). The bottom loss for the 8^o ray at 50 Hz is less than 1dB/reflection, regardless of which attenuation class is used.

(U) Sound attenuation by absorption has been measured recently (Ref. 16) during the KIWI ONE propagation measurements. The path of these measurements, from the Mexican Basin northeast toward the Florida shelf extends into the Church Stroke III area. The sources were aircraft-dropped SUS charges. The attenuation coefficient was determined by the deviation from the cylindrical spreading loss. The values of attenuation coefficient are compared with the Thorp formula in Fig. 3-9 (Ref. 16).

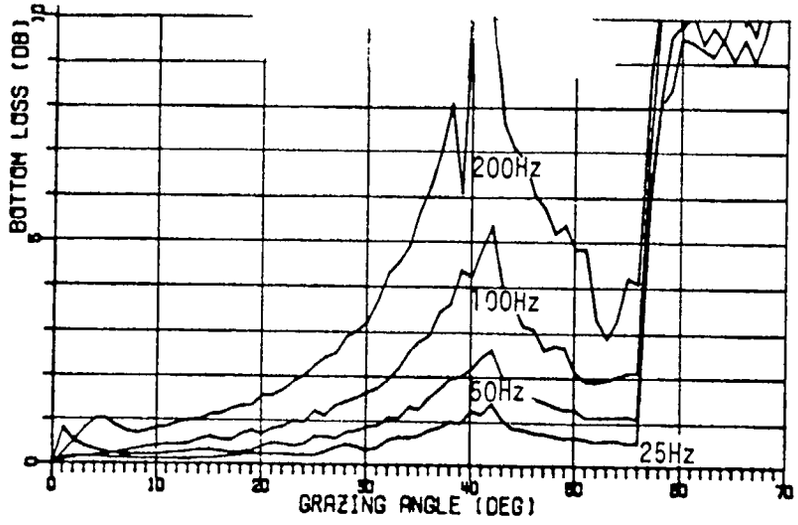

Low Attenuation

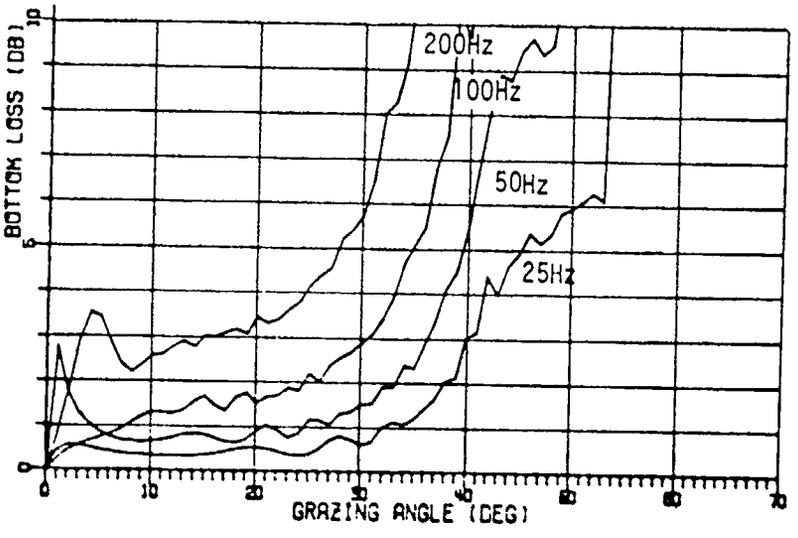

Medium Attenuation

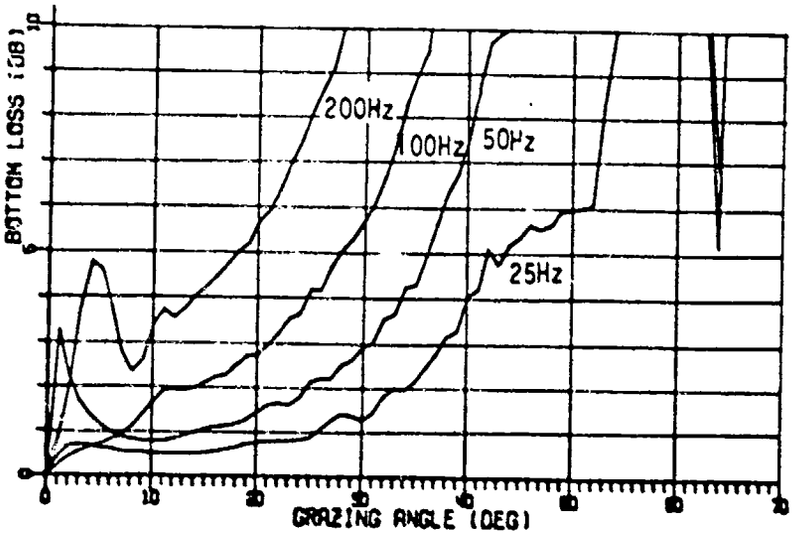

High Attenuation

Figure 3-8. (U) Bottom Loss Estimates for Mississippi Fan (U) (Ref. 15)

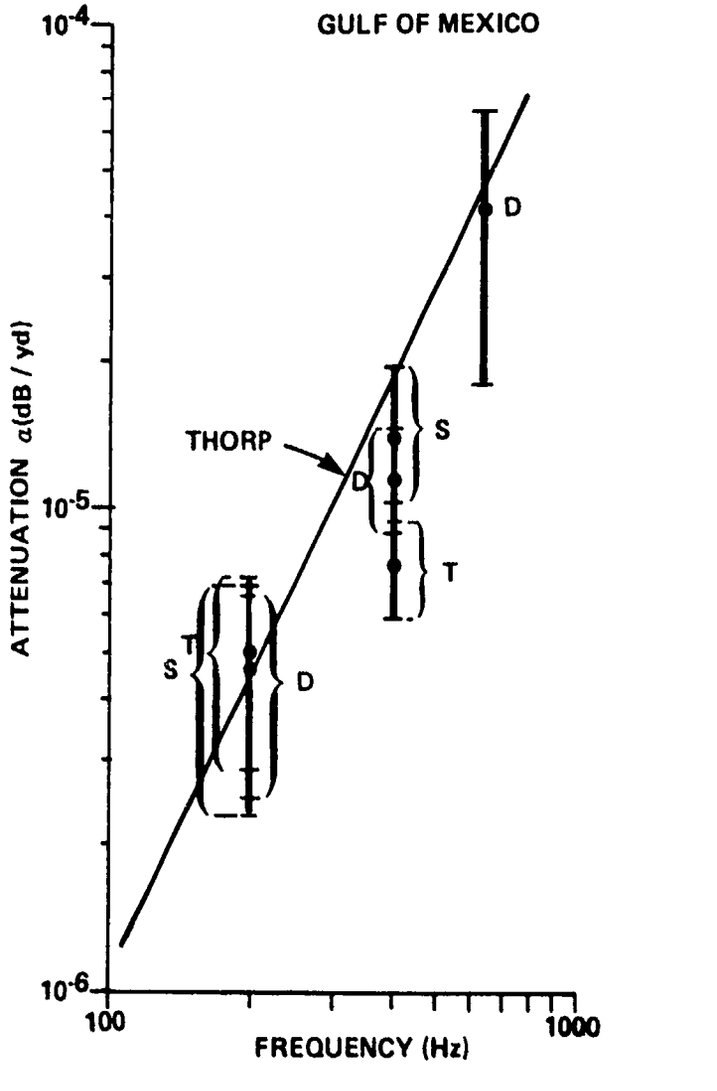

Figure 3-9. (U) Sound Attenuation Coefficient in Gulf of Mexico KIWI ONE Results (Ref. 16) (U)

3.2.5 Ambient Noise

(U) Ambient noise in the area is expected to be most strongly influenced by local shipping, particularly in the Straits of Florida. In addition, it is anticipated that oil exploration and recovery off the Texas - Louisiana shelf will influence the ambient noise in the exercise area.

(U) Shipping throughout the entire exercise area is dense. The greatest concentration of ships is through the Straits of Florida along the Florida Keys. The density of ships increases from east to west through the Straits reaching a maximum at that point beyond the Florida Keys where the ships fan out to the various ports of the Gulf of Mexico.

(C) An estimate of the density of the sum of merchant ships, tankers, and large tankers within the Gulf of Mexico is found in the Historical Temporal Shipping (HITS) data base.

(This page is unclassified.)

4. EXPERIMENTAL RESULTS

(U) Experimental data relating to sound propagation and towed array performance in the Florida plain region and the Catoche Tongue, were obtained over a three day period. The acoustic measurements with both a towed and a moored source were conducted along a Northeast-Southwest track as described in Section 3.2 and shown in Figure 3-3.
under relatively calm seas and clear weather. The LAMBDA III towed array was used as the receiver for signals from both sources. The M/V INDIAN SEAL deployed and towed this array at speeds of less than 1 to 1.5 knots in a direction so as to place the towed and moored source at a near broadside bearing during the acoustic measurements. The source ship USNS DESTEIGEUR opened or closed range with the nominal receiver location, E, on four legs designated F-E, E-G, G-E and E-F. Transmission Loss measurements were obtained on each of these legs and are presented by legs in Section 4.1. Section 4.2 presents the measured received signal characteristics including the array performance as measured by array signal gain, noise gain, array gain and measured beamwidth. Section 4.3 presents the results of signal fluctuation measurements for both short term (12 to 25 minutes) and long term (22 hour) periods.

4.1 TRANSMISSION LOSS AS A FUNCTION OF RANGE

(U) In order to meet the objectives of determining long range propagation loss as function of frequency, range, and receiver/source depth and of defining bathymetric effects a series of measurements were conducted in the operational area.

(U) The LAMBDA III system, towed at a slow speed in the Catoche Tongue at the vicinity of Site E by R/V INDIAN SEAL, was used as the receiver for CW signals transmitted by towed and moored sources. Signals at nominal 67 Hz and 173 Hz projected by the HX-231 F Towed Sound Projector were used to determine transmission loss as function of range. A detailed description of the Sound Projector and its characteristics can be found in Section 2.3 of this report. The Webb Moored Source described in Section 2.2 was used for array performance and signal fluctuation investigations.

PRECEDING PAGE BLANK-NOT FILM

4.1.1 Measurement Techniques

(U) Signal band levels received by each operational hydrophone group of the HF array were used in the estimation of transmission loss. The signal processing used is described in detail by Section 2.1.4 of this report.

(U) The signal level estimates used in the determination of transmission loss were derived by averaging 12 or 24 data ensembles.

(U) Figure 4-1 gives the mean levels and the negative and positive variance of the mean as function of frequency in three filter bands centered at 67, 173 and 175 Hz. The average is given for 24 ensembles.

(U) The same data are plotted in Figure 4-2. Doppler shifting of source frequencies at the receiver have been accounted for in the analysis. The spatial characteristics of the same received average signals as function of hydrophone group location in the HF array of the LAMBDA are represented in Figure 4-3. The length of the array is 300 meters.

(C) Examples of computer processed tabular and plotted values of received levels in the 0.08 Hz wide processing band are presented in Figures 4-4 and 4-5.

(U) The temporal characteristics for the data presented in Figures 4-1 to 4-3 were not determined, however Figures 4-4 and 4-5 present typical distributions of signal levels received by one hydrophone group as function of time (ensemble number). The duration of the 24 ensemble average is about 17 minutes.

(U) The extent of spatial averaging due to relative movement of the source and receiver was determined as less than 1 nautical mile. For most data ensembles it was found to be close to 0.5 nmi.

(U) Due to array tilt, the transmission loss data were acquired over a range of depths. This range was determined by the extent of the tilt and averaged less than 40 meters with occasional excursions to above 70 meters. Maximum variation in hydrophone group depths

DATE :16 AUG 1[illegible] TIME :193 14 59 4
THP III AVG TYPE : 1 NUMBER OF ENS. : 72
FILTER 1 : 67 00 FILTER 2 : 173 00 FILTER 3 :175 00
FILTER WEIGHT : 2 2 START ENS : 1
SAMPLE RATE :914 +1 FFT LINE SPACING : 0312
TYPE OF RECORD : TYPE OF ARRAY : 3
AVG SPECTRA : 00 HYDROPHONES NUMBER OF ENSEMBLES : 24

I	FREQ.	-SIG	MPS	+SIG	I	FREQ.	-SIG	MPS	+SIG	I	FREQ.	-SIG	MPS	+SIG	I	FREQ.	-SIG	MPS	+SIG
1	64.40	-6.9	88.2	3.8	49	68.30	-4.8	87.6	3.1	97	173.00	-8.6	64.7	4.2	145	173.70	-6.8	66.4	3.9
2	64.48	-6.9	87.2	3.8	50	68.38	-6.8	86.6	3.8	98	173.08	-8.1	64.9	4.1	146	173.78	-8.4	65.0	4.2
3	64.56	-6.5	85.8	3.7	51	68.46	-8.8	87.4	4.3	99	173.16	-8.1	65.5	4.1	147	173.86	-7.7	66.1	4.0
4	64.64	-5.7	86.2	3.4	52	68.54	-6.3	86.3	3.6	100	173.24	-6.5	69.9	3.7	148	173.94	-9.4	66.9	4.4
5	64.73	-6.5	85.1	3.7	53	68.62	-6.7	85.8	3.7	101	173.32	-6.0	82.6	3.5	149	174.03	-8.5	66.9	4.2
6	64.81	-6.4	84.6	3.7	54	68.71	-6.3	84.9	3.6	102	173.41	-5.8	83.7	3.4	150	174.11	-8.4	65.8	4.2
7	64.89	-7.5	84.2	4.0	55	68.79	-6.3	84.3	3.6	103	173.49	-6.6	73.9	3.7	151	174.19	-9.2	66.2	4.4
8	64.97	-10.2	81.4	4.6	56	68.87	-6.5	83.2	3.7	104	173.57	-7.4	66.0	3.9	152	174.27	-8.2	68.0	4.1
9	65.05	-10.1	80.3	4.5	57	68.95	-8.6	82.2	4.2	105	173.65	-6.4	66.1	3.6	153	174.35	-8.5	68.8	4.2
10	65.13	-11.6	78.3	4.8	58	69.03	-10.7	80.2	4.6	106	173.73	-7.6	65.8	4.0	154	174.43	-6.3	68.6	3.6
11	65.21	-12.2	76.8	4.9	59	69.11	-10.5	79.3	4.6	107	173.81	-7.4	65.4	3.9	155	174.51	-6.6	68.4	3.7
12	65.29	-15.0	75.8	5.2	60	69.19	-10.9	77.7	4.7	108	173.89	-7.9	66.5	4.1	156	174.59	-7.5	68.6	4.0
13	65.38	-12.1	75.2	4.9	61	69.27	-11.1	76.1	4.7	109	173.97	-9.6	67.1	4.4	157	174.68	-6.3	67.7	3.6
14	65.46	-12.5	75.6	4.9	62	69.36	-16.1	76.7	5.3	110	174.06	-8.7	66.2	4.2	158	174.76	-6.8	70.0	3.8
15	65.54	-21.5	76.7	5.6	63	69.44	-11.0	77.2	4.7	111	174.14	-9.1	66.1	4.3	159	174.84	-7.2	72.6	3.9
16	65.62	-10.4	77.6	4.6	64	69.52	-8.8	79.1	4.3	112	174.22	-8.0	66.5	4.1	160	174.92	-7.0	72.1	3.8
17	65.70	-8.9	79.6	4.3	65	170.40	-8.2	63.5	4.1	113	174.30	-8.8	68.6	4.3	161	175.00	-7.5	69.7	4.0
18	65.78	-7.8	82.2	4.0	66	170.48	-8.6	62.9	4.2	114	174.38	-7.1	68.8	3.8	162	175.08	-9.6	69.6	4.4
19	65.86	-7.8	83.2	4.0	67	170.56	-9.9	63.3	4.5	115	174.46	-6.7	68.4	3.7	163	175.16	-11.0	69.1	4.7
20	65.94	-5.2	85.4	3.2	68	170.64	-11.2	63.3	4.7	116	174.54	-6.9	68.7	3.8	164	175.24	-6.7	69.0	3.7
21	66.03	-6.6	85.6	3.7	69	170.73	-7.0	64.5	3.8	117	174.62	-6.1	68.4	3.6	165	175.32	-5.5	68.6	3.3
22	66.11	-7.2	84.4	3.9	70	170.81	-6.7	63.7	3.8	118	174.71	-6.7	68.3	3.7	166	175.41	-7.6	69.3	4.0
23	66.19	-7.5	84.1	4.0	71	170.89	-6.6	63.7	3.7	119	174.79	-6.8	71.2	3.8	167	175.49	-8.3	69.2	4.2
24	66.27	-5.6	84.2	3.4	72	170.97	-8.5	62.9	4.2	120	174.87	-7.0	73.1	3.8	168	175.57	-7.3	69.5	3.9
25	66.35	-6.4	81.6	3.6	73	171.05	-9.2	62.9	4.4	121	174.95	-7.3	70.9	3.9	169	175.65	-6.2	70.0	3.6
26	66.43	-6.7	79.5	3.7	74	171.13	-7.7	62.5	4.0	122	175.03	-7.7	69.9	4.0	170	175.73	-7.4	69.6	3.9
27	66.51	-7.7	79.4	4.0	75	171.21	-7.8	62.7	4.0	123	175.11	-10.7	69.6	4.6	171	175.81	-9.2	68.2	4.4
28	66.59	-7.5	78.8	4.0	76	171.29	-6.4	62.7	3.6	124	175.19	-10.0	69.1	4.5	172	175.89	-8.4	69.8	4.2
29	66.68	-9.2	77.7	4.4	77	171.38	-7.6	61.9	4.0	125	175.27	-5.4	69.3	3.3	173	175.97	-17.6	69.0	5.4
30	66.76	-7.5	78.8	4.0	78	171.46	-7.2	61.7	3.9	126	175.36	-5.8	69.0	3.4	174	176.06	-20.9	68.6	5.6
31	66.84	-9.1	76.9	4.3	79	171.54	-8.0	62.9	4.1	127	175.44	-8.2	69.9	4.1	175	176.14	-13.7	68.5	5.1
32	66.92	-7.5	75.5	4.0	80	171.62	-7.4	63.8	3.9	128	175.52	-7.6	69.7	4.0	176	176.22	-16.8	69.3	5.4
33	67.00	-8.6	80.1	4.2	81	171.70	-8.1	62.4	4.1	129	172.40	-7.1	63.6	3.8	177	176.30	-28.1	70.4	6.1
34	67.08	-9.3	80.5	4.4	82	171.78	-6.1	61.1	3.6	130	172.48	-7.4	62.8	3.9	178	176.38	-28.0	70.4	6.9
35	67.16	-8.6	86.3	4.2	83	171.86	-6.5	61.5	3.7	131	172.56	-7.1	63.0	3.9	179	176.46	-28.8	71.2	8.1
36	67.24	-6.8	75.1	3.8	84	171.94	-7.2	62.1	3.9	132	172.64	-7.3	63.5	3.9	180	176.54	-29.3	71.6	8.2
37	67.32	-7.4	74.0	3.9	85	172.03	-8.0	62.4	4.1	133	172.73	-8.4	63.4	4.2	181	176.62	-28.6	70.9	7.7
38	67.41	-7.5	74.1	4.0	86	172.11	-10.0	61.1	4.5	134	172.81	-8.1	64.0	4.1	182	176.71	-30.5	72.8	8.9
39	67.49	-8.5	74.8	4.2	87	172.19	-7.6	62.6	4.0	135	172.89	-6.6	64.6	3.7	183	176.79	-31.1	73.4	9.0
40	67.57	-8.8	75.4	4.3	88	172.27	-6.4	63.6	3.6	136	172.97	-7.9	64.9	4.1	184	176.87	-30.4	72.7	9.0
41	67.65	-8.9	76.0	4.3	89	172.35	-6.6	63.7	3.7	137	173.05	-8.4	64.8	4.2	185	176.95	-30.6	72.9	9.1
42	67.73	-9.1	76.9	4.4	90	172.43	-7.2	62.8	3.9	138	173.13	-7.8	65.4	4.0	186	177.03	-30.7	73.0	8.7
43	67.81	-9.8	77.8	4.5	91	172.51	-7.3	62.2	3.9	139	173.21	-8.4	65.7	4.2	187	177.11	-34.0	76.3	10.7
44	67.89	-8.6	78.1	4.2	92	172.59	-7.1	62.9	3.9	140	173.29	-6.1	79.1	3.5	188	177.19	-37.8	80.1	11.9
45	67.97	-7.5	80.8	4.0	93	172.68	-8.1	63.2	4.1	141	173.38	-5.9	84.5	3.5	189	177.27	-38.9	81.2	11.8
46	68.06	-7.5	83.0	4.0	94	172.76	-8.8	63.2	4.3	142	173.46	-5.9	79.0	3.5	190	177.36	-40.9	83.2	11.6
47	68.14	-7.6	84.4	4.0	95	172.84	-6.6	64.3	3.7	143	173.54	-7.6	67.6	4.0	191	177.44	-39.5	81.8	11.5
48	68.22	-7.1	86.0	3.9	96	172.92	-6.2	64.7	3.6	144	173.62	-6.8	65.3	3.8	192	177.52	-37.5	79.8	11.0

Figure 4-1. (C) Tabular Values of Received Levels and their Variances in the 0.08 Hz Processing Bands (C)

CONFIDENTIAL

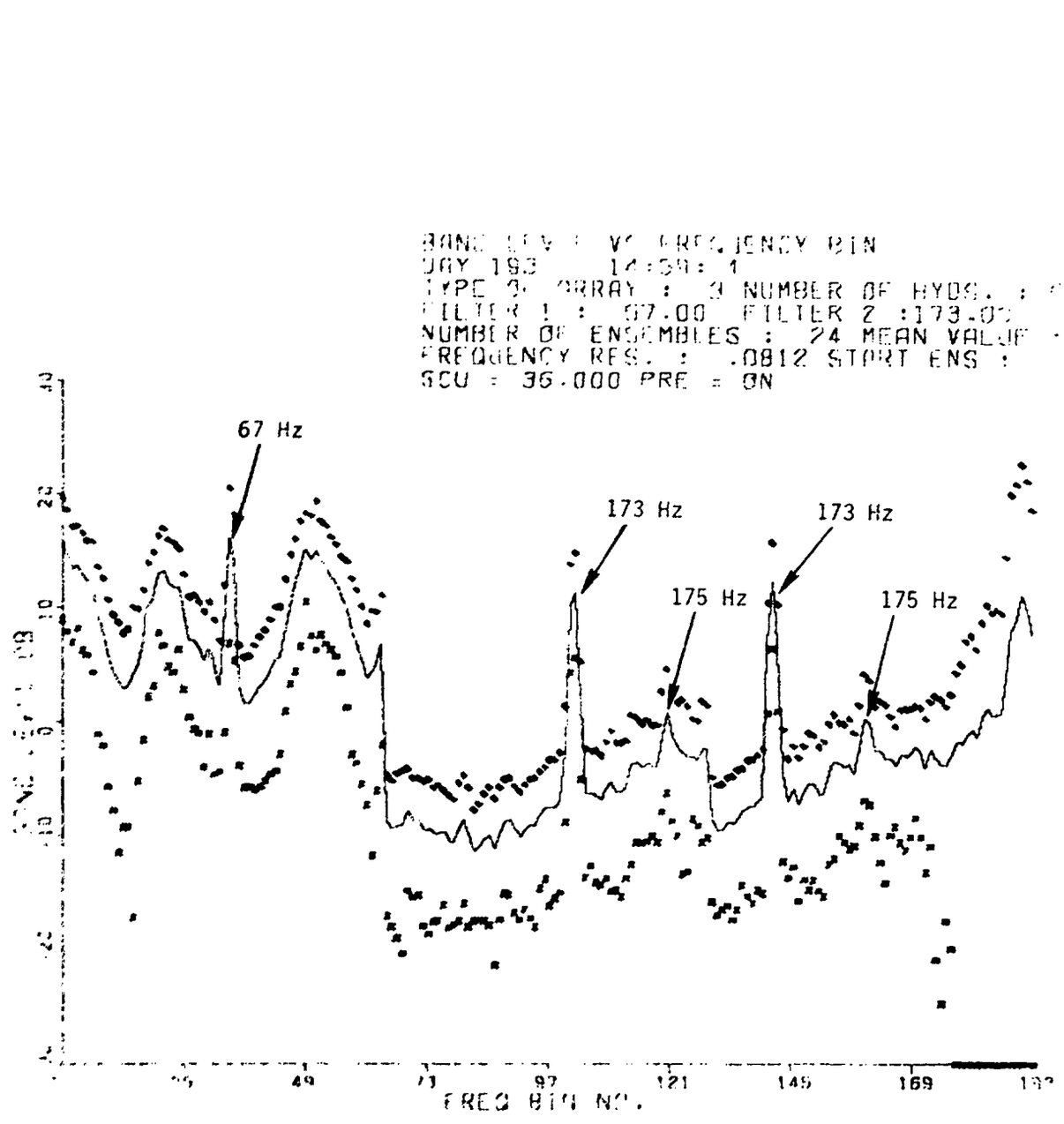

Figure 4-2 (C) Plotted Values of Received Levels and their Variances in the 0.08 Hz Processing Bands (C)

CONFIDENTIAL

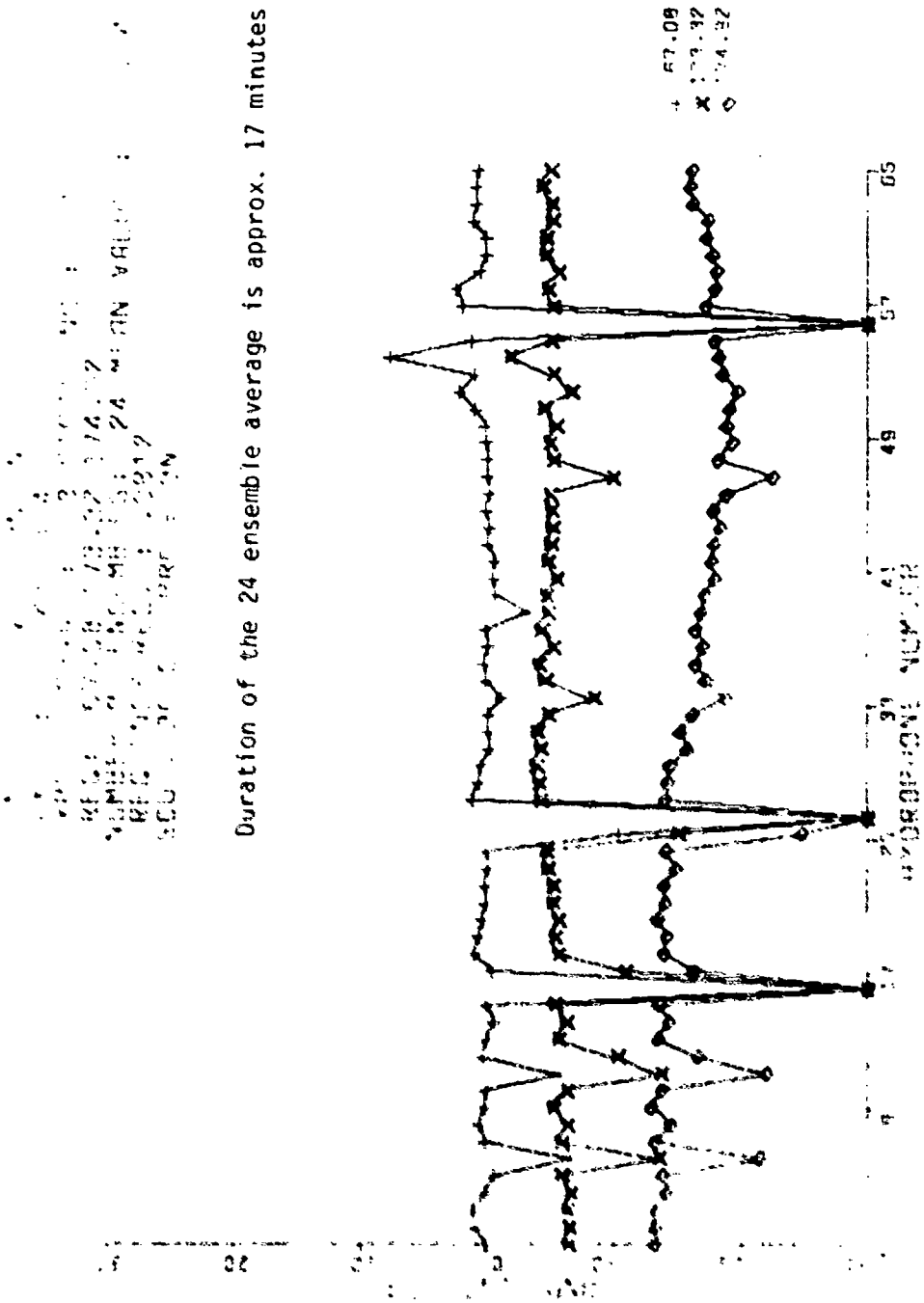

Figure 4-3 (C) Spatial Characteristics of Average Received Signals as Function of Hydrophone Group Location (U)

CONFIDENTIAL

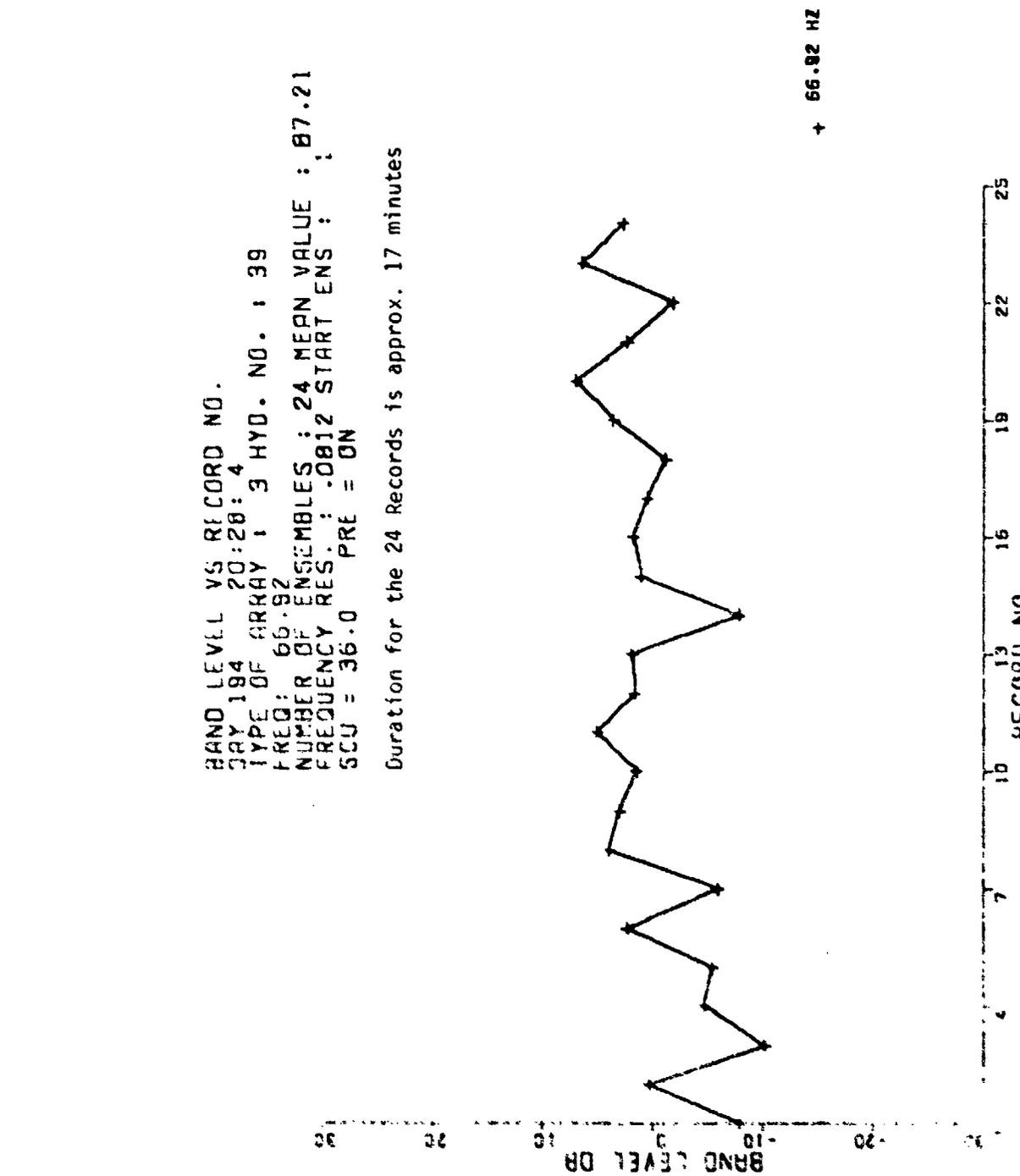

Figure 4-4. (C) Typical Characteristics of Received 67 Hz Signal Levels for One Hydrophone Group as Function of Time (U)

CONFIDENTIAL

CONFIDENTIAL

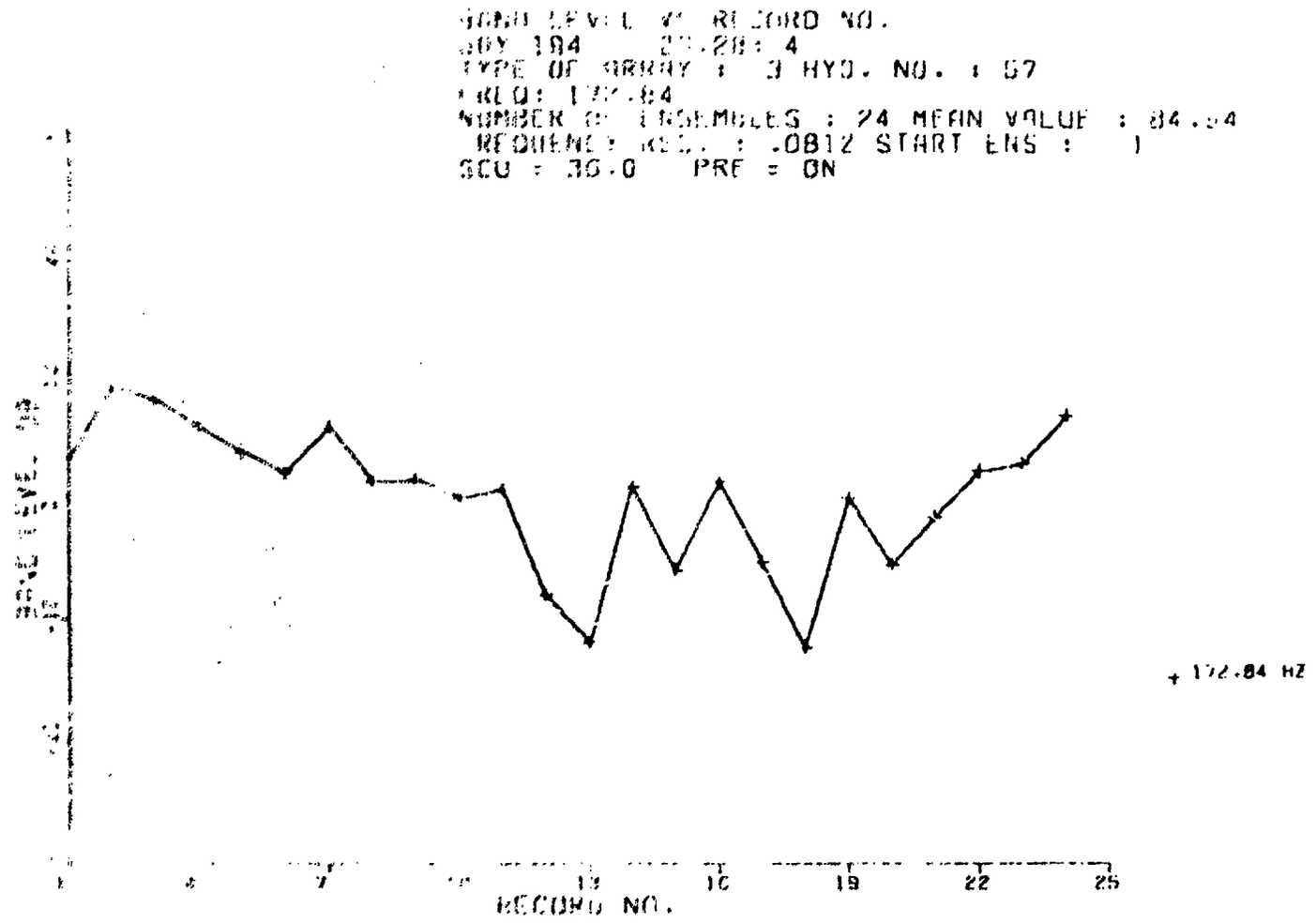

Figure 4-5. (C) Typical Characteristics of Received 173 Hz Signal Levels for One Hydrophone Group as Function of Time (U)

CONFIDENTIAL

(This page is unclassified.)

was 78 m. The effect of volumetric averaging of transmission loss was assumed negligible. This assumption was based on FACT model runs at several depths within the depth range of the hydrophone groups. The results of these runs showed no appreciable difference in predicted transmission loss as a function of depth within the observed depth range of the hydrophone groups.

(U) Noise levels were established by averaging the received levels in 3 processing bands on each side of the signal band located 4 processing bands away from the signal band. This noise value was used to determine signal plus noise-to-noise ratios for each received signal level.

(U) Transmission loss was derived by subtracting the received signal plus noise level from the calibrated source level of the sound projectors for signal to noise ratios greater than 2 dB.

4.1.2 Summary of Transmission Loss Data

(U) Tables 4-1 to 4-4 present a summary of the sound transmission loss for each of four legs as measured by the technique described earlier. TL values are given along with the measurement parameters relating to navigation, transmitted signal and signal processing. These parameters, used to establish the transmission loss estimates as a function of range in the headings for the Tables 4-1 to 4-4,are defined as follows:

Mean Time: The midpoint of the time interval during which the data ensembles were averaged. Time is reported as Greenwich Mean Time (Zulu).

Mean Receiver Location: The location of the tow ship at the Mean Time. Rectified navigation data provided by NORDA Code 340 were used in the determination of this location. The range error introduced by using the location of the tow ship instead the mean location of the hydrophones was considered negligible. Since the array was towed in a direction perpedicular to the bearing between the source and receiver this assumption is valid.

Mean Source Location: The location of the source ship at the Mean Time. Rectified navigation data provided by NORDA Code 340 were used in the determination of this location.

Signal Level: Received signal band level of one of the tones projected by the HX-231 F Sound Projector as determined by the spatial averaging of the output of at least 57 of the 64 hydrophones of the array and time averaging of a given number of ensembles (12 to 24) for each hydrophone.

Table 4-1. (C) Transmission Loss and Related Parameters for Leg F-E (U,

MEAN TIME	MEAN RECEIVER LOCATION		MEAN SOURCE LOCATION		* SIGNAL LEVEL 67 Hz	SIGNAL TO NOISE 67 Hz (dB)	TRANSMISSION LOSS 67 Hz (dB)	67 Hz	* SIGNAL LEVEL 173 Hz	SIGNAL TO NOISE 173 Hz (dB)	TRANSMISSION LOSS 173 Hz (dB)	173 Hz	RANGE (NM)	BEARING θ_T	R SOURCE (NM)	H SENSOR (NM)	D SENSOR (M)	MEAN DEPTH OF ARRAY (M)	ΔT	NUMBER OF AVERAGES	COMMENTS
	LAT N	LONG W	LAT N	LONG W																	
191 0120	33°08.3'	86°02.5'	34°15.2'	85°08.9'	88.1	8	91.4	2.7	85.1	15	98.4	2.9	55.8	60.1	1.76	0.08	110	787	18'44"	25	
0343	33°03.3'	86°02.0'	34°08.9'	85°19.3'	87.8	15	95.5	3.4	87.6	14	95.8	4.1	42.8	65.1	1.09	0.06	120	828	8'35"	12	
0353	33°03.3'	86°01.9'	34°08.3'	85°21.3'	87.8	8	91.7	3.7	88.9	18	94.5	4.1	40.8	65.3	0.92	0.06	121	828	8'35"	12	
0436	33°06.9'	86°02.0'	34°11.5'	85°25.1'	90.9	10	88.6	3.5	92.8	20	90.6	3.5	36.8	66.5	0.83	0.09	125	840	8'35"	12	
0446	33°06.8'	86°02.0'	34°11.1'	85°25.9'	86.9	9	92.6	3.7	90.7	20	92.7	3.7	36.0	66.5	0.83	0.12	126	846	8'35"	12	
0511	33°06.8'	86°02.0'	33°58.5'	85°28.7'	84.1	9	95.4	4.0	85.7	15	97.7	5.1	33.0	67.4	2.11	0.24	120	789	17'57"	24	
0539	33°06.1'	86°01.3'	33°54.3'	85°33.1'	96.3	15	85.2	4.4	93.5	18	91.9	3.6	24.5	66.4	0.76	0.13	?**	?**	8'35"	12	
0548	33°06.1'	86°01.3'	33°54.2'	85°33.8'	93.6	11	86.1	4.0	88.5	13	94.9	4.0	23.7	67.1	0.76	0.13	?**	?**	8'35"	12	

LEG F - E

SOURCE LEVEL 67 Hz 179.3 dB// 1 μPa
173 Hz 183.4 dB// 1 μPa

* SIGNAL LEVEL IN dB// 1 μPa

* SIGNAL LEVEL IN dB// 1 μPa

**DEPTH SENSOR(s) INOPERATIONAL

RECEIVER DEPTH: 720 - 950 M
SOURCE DEPTH 180 M

ARRAY ANGLE (VERTICAL)
22.8° TO - 19.14°

HORIZONTAL DISTANCE BETWEEN DEPTH SENSORS: 335.5 METERS

CONFIDENTIAL

Table 4-2. (C) Transmission Loss and Related Parameters for Leg E-F (U)

PAGE 1 of 3

MEAN TIME	MEAN RECEIVER LOCATION LAT N	MEAN RECEIVER LOCATION LONG W	MEAN SOURCE LOCATION LAT N	MEAN SOURCE LOCATION LONG W	SIGNAL LEVEL 67 Hz	SIGNAL TO NOISE 67 Hz (dB)	TRANSMISSION LOSS 67 Hz (dB)	σ 67 Hz	SIGNAL LEVEL 173 Hz	SIGNAL TO NOISE 173 Hz (dB)	TRANSMISSION LOSS 173 Hz (dB)	σ 173 Hz	RANGE (NM)	BEARING °T	ΔR SOURCE (NM)	ΔH SENSOR (NM)	ΔD SENSOR (M)	MEAN DEPTH OF ARRAY (M)	ΔT	NUMBER OF AVERAGES	COMMENTS
195 00 32	23°42.1'	85°58.8	24°11.5	85°19.6'	89.5	13	89.6		87.9		95.6		53.37	56.5	0.47	0.2	38	487	8'04"	12	
00 53	23°41.68'	85°58.34	24°11.9	85°18.9	91.8	13	87.9	2.0	87.2	18	96.2	2.5	54.36	56.8	0.47	0.2	37	488	8'04"	12	
01 35	23°41.59	85°57.80	24°10.7	85°18.8	92.2	8	89.8	2.6	91.2	22	92.2	2.5	57.28	56.5	0.75	0.18	37	485	8'04"	12	
01 53	23°40.97	85°57.57	24°10.5	85°18.8	87.4	8	91.9	2.7	85.1	16	98.3	2.9	58.28	53.8	0.75	0.2	38	482	8'04"	12	
02 15	23°40.17	85°57.00	24°12.1	85°17.7	90.9	6	92.5	2.8	83.5	15	99.9	3.1	61.85	53.2	0.79	0.2	40	481	8'04"	12	
02 36	23°39.70	85°56.70	24°10.2	85°17.1	83.9	6	95.4	3.1	84.8	17	107.4	2.9	63.75	52.6	0.78	0.2	37	399	8'04"	12	
02 53	23°39.68	85°56.55	24°10.6	85°16.5	86	9	93.3	3.1	80.2	12	103.2	2.8	64.52	52.6	0.71	0.2	40	400	8'04"	12	
03 41	23°38.48	85°55.50	24°11.4	84°55.9	87.5	9	91.4	2.8	81.3	15	102.1	3.0	69.58	51.5	0.88	0.2	35	398	8'04"	12	
03 49	23°38.23	85°55.45	24°12.1	84°55.2	88.3	10	92.6	2.8	79.4	12	104.9	3.2	70.38	51.2	0.88	0.2	35	398	8'04"	12	
195 00 00	23°37.92	85°55.19	24°12.1	84°53.9	87.3	10	92.8	3.0	80.5	14	102.9	3.1	71.93	50.9	0.73	0.16	34	400	8'04"	12	
00 13	23°37.75	85°55.01	24°13.4	84°53.1	87.3	12	91.6	2.7	82.3	17	101.1	3.7	72.72	50.8	0.73	0.16	31	398	8'04"	12	
00 27	23°37.60	85°54.76	24°14.2	84°53.9	88.6	12	90.5	2.3	82.6	19	100.8	2.5	74.85	50.5	0.73	0.16	37	396	8'04"	12	
00 36	23°37.29	85°54.63	24°14.6	84°53.2	85.3	8	94.0	2.8	85.3	16	98.1	2.6	74.74	50.5	0.64	0.16	35	395	8'04"	12	
00 49	23°37.27	85°54.60	24°14.6	84°54.2	85.1	5	94.2	2.7	82.8	17	101.4	2.7	75.87	50.4	0.73	0.15	36	385	8'04"	12	
03 56	23°37.06	85°54.60	24°14.5	84°54.5	86.6	5	92.7	2.5	79.6	15	104.6	2.8	76.87	50.4	0.73	0.15	32	390	8'04"	12	
00 00	23°37.25	85°54.5	24°14.8'	84°54.1	85.6	6	93.7	3.0	81.3	17	102.1	2.8	76.78	50.8	0.57	0.15	32	381	8'04"	12	
00 17	23°37.09	85°54.43	24°14.8'	84°53.7	84.4	5	94.9	3.1	82.4	17	101.8	2.6	77.38	48.8	0.57	0.24	36	381	8'04"	12	
00 37	23°36.89'	85°54.38	24°14.2	84°53.5	84.7	7	94.4	2.8	80.8	15	102.6	2.8	78.88	48.5	0.57	0.24	35	378	8'04"	12	

LEG E-F SOURCE LEVEL 173 Hz 183.3 dB//1 μPa; 67 Hz 183.4 dB//1 μPa RECEIVER DEPTH 362 - 423 M SOURCE DEPTH 100 M ARRAY ANGLE (VERTICAL) +5.2 TO +7.6 HORIZONTAL DISTANCE BETWEEN DEPTH SENSORS = 335.5 METERS

* SIGNAL LEVEL IN dB//1 μPa

CONFIDENTIAL

Table 4-2. (C) Transmission Loss and Related Parameters for Leg E-F (U) (Con't)

MEAN TIME	MEAN RECEIVER LOCATION LAT N	MEAN RECEIVER LOCATION LONG W	MEAN SOURCE LOCATION LAT N	MEAN SOURCE LOCATION LONG W	SIGNAL LEVEL 63 Hz	SIGNAL TO NOISE 63 Hz dB	TRANSMISSION LOSS 63 Hz dB	63 Hz	SIGNAL LEVEL 173 Hz	SIGNAL TO NOISE 173 Hz dB	TRANSMISSION LOSS 173 Hz dB	173 Hz	RANGE (NM)	BEARING °T	A SOURCE (NM)	H SENSOR (NM)	D SENSOR (M)	MEAN DEPTH OF ARRAY (M)	T	NUMBER OF AVERAGES	COMMENTS
1900 30 JU	33° 57.9	75° 54.1	34° 26.6	65° 39.6	95.7	9	93.6	2.9	92.3	15	104.1	3.1	98.77	49.15°	0.57	0.24	34	384	8'84"	12	
05 02	33°51.9	65°56.1	34° 38.6	66°20.3	91.2	4	92.6	2.9	82.6	15	100.6	2.5	101.95	48.55°	0.63	0.28	34	383	8'84"	12	
05 17	33°51.8	65°56.6	34°38.8	66°38.8	87.6	8	91.1	2.8	88.6	16	103.0	2.5	101.98	48.34°	0.63	0.28	35	380	8'84"	12	
05 33	33°51.8	65°56.8	34°48.1	66°58.7	84.5	3	94.8	3.2	79.5	15	104.4	3.5	103.61	48.01°	0.73	0.27	37	381	8'84"	12	
05 48	33°50.8	65°53.9	34°48.7	66°28.7	87.1	6	93.2	2.9	77.1	16	105.7	2.9	104.46	47.83°	0.73	0.22	36	385	8'84"	12	
06 02	33°50.7	65°53.6	34°51.1	66°27.5	88.0	5	93.1	2.8	77.6	13	105.7	3.3	106.02	47.58°	0.73	0.22	38	387	8'84"	12	
06 17	33°50.8	65°53.5	34°43.6	66°26.8	85.8	5	93.5	3.2	77.6	13	105.6	3.2	106.99	47.39°	0.73	0.22	38	389	8'84	12	
06 30	33°50.7	65°53.1	34°43.7	66°25.7	86.7	6	92.6	3.1	79.8	11	103.6	2.6	109.86	47.10°	0.69	0.28	35	384	8'84"	12	
06 43	33°49.5	65°53.0	34°40.2	66°24.9	86.2	5	92.6	3.1	79.8	8	103.6	2.6	109.83	47.01°	0.69	0.28	36	392	8'84"	12	
06 58	33°49.3	65°52.8	34°40.8	66°23.7	87.6	6	91.7	2.9	80.7	10	102.7	3.1	110.84	46.98°	0.69	0.28	41	384	8'84	12	
07 02	33°48.5	65°52.7	34°40.7	66°23.0	88.8	3	90.5	2.6	81.5	12	101.9	3.7	111.78	46.84°	0.69	0.99	39	397	8'84	12	
07 09	33°48.8	65°54.1	34°40.8	66°18.6	88.3		91.1	3.2	85.7	13	98.2	2.5	117.17	47.72°	0.66	0.22	39	411	8'84"	12	
07 13	33°51.8	65°56.3	34°40.3	66°18.8	89.1	8	90.7	3.6	85.5	13	97.9	3.2	117.91	47.83°	0.66	0.22	39	411	8'84	12	
07 25	33°51.9	65°56.3	34°42.1	66°18.2	86.8	8	92.5	3.6	83.6	14	99.8	2.9	122.25	48°59°	0.65	0.29	39	411	8'84"	12	
07 37	33°51.8	65°56.4	34°42.7	66°17.8	83.5	7	93.8	3.6	79.4	11	104.4	2.8	122.69	48°74°	0.65	0.25	38	410	8'84"	12	
07 50	33°52.6	65°56.7	34°43.8	66°17.7	84.2	6	95.1	2.9	78.1	9	105.3	3.0	124.09	48°26°	0.65	0.18	39	411	8'84"	12	
10 00	33°52.9	65°56.3	34°43.5	66°18.3	84.0	6	95.3	2.5	75.6	6	108.8	3.1	125.03	48°76°	0.98	0.22	41	410	8'84"	12	
10 13	33°52.8	65°56.4	34°43.8	66°18.8	85.2	6	93.6	3.0	72.6	6	111.8	3.3	125.45	49°83°	0.98	0.22	40	409	8'84"	12	

LEG E-F SOURCE LEVEL: 63 Hz 179.3 dB/1 μPa; 173 Hz 183.6 dB/1 μPa. RECEIVER DEPTH 363 637 M. SOURCE DEPTH 198 M. ARRAY ANGLE (VERTICAL) +5.3 TO -7.6. HORIZONTAL DISTANCE BETWEEN DEPTH SENSORS = 335.5 METERS

* SIGNAL LEVEL 10 dB/1 μPa

CONFIDENTIAL

Table 4-2. (C) Transmission Loss and Related Parameters for Leg E-F (U) (Con't)

MEAN TIME	MEAN RECEIVER LOCATION LAT °N	MEAN RECEIVER LOCATION LONG °W	MEAN SOURCE LOCATION LAT °N	MEAN SOURCE LOCATION LONG °W	* SIGNAL LEVEL 67 Hz	SIGNAL TO NOISE 67 Hz (dB)	TRANSMISSION LOSS 67 Hz (dB)	67 Hz	* SIGNAL LEVEL 173 Hz	SIGNAL TO NOISE 173 Hz (dB)	TRANSMISSION LOSS 173 Hz (dB)	173 Hz	RANGE (NM)	BEARING °T	A SOURCE (NM)	H SENSOR (NM)	D SENSOR (M)	MEAN DEPTH OF ARRAY (M)	T	NUMBER OF AVERAGES	COMMENTS
09 31	23°33.7	85°58.7	20°56.7	86°09.1	63.6	7	95.7	2.7	70.8	5	108.6	3.4	127.48	50.0	8.98	0.20	36	400	12	8'84"	
09 39	23°33.5	85°58.9	20°56.5	86°08.3	62.9	5	95.4	2.5	71.4	2	112.0	2.9	128.88	50.0	8.98	0.20	36	411	12	8'84"	
11 00	23°34.5	85°57.7	20°58.6	86°07.8	63.5	7	95.8	3.3	73.6	2	109.8	3.2	129.68	50.2	8.98	0.22	35	142	12	8'84"	
11 29	23°34.8	85°57.9	20°57.3	86°08.8	63.9	7	95.8	3.5	69.6	1	113.8	3.2	130.90	50.3	8.98	0.22	38	409	12	8'84"	
11 58	23°35.0	85°58.9	20°58.2	86°09.3	64.0	8			72.4	0			132.07						*2	8'84"	
11 58	23°35.5	85°58.7	20°58.7	86°09.0	62.7	5			71.5	0			132.56						12	8'84"	
12 16	23°35.0	85°58.5	20°58.0	86°08.0	62.1	6			73.3	0			134.09						12	8'84"	
12 30	23°35.0	85°58.6	20°59.1	86°08.6	62.6	6			72.1	0			134.47						12	8'84"	
12 35	23°35.2	85°58.8	20°58.7	86°08.6	63.3	6			70.6	0			135.02						12	8'84"	
12 45	23°35.4	85°58.8	20°58.1	86°08.9	61.9	8			72.8	0			136.26						12	8'84"	
12 58	23°35.0	85°58.1	20°58.0	86°08.3	61.4	0			72.5	0			136.91						12	8'84"	
13 08																					
13 25																					
13 38																					
13 58																					
13 58																					
14 11																					
14 28																					

LEG E-F SOURCE LEVEL 67 Hz 178.3 dB// 1 μPa
173 Hz 182.4 dB// 1 μPa
RECEIVER DEPTH 362 - 427 M
SOURCE DEPTH 100 M
ARRAY ANGLE (VERTICAL) +5.3 TO -7.8
HORIZONTAL DISTANCE BETWEEN DEPTH SENSORS = 335.5 METERS

* SIGNAL LEVEL IN dB// 1 μPa

CONFIDENTIAL

Table 4-3. (C) Transmission Loss and Related Parameters for Leg E-G (U)

MEAN TIME	MEAN RECEIVER LOCATION		MEAN SOURCE LOCATION		* SIGNAL LEVEL 67 Hz	SIGNAL TO NOISE 67 Hz (dB)	TRANSMISSION LOSS 67 Hz (dB)	Δ 67 Hz	* SIGNAL LEVEL 173 Hz	SIGNAL TO NOISE 173 Hz (dB)	TRANSMISSION LOSS 173 Hz (dB)	Δ 173 Hz	RANGE (NM)	BEARING °T	ΔR SOURCE (NM)	ΔH SENSOR (M)	ΔD SENSOR (M)	MEAN DEPTH OF ARRAY (M)	ΔT	NUMBER OF AVERAGES	COMMENTS
	LAT N	LONG W	LAT N	LONG W																	
192 00:23	24°01.4'	85°50.6'	23°22.5'	86°21.9'	89.6	9		3.5	91.8	18	91.6	3.5	48.32	216.49°	1.65	0.43	33	665	16'51"	25	
00:46	24°01.2'	85°50.0'	23°22.8'	86°24.1'	87.3	8	92.2	3.0	90.6	20	92.8	3.2	50.12	218.65°	2.20	0.61	31	666	23'56"	25	
01:46	24°00.5'	85°48.4'	23°28.0'	86°28.5'	89.5	7	90.0	3.1	89.4	18	94.1	3.5	54.67	222.34°	1.17	0.35	51	745	16'51"	25	
02:15	24°00.15'	85°48.1'	23°18.5'	86°30.7'	90.7	3	88.8	4.9	85.5	14	97.9	3.7	57.07	223.28°	1.81	0.20	73	769	16'51"	25	
02:36	23°59.9'	85°48.0'	23°17.0'	86°32.6'	87.4	4	92.1	3.4	82.7	12	100.8	3.7	59.24	223.75°	0.71	0.07	78	776	6'35"	10	
05:30	23°56.2'	85°45.6'	23°06.1'	86°43.4'	91.4	11	88.1	2.8	85.7	12	97.7	3.7	72.93	226.80°	1.12	0.25	59	751	16'51"	25	
06:44	23°56.1'	85°45.5'	23°05.4'	86°43.9'	91.6	12	87.9	2.8	82.9	12	100.6	3.4	73.74	226.76°	0.50	0.11	59	751	8'16"	12	
07:38	23°55.3'	85°44.9'	23°02.6'	86°47.9'	87.5	9	92.0	3.3	78.9	11	104.5	3.1	78.20	227.84°	0.81	0.13	63	755	8'16"	12	
07:56	23°55.1'	85°44.7'	23°01.7'	86°49.5'	92.3	11	87.2	2.7	80.7	12	102.7	3.0	79.90	228.28°	0.81	0.13	68	761	8'16"	12	
08:16	23°54.9'	85°44.6	23°00.8'	86°51.3'	89.4	7	90.1	2.7	77.1	11	105.3	3.2	81.67	228.74°	0.78	0.09	72	767	8'16"	12	
08:34	23°54.7'	85°44.5'	22°59.9'	86°52.9'	87.1	7	92.4	2.8	78.7	10	104.7	3.3	83.31	229.10°	0.78	0.09	78	774	8'16"	12	
08:48	23°54.6'	85°44.4'	22°59.2'	86°54.2'	86.7	6	92.8	3.0	76.6	10	106.8	2.9	84.67	229.37°	0.78	0.14	78	759	8'16"	12	
09:07	23°54.2'	85°44.2'	22°58.2'	86°55.7'	87.8	0	-	3.4	81.1	5	103.3	3.6	86.25	229.75°	0.82	0.20	75	744	8'30	12	67 Hr Widening Ship's Noise
09:25	23°53.9'	85°44.0'	22°56.9'	86°56.9'	87.5	5	-	3.1	71.6	6	112.8	3.3	87.88	229.81°	0.82	0.14	57	738	8'30	12	
09:43	23°53.6'	85°43.8'	22°55.5'	86°58.1'	86.0	3	-	3.1	73.15	8	111.25	3.3	89.58	229.81°	0.82	0.14	51	737	8'30"	12	
09:57	23°53.4'	85°43.7'	22°54.5'	86°59.1'	86.2	0	-	2.8	74.4	7	110.0	2.8	90.87	229.85°	0.82	0.16	50	735	8'30	12	
10:15	23°53.1'	85°43.4'	22°52.9'	87°00.0'	86.5	3	-	3.1	74.0	10	110.4	2.5	92.56	229.68°	0.89	0.16	50	737	8'30	12	
10:33	23°52.9'	85°43.2'	22°51.2'	87°00.9'	-	-	-	-	67.6	0	-	3.8	94.31	229.40°	0.89	0.15	-	-	8'30	12	
10:52	23°52.7'	85°42.9'	22°49.4'	87°01.9'	-	-	-	-	64	0	-	3.3	96.27	229.15°	0.89	0.14	-	-	8'09"		

LEG E G

SOURCE LEVEL: 67 Hz 179.3 dB// 1 μPa
173 Hz 183.4 dB// 1 μPa

RECEIVER DEPTH: 648 – 813 M
SOURCE DEPTH 100 M

ARRAY ANGLE: −5.3 TO −13.4°
ARRAY LENGTH: 335.5 METERS

HORIZONTAL DISTANCE BETWEEN DEPTH SENSORS = 335.5 METERS

* SIGNAL LEVEL IN dB// 1 μ Pa

CONFIDENTIAL

CONFIDENTIAL

Table 4-4. (C) Transmission Loss and Related Parameters for Leg G-E (U)

PAGE 1 of 1

MEAN TIME	MEAN RECEIVER LOCATION		MEAN SOURCE LOCATION		* SIGNAL LEVEL 67 Hz	SIGNAL TO NOISE 67 Hz (dB)	TRANSMISSION LOSS 67 Hz (dB)	σ 67 Hz	* SIGNAL LEVEL 173 Hz	SIGNAL TO NOISE 173 Hz (dB)	TRANSMISSION LOSS 173 Hz (dB)	σ 173 Hz	RANGE (NM)	BEARING °T	Δ R SOURCE (NM)	Δ H SENSOR (NM)	Δ D SENSOR (M)	MEAN DEPTH OF ARRAY (M)	Δ T	NUMBER OF AVERAGES	COMMENTS
	LAT. N	LONG. W	LAT. N	LONG W																	
193 1414	23°29.9'	85°54.7'	23°05.7'	86°48.5'	85.2	10	94.1	4.7	76.9	10	106.5	5.1	55.02	244.1°	1.51	0.46	31	388.5	16'52"	24	
1432	23°29.8'	85°54.4'	23°07.1'	86°47.6'	88.4	11	90.9	3.9	80.5	15	102.9	4.3	53.79	245.5°	1.51	0.35	36	386	16'52"	24	
1449	23°29.3'	85°54.2'	23°08.4'	86°46.8'	88.5	11	90.8	3.7	80.5	14	102.9	3.8	52.63	246.8°	1.51	0.35	34	385	16'52"	24	
1508	23°28.9'	85°53.9'	23°09.3'	86°45.7'	88.5	10	90.8	4.4	84.5	15	98.9	3.5	51.45	247.8°	0.98	0.36	39	387.5	17'02"	24	
1525	23°28.6'	85°53.7'	23°09.6'	86°44.7'	90.1	15	89.2	4.1	84.6	19	98.8	3.8	50.54	248.1°	0.97	0.46	34	390	16'52"	24	
1623	23°27.3'	85°52.5'	23°12.5'	86°39.9'	87.6	10	91.7	4.0	87.9	19	95.5	4.1	45.97	251.4°	–	–	31	392.5	–	23	
1643	23°26.8'	85°52.1'	23°12.6'	86°38.5'	85.2	5	94.1	4.2	86.9	11	96.5	6.2	44.91	251.7°	0.90	0.31	33	390.5	16'56"	24	
1659	23°25.5'	85°51.9'	23°12.3'	86°37.7'	88.3	8	91.0	3.9	87.3	14	96.1	4.7	44.39	251.5°	0.89	0.31	35	393.5	16'53"	24	
1821	23°27.8'	85°53.8'	23°13.9'	86°31.1'	91.4	12	87.9		91.6	20	91.8	3.4	37.64	248.5°	0.46	0.46	30	375	8'33"	12	
1903	23°29.2'	85°54.8'	23°15.1'	86°28.8'	96.1	17	83.2	3.0	94.5	25	88.9	2.8	34.92	246.3°	1.14	0.40	28	384	18'37"	12	
1926	23°30.8'	85°54.4'	23°16.4'	86°26.5'	96.9	17	82.4	2.6	95.7	22	87.7	2.8	32.45	245.3°	1.14	0.40	28	383	18'36"	12	
1949	23°30.8'	85°54.9'	23°17.7'	86°24.3'	87.9	9	91.4	3.1	90.2	20	93.2	3.3	29.99	244.2°	1.09	0.43	30	379	18'36"	12	
2026	23°32.8'	85°55.7'	23°19.5'	86°21.1'	85.06	5	94.2	3.3	81.85	10	101.55	3.2	26.26	242.7°	1.05	0.39	29	378.5	18'36"	12	
2048	23°32.5'	85°56.1'	23°21.3'	86°19.3'	89.16	8	90.1	3.2	88.1	15	95.3	3.5	24.05	242.3°	1.05	0.30	28	374	18'36"	12	
2111	23°33.1'	85°56.7'	23°22.8'	86°17.5'	97.16	20	82.1	2.9	94.4	19	89.0	3.5	21.68	241.7°	1.03	0.56	31	378.5	18'36"	12	
2128	23°34.1'	85°57.5'	23°24.7'	86°15.3'	94.3	15	85.8	3.9	97.1	22	86.3	4.2	18.84	240.13°	1.03	0.38	29	380.5	18'36"	12	

LEG G-E SOURCE LEVEL: 179.3 dB//1 μPa
183.4 dB//1 μPa

RECEIVER DEPTH: 356 – 411 M
SOURCE DEPTH 180 M

ARRAY ANGLE (VERTICAL) +4.4 TO -6.7

HORIZONTAL DISTANCE BETWEEN DEPTH SENSORS = 235.5 METERS

* SIGNAL LEVEL IN dB//1 μ Pa

CONFIDENTIAL

Signal to Noise Ratio: Determined by the difference between the averaged signal band level and a noise level defined by the average of three spatially and temporally averaged noise band levels at each side of the signal band, starting four processing bands away from the signal band.

Standard Deviation (σ): The value of standard deviation for the spatially and temporally averaged signal levels.

Transmission Loss: Determined by the subtraction of the received signal level from the calibrated signal level of the source frequency.

Range: Calculated great circle distance between the Mean Receiver and Mean Source locations in nautical miles.

Bearing: Calculated true bearing from the Mean Receiver location to the Mean Source location.

ΔR Source: The distance traveled by the source in the direction of the tow during the duration of the averaging time for the determination of received signal level. Rectified navigational parameters provided by NORDA Code 340 were used in the determination of this value.

ΔH Sensor: The distance traveled by the receiver in the direction of the tow during the duration of the averaging time for the determination of received signal level. Rectified navigational parameters provided by NORDA Code 340 were used in the determination of this value. This value is given in nautical miles.

Mean Depth of Array: The depth of the center of the array at the Mean Time in meters. This value was determined by averaging of the depths indicated by the depth sensors located of the front and at the end of the HF array. This value is given in meters.

ΔD Sensor: The difference in depth between the depth sensors at the front and at the end of the HF array. This value is given in meters.

ΔT: The elapsed time over which the number of data ensembles were averaged to establish the value of Received Signal Level.

Number of Averages: The number of data ensembles averaged to obtain the value of Received Signal Level.

(U) TL values are given for the two towed source frequencies, 67 Hz and 173 Hz, for ranges from 48 nm to 136.9 nm depending upon which leg is selected.

(U) The measured transmission loss (TL) for each of three legs E-G, G-E and E-F is plotted as a function of range for the two frequencies, 67 Hz and 173 Hz, in Figures 4-6 to 4-8. Measured bathymetry for each leg is also shown on the figures. The depth values are based upon PDR (Precision Depth Recorder) readings corrected for local sound velocity and were provided by NORDA Code 340. Each point on the plots of TL versus range is a space and time averaged value as indicated on the figure and discussed previously. Lines connecting these points are meant only to identify the data and have no other purpose.

(U) No plot is presented for the legs F-E since there are only eight data points at source depth of 100 m and receiver depth of 800 m.

(U) Depth-range relationships derived by using Site E as reference point and presented in Figure 3-4 were corrected for variations introduced by the fact that the receiver did not always remain in the close proximity of Site E.

The correction was defined by

$$r = D\cos(\theta)$$

where r = range correction

θ = Bearing of the location from E - Bearing of the track used for the measurement of the depth profile.

D = Distance between the receiver and E at the time of the measurement of TL.

(U) Corrections for legs G-E and E-F where negligible (at or less than 1 nm) and therefore no corrections were applied. An average 22 nm were added to the ranges for leg E-G due to the fact that the receiver was between 21.5 and 23 miles east from Site E on the track of the towship (nominal 232°T).

(U) The location of each leg was shown earlier in Figure 3-3. The bathymetry along the entire path F-G was shown in Figure 3-4 along with representative sound velocity profiles constructed by NORDA Code 340 from XBT records obtained on the DESTEIGEUR along the source tow track. Sound propagation has been discussed in general in Section 3.2.4.

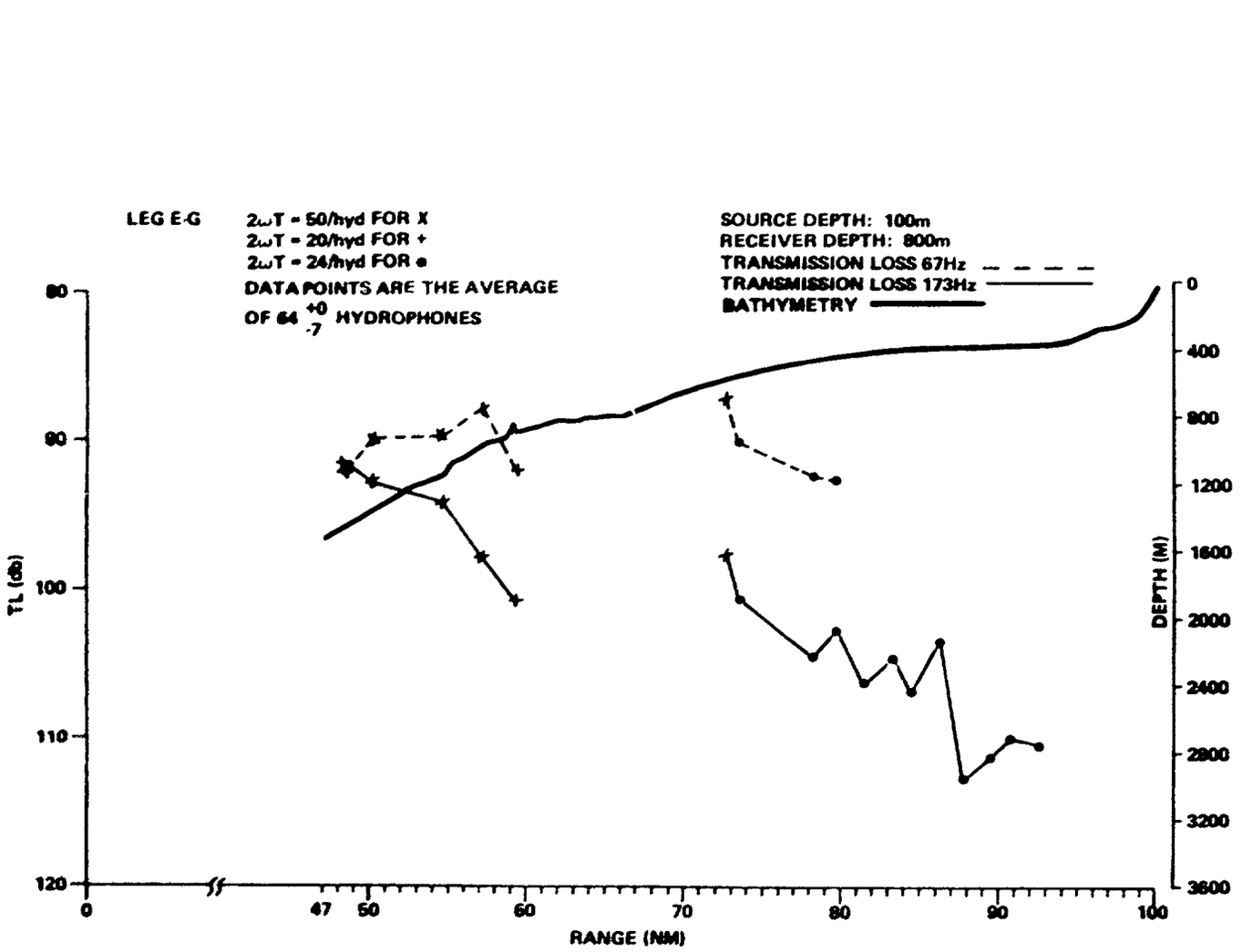

Figure 4-6. (U) Measured Transmission Loss as Function of Range and Bathymetry for Leg E-G (U)

UNCLASSIFIED

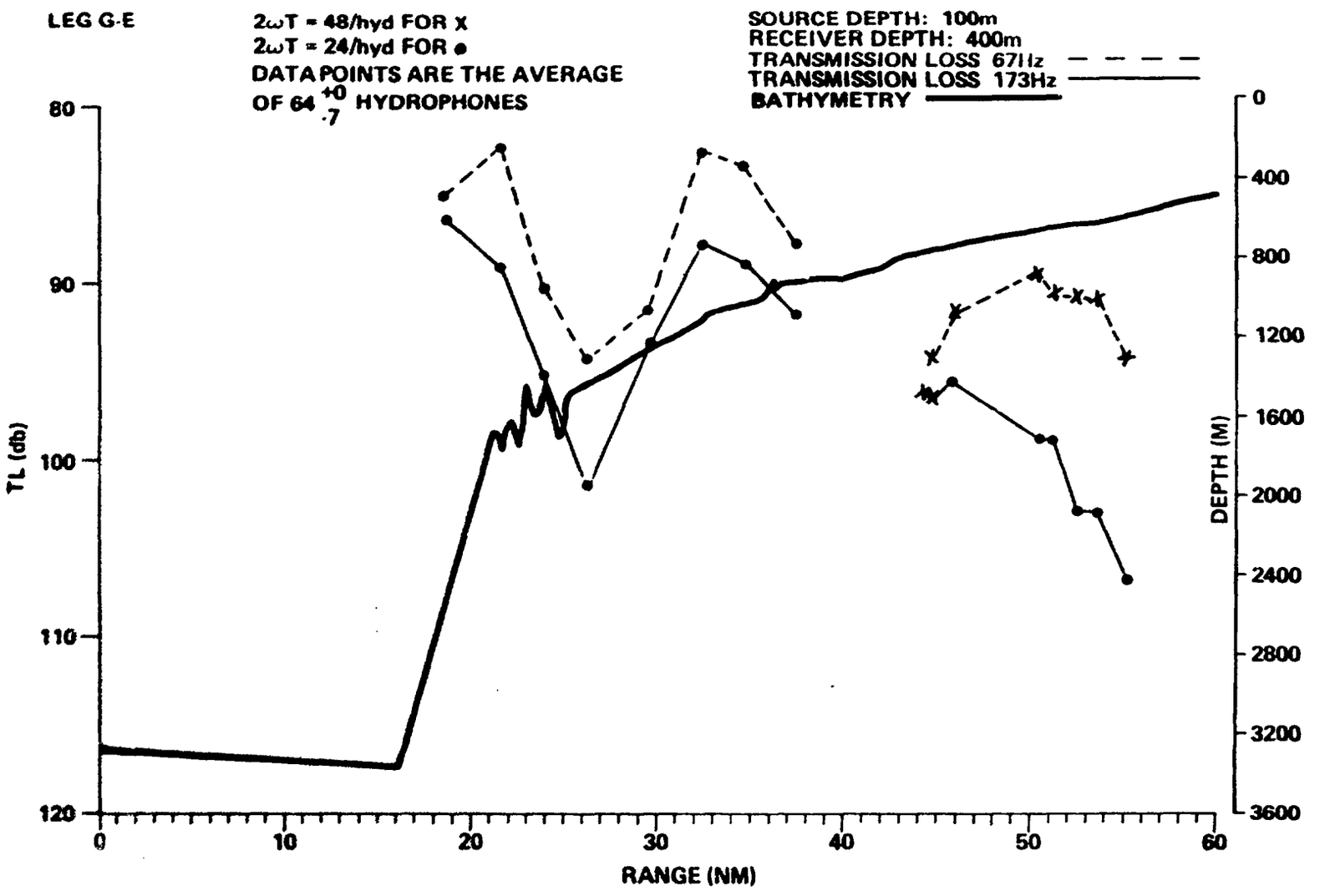

UNCLASSIFIED

Figure 4-7. (U) Measured Transmission Loss as Function of Range and Bathymetry for Leg G-E (U)

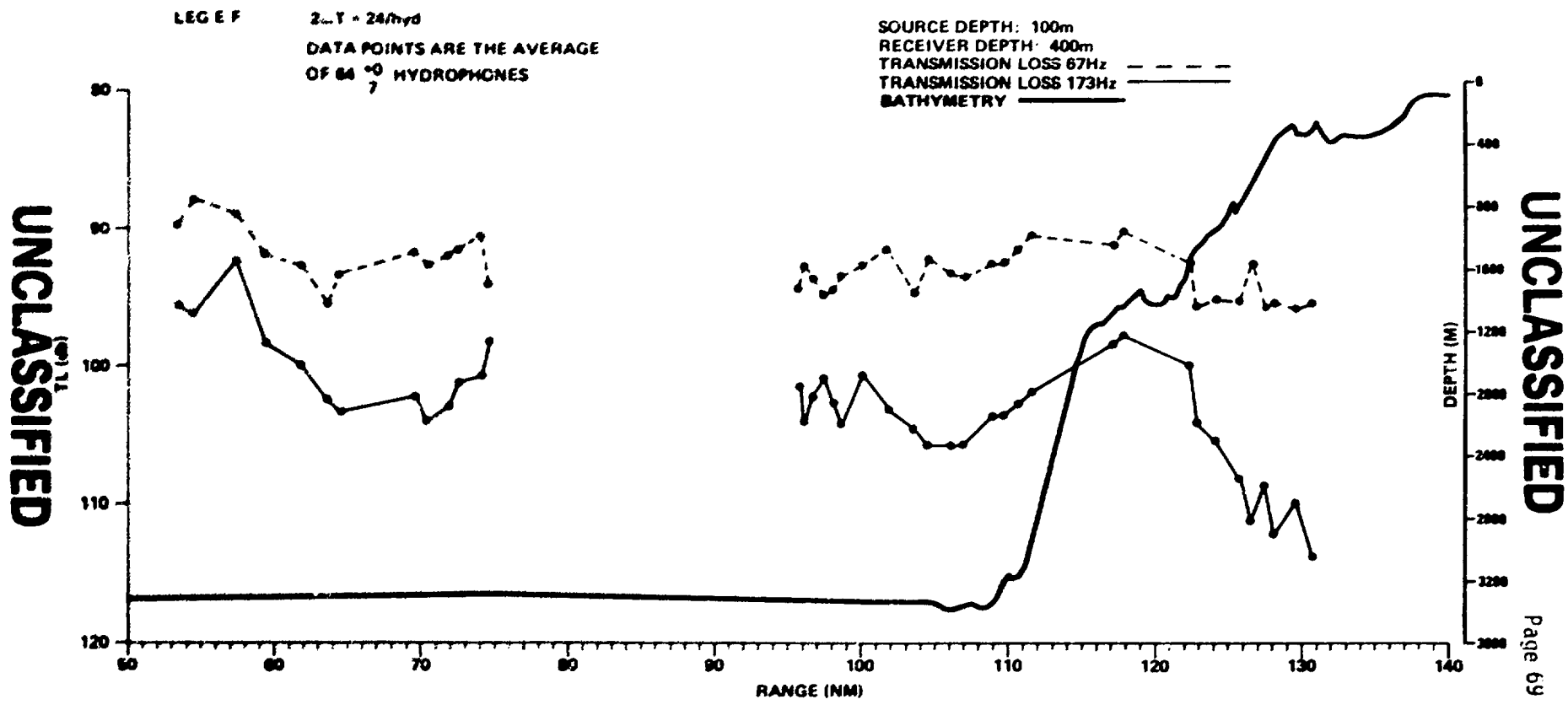

Figure 4-3. (U) Measured Transmission Loss as Function of Range and Bathymetry for Leg E-F (U)

4.1.3 Transmission Loss Characteristics (U)

(U) The measured transmission loss (TL) as a function of range along the track covered during CHURCH STROKE III, CRUISE 1, is influenced by several effects including:

1. Refraction of sound in water and sub bottom,
2. Bottom loss upon bottom reflection,
3. Changing bathymetry along the track,
4. Absorption by water,
5. Presence of ocean currents.

(U) Of these effects the influence of the first three may be seen in the TL measurements although accounting for each effect by itself in detail is not possible. Since absorption of sound has been measured and reported previously (Ref. 16), data may be corrected for this effect. The exact influence of the loop current on transmission loss is difficult to isolate from the bathymetric effect since the two effects appear in the same range interval. (See the discussion on the data of leg G-E and E-G).

(U) Little meaning can be given to the data without reference to the general propagation characteristics. Thus, as a preparation to the discussion of the TL data, a short summary of the theoretical basis for data treatment is given.

(U) The refraction of sound due to the variable sound velocity with depth combined with the shallow bottom depth produces a bottom-limited sound propagation condition. This condition, coupled with a bottom loss that increases with grazing angle, will cause the transmission at long ranges to be confined to an initial angle sector near the upgoing limiting ray. This ray grazes the surface and strikes the bottom at the longest range of any ray produced by the source. The downgoing ray strikes the bottom at the critical angle of bottom interaction. Steeper rays than those at the critical angle are highly attenuated and suffer more bottom bounces to a given range due to their foreshortened cycle distance. This is somewhat the case for rays which have elevation angles that exceed the limiting ray since they strike the bottom at a shorter distance and steeper angle than the limiting ray. The

sum effect is to concentrate the sound energy "near" the limiting ray especially at the higher frequency. It would be expected then that local minima in the transmission loss would occur at ranges where the limiting ray reaches the receiver depth and that the distance between such minima (actually pairs of minima since the up-coming and down-going rays will be met at slightly different ranges when the receiver depth is not zero) should match closely the cycle distance of the limiting ray. To carry the argument further would require a detailed knowledge of the number of rays that reach a given depth and range. Ray tracing and transmission loss models were used during the analysis to accomplish this purpose and to produce detailed comparisions with an interpretation of the data. At ranges of the TL minima, the TL values are determined by the expression

$$TL = 20 \log R_0 + 10 \log (R/R_0') + \alpha R + \bar{N}B \qquad (4\text{-}1)$$

where R_0 is the range at which the transition from spherical spreading to cylindrical spreading occurs. R_0 is in meters and R_0' is expressed in the measurement units of R. $\bar{N}$ is the mean number of bounces taken by the rays between the limiting ray and critical ray and B is a mean loss per bounce. The last term is an approximation to the actual contribution of the rays after bottom reflection. The constant, α, is the absorption coefficient in dB/unit range (dB/nm).

(U) It is necessary to estimate the bottom loss in the experimental data so that the residual effects such as proximity to a sloping bottom may be treated. The term "slope effect" is used to express the difference between measured and estimated transmission loss when the source is over the sloping bottom. Each leg is treated from this viewpoint in the next three sections. The TL versus range data is fitted to a form similar to Eq. 4-1 and the bottom loss and residual effects are then estimated from the data.

(U) Of the four acoustic data legs that were run during CHURCH STROKE III, CRUISE 1 exercise, three resulted in data over a range interval that was long enough to warrant closer analysis. In this section the data is examined in

order to separate the several factors that contribute to sound transmission loss: spreading, bottom loss, absorption, and bathymetric effects. The data is considered and discussed separately by leg.

4.1.3.1 Leg E-F

(U) The received signal data on leg E-F covers the largest range interval of the four legs that were run, (53 nm - 131 nm). It is also the only leg where the source was in uniformly deep water (3400 m) for a significant part of the run (53 nm - 108 nm). Thus this leg offers the best opportunity to observe the characteristics of bottom-limited sound propagation without the complications of a changing bathymetry, at least until the longer range portions of the leg are reached.

(U) The location of measurement leg E-F is shown in Figure 3-3. The bathymetry along leg is sketched in Figure 3-4 with representative sound velocity profiles constructed by NORDA Code 340 (Ref.13) from the XBT records obtained on the DESTEIGEUR along the towed source track. Sound propagation has been discussed in general in Section 3.2.4 and these data are shown in Figure 4-8.

(U) The general character of the data may be described as follows:

(1) At ranges between 50 and 102 nm TL values tend to increase with range. However, peaks of minimum TL occur for the 67 Hz data at 55 nm, and for the 173 Hz data at 57 nm. A sharp rise for 173 Hz at 73 nm and with a less well defined peak in the region near 100 nm is also observed.

(2) At ranges between 102 nm and 108 nm the 67 Hz TL data shows no strong trend but the 173 Hz TL values increase with range.

(3) At ranges between 108 nm and 118 nm, the TL values decrease with range. The 173 Hz data shows a higher rate of decrease with range than the 67 Hz data. The TL values at both frequencies display minimum values at 118 nm range.

(4) At ranges greater than 118 nm, the TL values increase with range with the higher frequency data increasing at a higher rate than the lower frequency data.

(U) By comparing the TL values with the bathymetry, it is clear that the strong reversal in the TL versus range trend occurs in the vicinity of the sloping bottom and is associated with this bathymetric feature. This effect is discussed further in this section.

(U) To obtain an empirical relationship for transmission loss for leg E-F as a function of its parameters, we assume the form given in Equation 4-2. (Refer to Equation 4-1 for definitions).

$$TL = 20 \log R_0 - 10 \log R_0' + 10 \log R + B\,\bar{N}(R) + \alpha R. \qquad (4\text{-}2)$$

For example, if the transition range between spherical and cylindrical spreading, R_0, is taken as 10,000 meters and the horizontal range, R, expressed in nm units, Eq 4-2 becomes, with $\bar{N} = 0$,

$$TL = 80\ dB - 7.3\ dB + 10 \log R + B\bar{N}$$
$$TL = A + 10 \log R + \bar{N}B + \alpha R, \qquad (4\text{-}3)$$
$$A = 72.7\ dB\ .$$

Equation 4-3 assumes a flat uniform bottom and an acoustic energy distribution that, at sufficient range, becomes uniform over the extent of the water depth. At the two source frequencies, the value of α taken from Figure 3-9 is

f(Hz)	α(dB/Yard)	α(dB/nm)
67	$\cdot 10^{-6}$	$<2 \times 10^{-3}$
173	3×10^{-6}	6×10^{-3}

Absorption is negligible at 67 Hz and of marginal importance at 173 Hz when compared to our constant of A=72.7dB. Absorption will not be considered further in the TL estimates presented in this section. The acoustic energy which propagates near the limiting ray will also follow a cylindrical spreading law. The physical reason for this is that minima in the TL versus range curve are caused by focusing of rays near the limiting ray. The locus of these minima are on a ring of radius r from the source. Losses due to dispersion and absorption when secondary thus imply that successive minima will follow a cylindrical spreading law. Thus a cylindrical spreading law was used to estimate the bottom loss per bounce B from our measured data. We assume that the energy from minima to minima is described by

$$TL = (A_0 - \bar{N}(R_1) \cdot B) + 10 \log (R) + \bar{N}(R) \cdot B \quad (4\text{-}4)$$

where

A_0 = TL (Measured) - 10 log (R_1)

R_1 = Range to first minima.

R = Range

$\bar{N}(R)$ = Average number of bounces for ray bundle between critical and limiting ray

B = Bottom loss per bounce.

The value A_0 is determined for the first experimentaly observed minima and corresponds to the case where the bottom loss per bounce is zero. Once A_0 is determined we parametrically vary the bottom loss per bounce (B = 0, 0.5, 1.0, 1.5...) until we observe a good fit to the data prior to the initiation of the slope. Once an estimate of the value of B was obtained for each frequency, the extrapolated TL curve in the vicinity of the slope was used as a basis for the determination of the "slope effect". The "slope effect" is defined as the deviation of the measured TL data from the best fit curves. Caution must be taken in this regard since the TL values have several local minima. A minimum value of TL is shown as a maximum in the TL versus range data due to the unusual method of plotting curves of TL versus range. These minima are formed "near" the cycle distance intervals of the limiting ray.

(U) Crucial to this estimating process is the determination of $\bar{N}$, the number of bounces at a given range, since the minimum number of bounces is clearly the value for the limiting ray. Figure 4-9 shows the ranges for the limiting ray based on a measured sound velocity profile listed in Table 4-5. This profile represents the conditions at the receiver; Site E. Although the SVP changed with range this change is ignored in the approximate methods used here. The limiting ray is launched at an elevation angle of 5.08° angle and strikes the bottom at a grazing angle of 9.23°. Figure 4-9 estimates the minimum number of bounces determined by the limiting ray at any range. In particular, the ranges at which the receiver intersects the limiting ray are in-

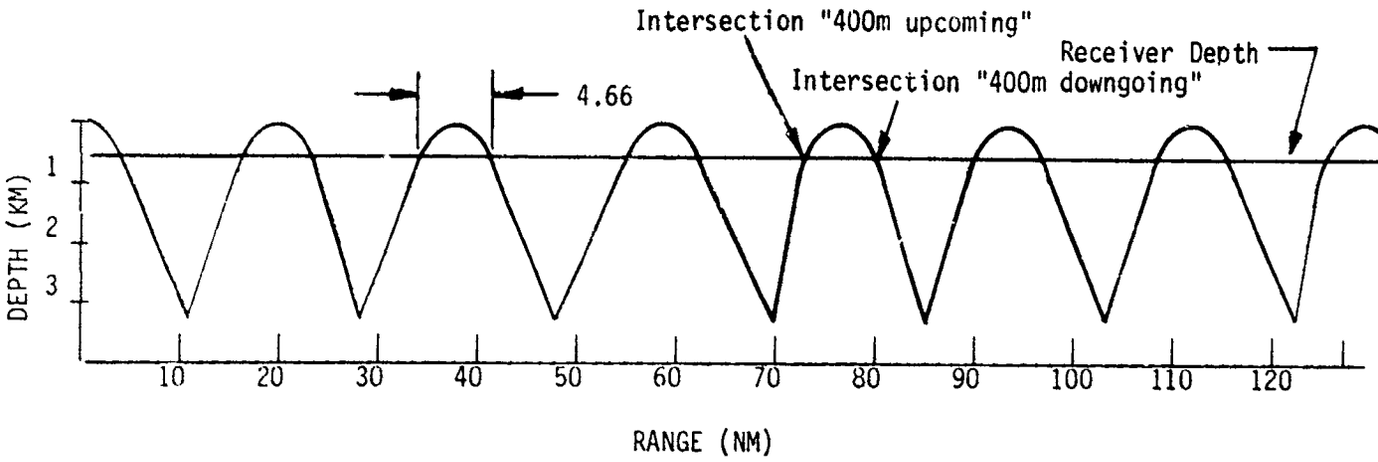

Bounce No.	Range (nm) Bottom Bounce	Range (nm) 400m depth upcoming	Range (nm) Zero depth --	Range (nm) 400m depth downgoing
N (min)				
0	--	--	1.18	3.51
1	10.58	17.64	19.97	22.31
2	29.37	36.43	38.76	41.09
3	48.16	55.22	57.55	59.88
4	69.95	74.00	76.34	78.67
5	85.74	92.80	95.13	97.46
6	104.53	111.99	113.92	116.25
7	123.32	130.4	132.71	135.04

Figure 4-9. (U) Ranges for Limiting Ray Propagation (U)

Table 4-5. (U) Sound Velocity Profile for Ray Tracing Analysis (U)

Z(m)	C(m/sec)
0	1544.12
50	1540.85
100	1538.04
150	1536.74
200	1529.04
250	1524.16
300	1521.57
350	1519.17
400	1515.43
500	1508.39
600	1501.43
700	1495.79
800	1491.72
900	1489.05
1000	1488.30
1230	1486.45
1400	1489.21
2000	1499.32
3000	1516.40
3400	1523.32

dicated as "400m depth, upcoming" and "400m depth, downgoing" in separate columns of the table on Figure 4-9. The zero depth column indicates the ranges at which successive cycles graze the sea surface.

(U) Ray tracing was used to determine $\overline{N}$. The number of bounces to a given range were counted for launch angles between the limiting ray and the critical ray. Table 4-6 shows the resulting values for $\overline{N}$ at 50, 75 and 100 nm. These values are used to compute transmission loss values. The summary of the computation for the 67 Hz data is shown in Table 4-7.

(U) Curves of TL versus range for the three bottom loss assumptions are shown overplotted on the 67 Hz data for leg E-F on Figure 4-10. The following is noted,

(1) at 73 m the data maximum lies between the 0.5 dB and 1.0 dB/bounce loss curves.
(2) between 96 and 108 m, several data points lie between the same two curves.
(3) at 96 m, local minima in the data lie above the 1.0 dB/bounce curve.
(4) at 102 m and 105 m, two minima agree with the 0.5 dB curve.

The conclusion from this analysis is that the bottom loss value is between 0.5 and 1.0dB/bounce which gives this area a "low-loss" bottom classification as described by Mitchell (Ref.4) and in Section 3.2.4, Figure 3-8.

With this empirical determination of bottom loss we may now characterize the slope effect at 67 Hz. If a 0.5dB/bounce loss is assumed the equation for TL versus range in the absence of the slope is

$$TL = 69.1 + 10 \log R + \overline{N}B.$$

At 108nm, the median range from receiver to the slope base, the TL value is 93dB.

Table 4-6. (U) BOTTOM BOUNCE ESTIMATES FROM RAY TRACING

	Range (nm)		
θ°	50	75	100
Limiting Ray 5.08°	3	4	5
+6 to +10	3	4	6
+12 to +16	4	7	9
-6 to -10	3	4	6
-12 to -16	4	7	9
$\overline{N}$	4	5	7

Table 4-7. (U) COMPUTATIONS OF TRANSMISSION LOSS AT 67 HZ BASED ON EQ. 4-4 (U)

Range (nm)	A	B	$\bar{N}$	$\bar{N}B$	10 log(R)	TL(dB)
55	70.6	0	3	0	17.3	87.9
	69.1	0.5	3	1.5	17.3	87.9
	67.6	1.0	3	3	17.3	87.9
75	70.6	0	5	0	18.7	89.3
	69.1	0.5	5	2.5	18.7	90.3
	67.6	1.0	5	5	18.7	93.3
100	70.6	0	7	0	20.0	90.6
	69.1	0.5	7	3.5	20.0	92.6
	67.6	1.0	7	7	20.0	94.6

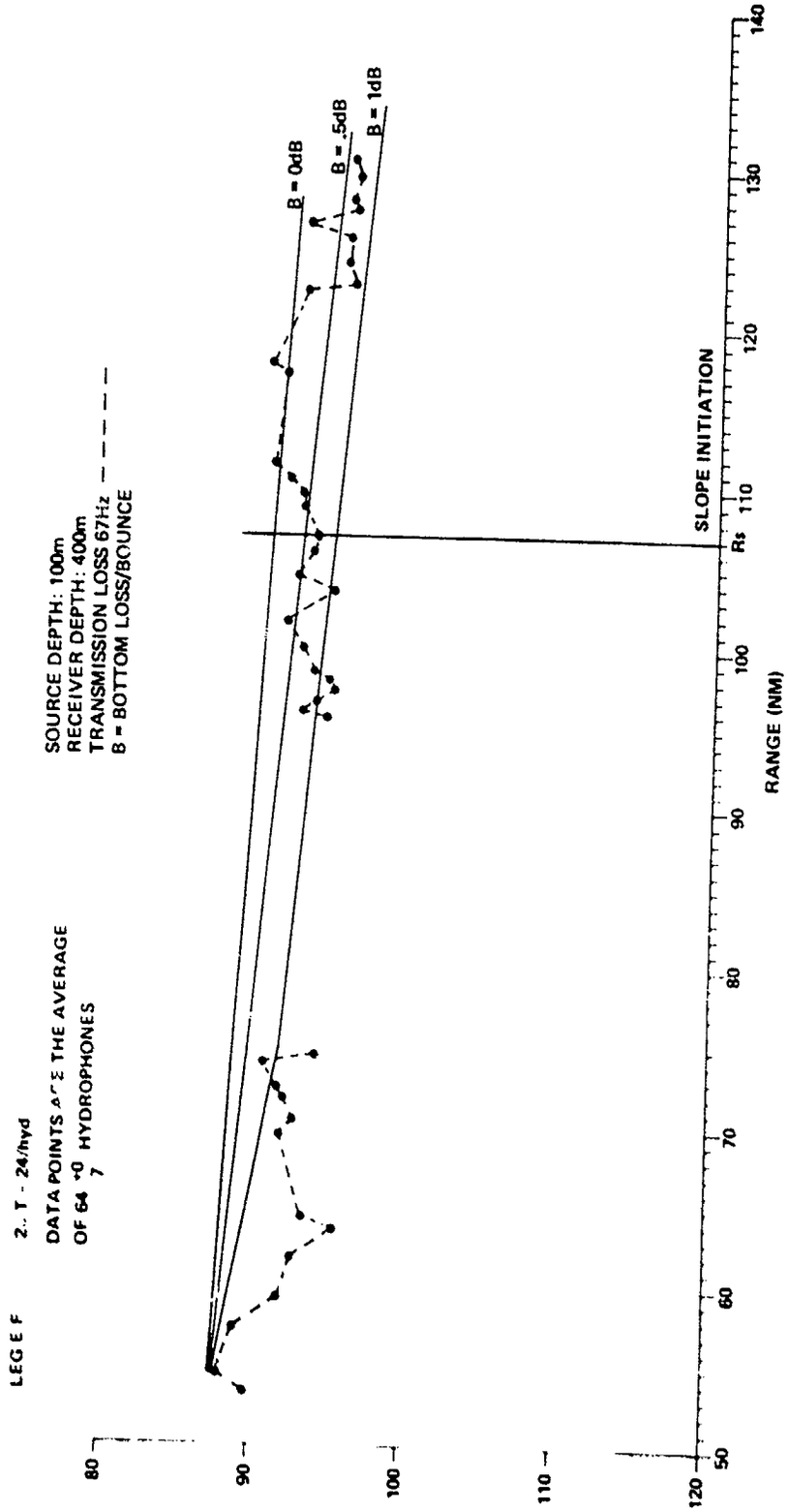

Figure 4-10. (U) Measured Transmission Loss and Bottom Loss Estimates Along Leg E-F for Towed Source at 67 Hz (U)

Between 108nm and 112nm we see an actual decrease in the transmission loss. The empirical fit in this region is

$$TL = 93 - 560[\log(R) - \log(R_s)], \quad 108 < R \leq 112 \text{ n.m}, \quad R_s = 108 \text{ n.m.}$$

Between ranges of 112 and 118nm the TL is almost constant, decreasing by less than 1dB. At ranges greater than the minima value at 118nm the TL increases from 90dB to 96dB at 131nm. The empirical fit in this region is

$$TL = 90 + 132 \log(R/R_m), \quad 118 < R \leq 131 \text{ nm}, \quad R_m = 118 \text{ nm.}$$

For the 173 Hz data a similar analysis was performed. The reference range was taken as 57nm; and the measured TL value is 92.0dB. Parameter values 0, 1, 2 and 3dB/bounce were used for B. The empirical transmission loss constant at 173 Hz is

$$A_o + NB = 74.5\text{dB}, \quad R = 57\text{nm.}$$

The values for N were mean number of bounces. The result is overplotted on the 173 Hz data for leg E-F on Figure 4-11. The following is noted:

(1) At ~ 75nm the measured data fall between the 2.0dB/bounce and 3.0dB/bounce curves. The minimum is near the 2.0 dB/bounce curve.

(2) Between 95nm and 104nm the measured data fall between the 1.5dB/bounce and the 3.0dB/bounce with the data minima centered on 1.5dB/bounce curve.

(3) The 1.5dB/bounce curve meets the rising measured data at 113nm.

(4) At 118nm the TL data rises ~ 8.0dB above the 2dB/bounce curve and 6dB above the 1.5dB/bounce curve.

To further detail the slope effect and to obtain an empiri l fit for the 173 Hz data as we did before with the 67 Hz data the following estimates were made:

$$TL = (69.9) + 10 \log(R) + N(B), \quad 50\text{nm} < R < 108\text{nm}, \quad B = 1.5\text{dB/bounce}$$

$$TL = 106 - 208.0 \log(R/R_s), \quad 108\text{nm} < R < 118\text{nm}, \quad R_s = 108\text{nm.}$$

$$TL = 100 + 452 \log(R/R_m), \quad 122\text{nm} < R < 131\text{nm}, \quad R_m = 122\text{nm.}$$

UNCLASSIFIED

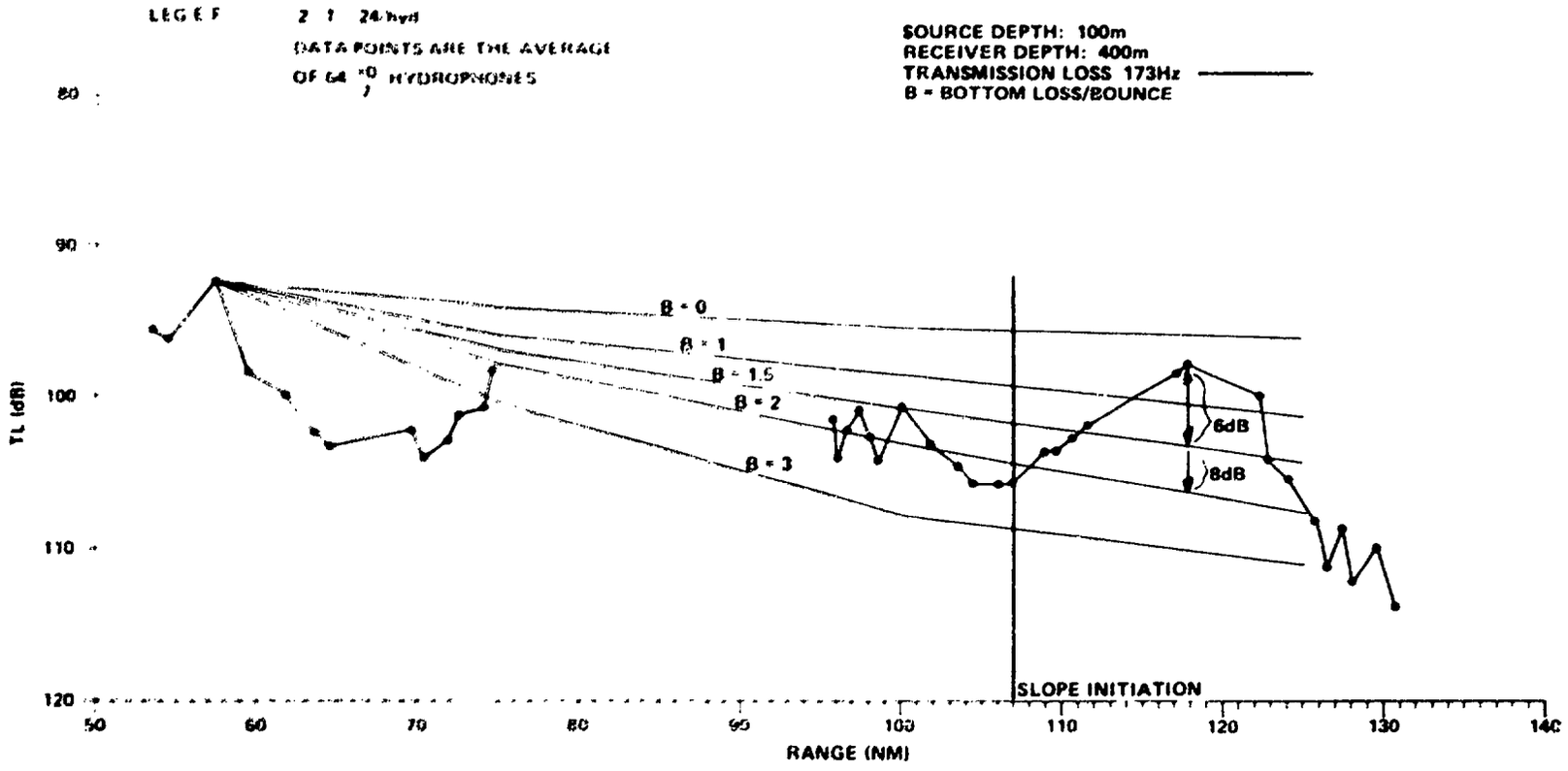

Figure 4-11. (U) Measured Transmission Loss and Bottom Loss Estimates Along Leg E-F for Towed Source at 173 Hz (U)

UNCLASSIFIED

CONFIDENTIAL

(This page is unclassified.)

4.1.3.2 Leg E-G

(U) The receiver depth for this leg is 800m. The data on this leg begins at ranges where the source is well over the slope as can be seen by reference to Figure 4-6. Thus no comparison with the source in deep water is possible unless a calibrated model calculation is available. The TL values are increasing with depth at the higher frequency and decreasing slightly at the lower frequency in the range interval 47-60nm. From 70nm to maximum range, 100nm, the TL values at both frequencies are decreasing with range. The empirical fit expressions for transmission loss are as follows:

At 67 Hz,

$TL = 92 - 54.6 \log (R/R_0)$; $47nm \leq R \leq 60nm$, $R_0 = 49nm$,

$TL = 87 + 150.9 \log (R/R_1)$, $73nm \leq R \leq 79nm$, $R_1 = 73nm$.

At 173 Hz,

$TL = 92 + 111.6 \log (R/R_0)$, $49nm \leq R \leq 60nm$, $R_0 = 59nm$

$TL = 98 + 119 \log (R/R_1)$, $73nm \leq R \leq 92nm$, $R_1 = 73nm$

4.1.3.3 Leg G-E

Leg G-E was the return leg from the leg E-G with an actual mean difference of receiver position of 2.2nm. The receiver depth was 400m. The outstanding feature of this run is the deep dip in the TL plot (Figure 4-4) at 26nm. This dip shows for both the 67 Hz and 173 Hz. This range coincides with two oceanographic features, that of the loop current and the area of special bottom roughness. The evidence for the loop current has been shown in Figure 4-4. The bottom roughness shows on the bathymetric curves of Figure 4-5. There is nothing in the present analysis to separate the loop current from bathymetric effects. The deep dip in TL may be due to either effect.

CONFIDENTIAL

4.2 RECEIVED SIGNAL CHARACTERISTICS

(U) The data obtained in these series of experiments using the LAMBDA III measurement system were performed by the preservation of amplitude and phase information from omnidirectional hydrophone groups and beams. These data were processed to yield the individual phone spectra, acoustic band level as a function of beam number, acoustic band level as a function of hydrophone position, beam band level spectra, crosspower spectra, magnitude squared coherence, and signal fluctuation statistics. This processing resulted in a rather complete but voluminous set of data on the performance of the LAMBDA III array.

(C) During the CHURCH STROKE III Cruise 1, exercise data was obtained from a moored source and a towed source. During one period of operation on July 13 (194:20:28:04) data was obtained from both sources under favorable operating conditions. During this period of time the LAMBDA III platform, the R/V INDIAN SEAL, was 53.9 nm from the towship at a relative bearing of 93.5° and 99.92 nm from the moored source with a relative bearing of 96°. The moored source was at a depth of 988 m in 3,416 m of water. The towed source was at a depth of 91 m and towed at a 1.76 kt speed. The LAMBDA III array was towed at a nominal 1 kt at a depth of 400 meters. The array was determined to have a tilt from fore to aft of +6.17°.

(C) Figures 4-12 to 4-14 show the beam response levels for the 67, 173 and 175 Hz sources. These beam band levels are the voltage level of each beam corrected for the omnidirectional hydrophone sensitivity. The beamformer was the TAP III frequency domain beamformer. The output of the processor is shown in the 'a' parts of these figures which show the band level for the source frequency bin and four selected noise bins. The source frequency bin was the bin with the maximum level. We observed that these maximum levels occur at 66.92 (Δf = -.08 Hz), 172.84 (Δf = -.16 Hz) and 174.84 (Δf=0Hz). The Δf value of -0Hz is what we would predict for the doppler shift between the moored source and the LAMBDA III source ship; but the

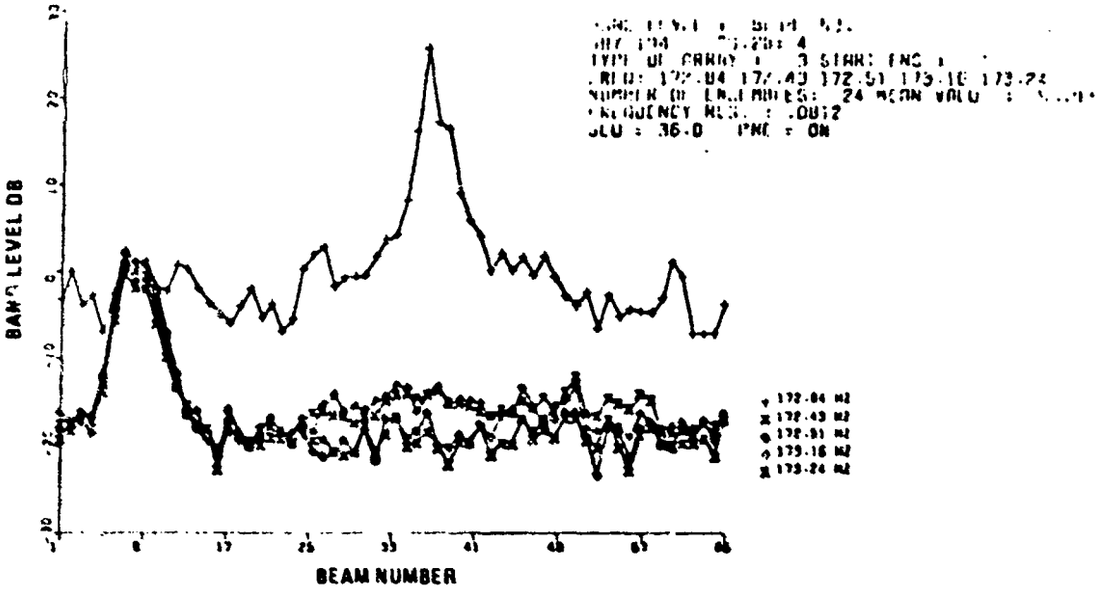

a) (C) Beam Band Level Versus Beam Number (U)

b) (C) Beam Band Level Versus Relative Bearing (U)

Figure 4-17. (C) Beam Band Levels of the 173 Hz Signal as a Function of Beam Number and Relative Bearing (U)

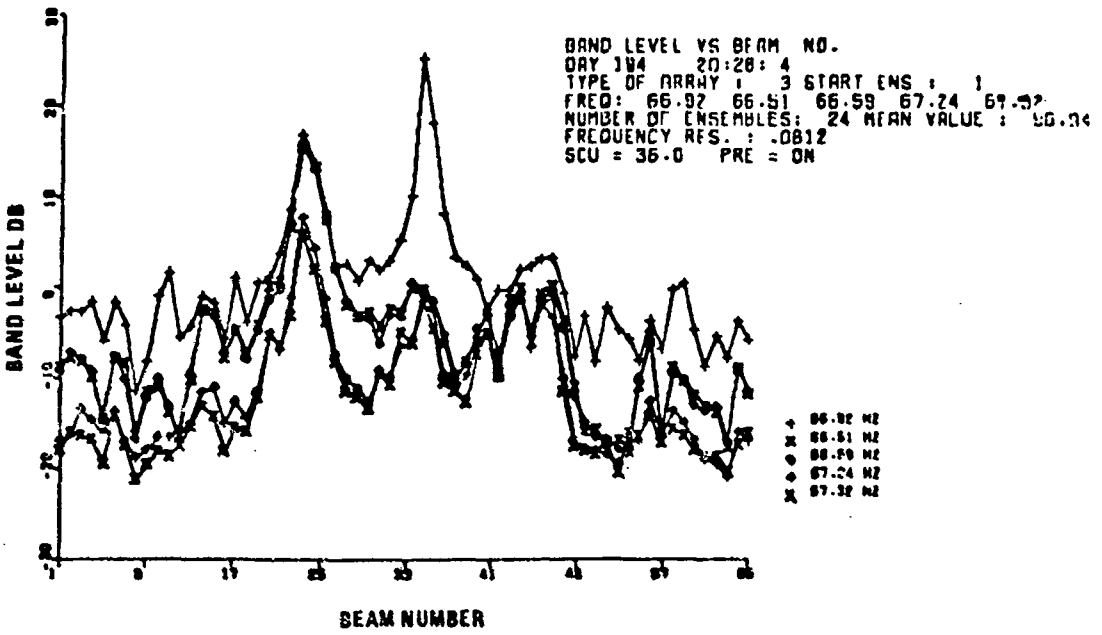

a) (C) Beam Band Level Versus Beam Number (U)

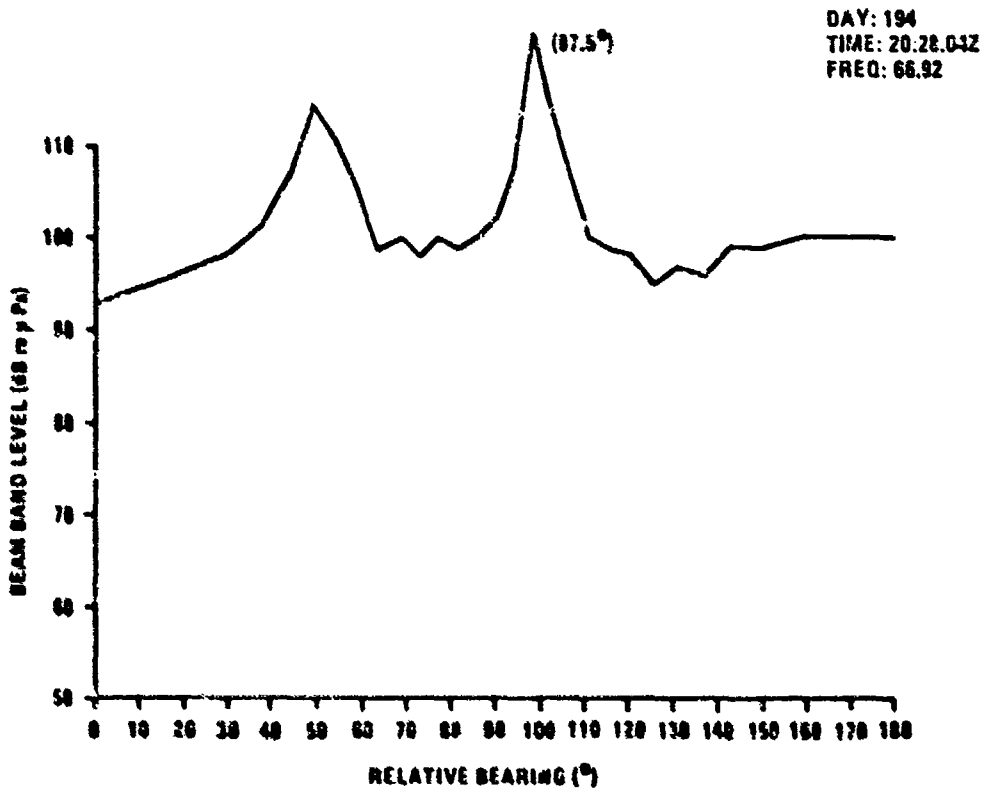

b) (C) Beam Band Level Versus Relative Bearing Angle (U)

Figure 4-13. (C) Beam Band Levels of the 67 Hz Signal as a Function of Beam Number and Relative Bearing (U)

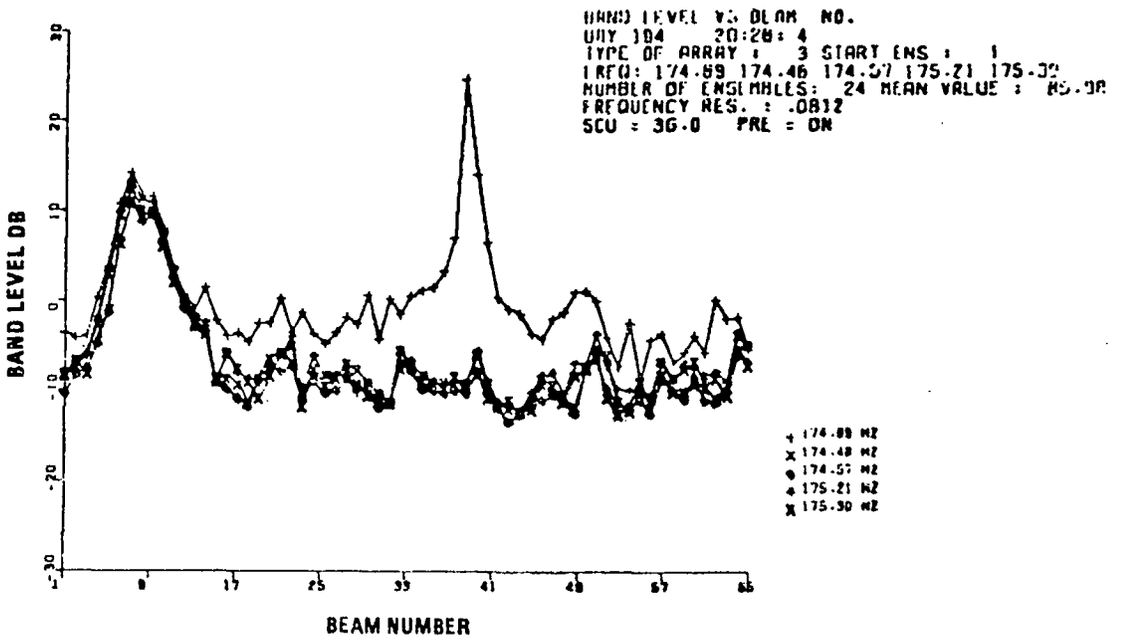

a) (C) Beam Band Level Versus Beam Number (U)

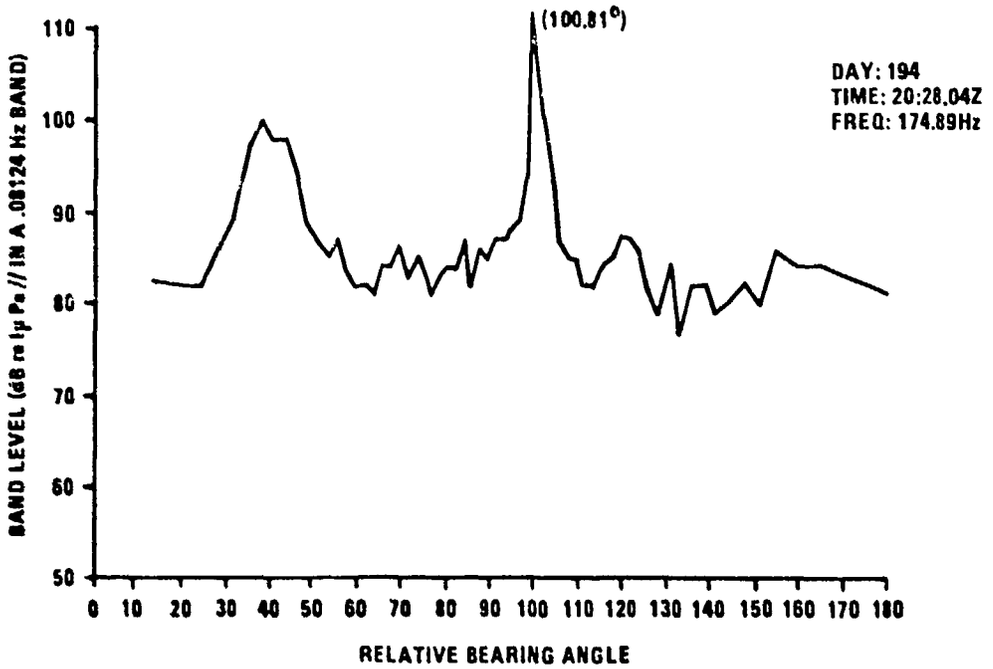

b) (C) Beam Band Level Versus Bearing Angle (U)

Figure 4-14. (C) Beam Band Levels of the 175 Hz Signal as a Function of Beam Number and Relative Bearing (U)

values for the towed source are less than one would expect for a relative receding velocity of 2.3 kts. These shifts in frequencies are consistent with a relative motion on the order of 1.34 to 1.73 kts. The output of the processor is band level versus beam number. As one would expect, the look direction for each beam member is a function of frequency for this FFT beamformer. The 'b' portion of figures 4-12, 4-13, 4-14 show the correct relative bearing angle for arrival of acoustic energy. The effect of the tow ship's radiated noise is clearly seen in the noise curves of Fig. 4-12a, 4-13a, 4-14a, 4-12b and 4-14b. The received signal level for the 172.84 Hz Signal (Fig. 4-13a and 4-13b) is such that the presence of the ship is not readily observed in the beam response pattern. In other words, beam #9 which looks in the relative direction of 39^0 sees not only the acoustic noise radiated from the tow ship but also the signal from the 173 Hz source on its side lobe in the direction of 97.18^0. This implies that the side lobe levels are less than -20 dB with a few as low as -30 dB and a mean side lobe level of approximately -25 dB. Examination of Fig. 4-14b shows the case for a lower signal energy. In this instance, the tow ship radiated noise is discernable as a separate signal at 100.81^0. Likewise we see that the tow ship response (-25dB) is not dominant in the beam which had signal. These response curves show that the LAMBDA III array clearly sees both the sources and the tow ship's radiated noise.

(U) The relative bearing to the sources determined from the beam angle of maximum response compare favorably with known positions. A bias error is observed as shown in the following table.

FREQ.	MEASURED RELATIVE BEARING	ARRAY HEADING	MEASURED TRUE BEARING	TRUE BEARING	ERROR
61.92	97.5^0	151.4^0	53.9^0	55.5^0	-1.6^0
172.84	97.18^0	151.4^0	54.2^0	55.5^0	-1.3^0
174.89	100.81^0	151.4^0	50.59^0	53^0	-2.4^0

These errors could be due to a variety of factors including the array tilt.

(C) The data for the 172.84 Hz data shown in Fig. 4-13b is replotted in Fig. 4-15. We have chosen this higher signal-to-noise ratio case to determine the best estimates of the array beam pattern. The beam levels shown in Fig.

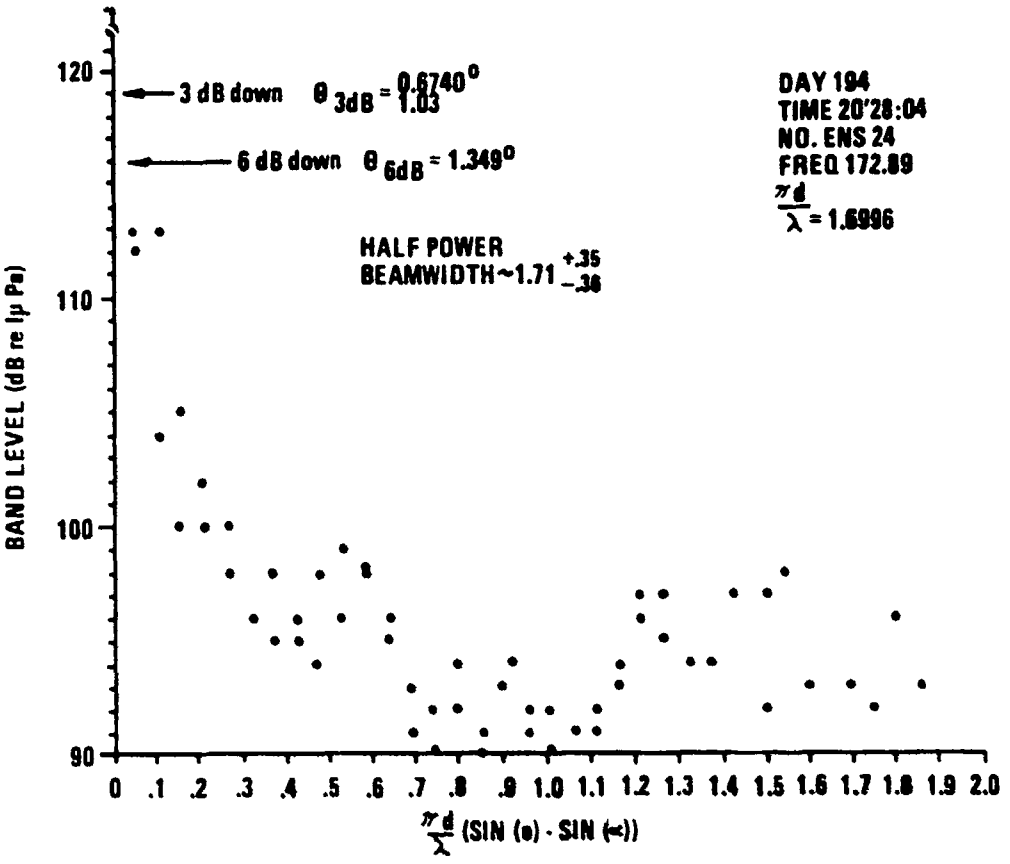

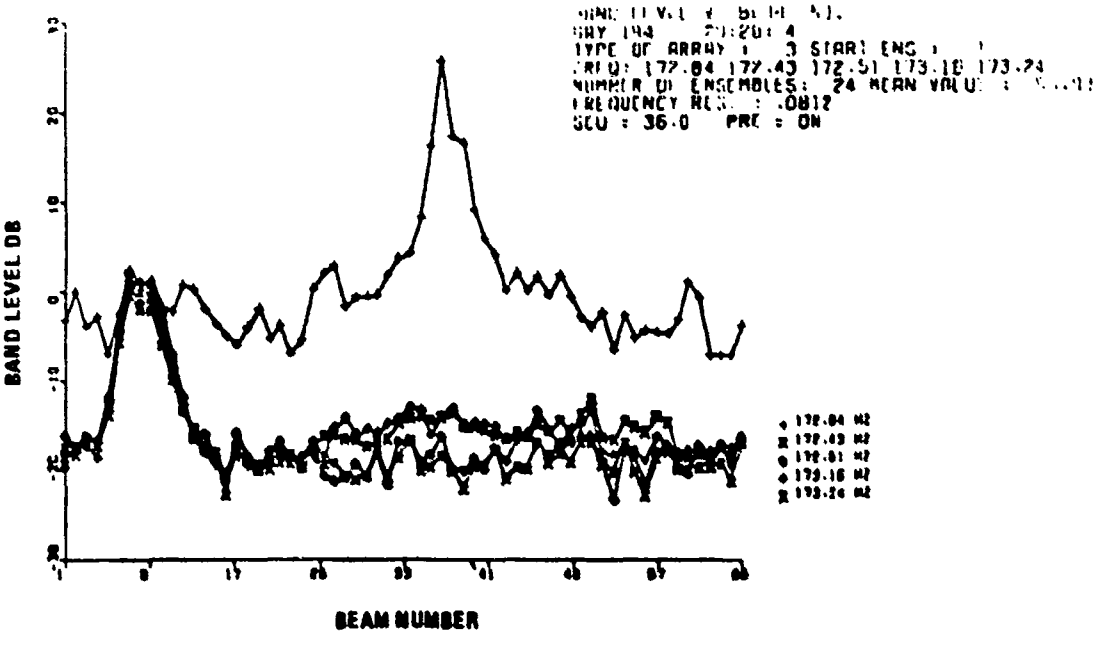

Figure 4-15. (C) The LAMBDA III HF Beam Response (U)

4-13 are clearly dominated by the source on most beams. Each data point represents the response of a beam with its main axis of response in α direction to the source at angle θ, where both angles are measured from broadside. A sampling of the range of side lobe level values in this data corresponds to the range of the variable Ψ ($\Psi = \pi\ d/\lambda\ (\sin(\theta) - \sin(\alpha))$) between 0.0 and 1.9. The data shown in Fig. 4-15 are the relative band levels versus the variable Ψ. This plot reveals several interesting characteristics of the LAMBDA III HF array.

(C) The beam width which is defined as the angular width of the beam at the -3 dB point is determined to be $1.71 \pm .35^{o}$. The side lobe level can be inferred from this plot. In the region of the main lobe, the first appears at -9dB and the second at -17dB. The remaining side lobes are seen to be less than -20 dB with an average level of -27.5 dB. This performance is comparable to the $\left| \sin(n\Psi)/n \sin(\Psi) \right|^2$ response of a uniform line array with several missing hydrophones for a signal plus noise measurement.

4.2.1 Measured Spectral Values

(C) The characteristics of the beam response curves previously discussed can be studied best by examination of the mean hydrophone and beam band level spectra. We employ the term "band" because we have not applied any bandwidth correction to the measured levels. The hydrophone sensitivity correction has been applied, however, yielding absolute pressure levels in a 0.08124 Hz analysis band.

(C) Figure 4-16 shows the mean band level spectra for all 60 hydrophones. The figure shows the three TAP III filters centered at 67 Hz, 173 Hz and 174 Hz side by side in order of increasing processor frequency bin number (.08124 Hz). This spectra represents the linear power average of 24 individual estimates of power for each of the 60 hydrophones, 2,880 degrees of freedom. Also shown in this figure are the standard deviations for this measurement as determined by power averaging and then converted to dB's. Tabular values of the 192 bins of information are presented in Fig. 4-17. We present this information, since further discussion is restricted to 64 frequency bins (5.2 Hz) of information. The first filter region for the tag 194:20:28:04 sample is shown in Figure 4-18a for both the mean hydrophone and beam #34, the beam of maximum response that appeared in Fig. 4-12. The beam level has been

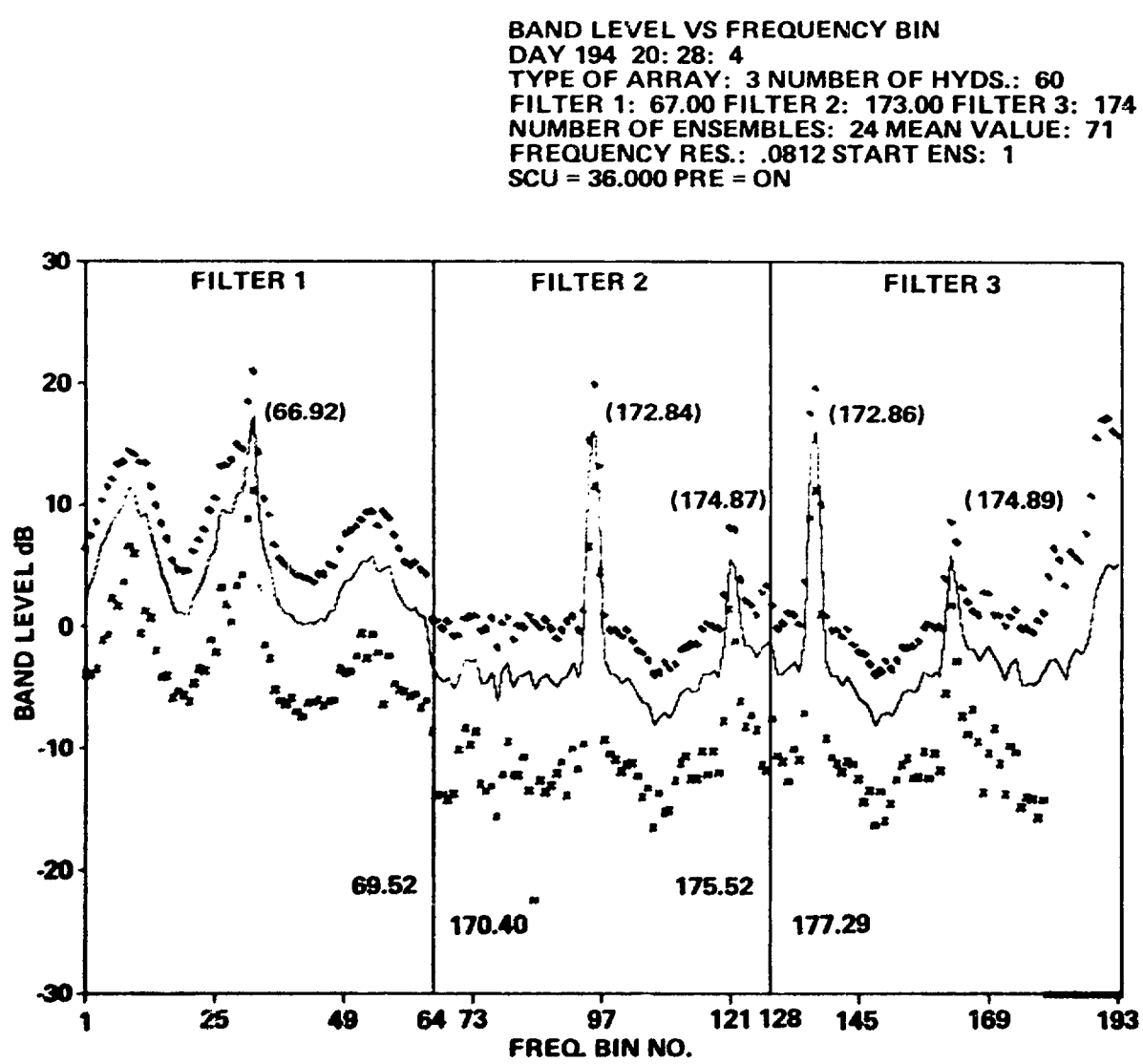

Figure 4-16. (C) Band Level Spectra in the 67 Hz, 173 Hz 175 Hz Filter Bands (U)

CONFIDENTIAL

DATE :13 JULY 1979 TIME :194: 20: 28: 4
TMP III AVG. TYPE : 1 NUMBER OF ENS. : 24
FILTER 1 : 67.00 FILTER 2 :173.00 FILTER 3 :174.89
FILTER WEIGHT : 2: 2: 2 START ENS : 1
SAMPLE RATE :914.91 FFT LINE SPACING : .0812
TYPE OF RECORD : 3 TYPE OF ARRAY : 3
AVG. SPECTRA : 60 HYDROPHONES. NUMBER OF ENSEMBLES : 24

I	FREQ.	-SIG	APS	+SIG	I	FREQ.	-SIG	APS	+SIG	I	FREQ.	-SIG	APS	+SIG	I	FREQ.	-SIG	APS	+SIG
1	64.40	-6.6	73.6	3.7	49	68.30	-7.5	74.6	4.0	97	173.00	-6.6	68.1	3.7	145	173.59	-8.1	64.6	4.1
2	64.48	-7.4	74.5	3.9	50	68.38	-7.6	74.8	4.0	98	173.08	-6.6	67.0	3.7	146	173.67	-6.7	64.2	3.7
3	64.56	-8.0	75.5	4.1	51	68.46	-6.9	75.4	3.8	99	173.16	-6.9	66.9	3.8	147	173.75	-8.3	62.9	4.2
4	64.64	-7.6	77.4	4.0	52	68.54	-5.9	76.2	3.5	100	173.24	-7.3	66.3	3.9	148	173.83	-6.3	63.7	3.6
5	64.73	-8.0	78.4	4.1	53	68.62	-7.9	76.2	4.1	101	173.32	-7.2	66.8	3.9	149	173.92	-8.8	63.8	4.3
6	64.81	-6.2	79.5	3.6	54	68.71	-6.4	76.7	3.7	102	173.41	-6.5	66.2	3.7	150	174.00	-7.2	63.6	3.9
7	64.89	-7.7	80.2	4.0	55	68.79	-6.7	75.4	3.7	103	173.49	-6.6	65.2	3.7	151	174.08	-6.2	64.5	3.6
8	64.97	-6.3	80.9	3.6	56	68.87	-11.1	75.7	4.7	104	173.57	-7.8	64.7	4.0	152	174.16	-6.1	65.7	3.6
9	65.05	-4.8	82.4	3.1	57	68.95	-7.4	75.9	3.9	105	173.65	-6.7	64.4	3.8	153	174.24	-5.7	65.8	3.4
10	65.13	-5.1	82.0	3.2	58	69.03	-8.1	74.3	4.1	106	173.73	-8.5	62.9	4.2	154	174.32	-7.1	65.6	3.8
11	65.21	-9.6	80.0	4.5	59	69.11	-7.6	73.3	4.0	107	173.81	-6.3	63.6	3.6	155	174.40	-7.3	65.9	3.9
12	65.29	-8.1	80.2	4.1	60	69.19	-6.8	72.5	3.8	108	173.89	-8.3	63.9	4.2	156	174.48	-6.5	67.2	3.7
13	65.38	-7.0	78.6	3.8	61	69.27	-6.9	72.1	3.8	109	173.97	-7.7	63.5	4.0	157	174.57	-8.5	66.9	4.2
14	65.46	-7.9	76.9	4.1	62	69.36	-6.9	72.4	3.8	110	174.06	-6.0	64.3	3.5	158	174.65	-6.6	67.2	3.7
15	65.54	-8.4	75.2	4.2	63	69.44	-7.4	71.7	3.9	111	174.14	-5.9	65.6	3.5	159	174.73	-7.8	66.9	4.0
16	65.62	-7.4	74.2	3.9	64	69.52	-6.6	71.5	3.7	112	174.22	-5.6	65.9	3.4	160	174.81	-5.9	71.4	3.5
17	65.70	-7.3	72.4	3.9	65	170.40	-5.8	68.1	3.4	113	174.30	-7.2	65.6	3.9	161	174.89	-4.0	76.7	2.7
18	65.78	-6.3	72.0	3.6	66	170.48	-9.9	66.9	4.5	114	174.38	-7.3	65.6	3.9	162	174.97	-6.2	74.3	3.6
19	65.86	-6.5	71.9	3.7	67	170.56	-9.3	66.4	4.4	115	174.46	-6.5	67.1	3.7	163	175.05	-6.9	70.4	3.8
20	65.94	-6.9	71.8	3.8	68	170.64	-10.2	66.8	4.6	116	174.54	-8.2	67.0	4.1	164	175.13	-7.0	69.1	3.8
21	66.03	-7.0	73.3	3.8	69	170.73	-8.7	65.9	4.3	117	174.62	-6.6	67.2	3.7	165	175.21	-4.9	69.0	3.1
22	66.11	-6.9	74.3	3.8	70	170.81	-6.0	66.8	3.5	118	174.71	-7.8	66.7	4.0	166	175.30	-6.7	68.2	3.7
23	66.19	-7.6	74.9	4.0	71	170.89	-5.6	68.2	3.4	119	174.79	-6.7	69.8	3.7	167	175.38	-11.6	69.0	4.8
24	66.27	-6.9	76.7	3.8	72	170.97	-6.8	68.0	3.8	120	174.87	-4.0	76.3	2.7	168	175.46	-8.9	69.4	4.3
25	66.35	-8.5	77.3	4.2	73	171.05	-6.0	68.3	3.5	121	174.95	-5.7	75.4	3.4	169	175.54	-5.9	68.4	3.5
26	66.43	-6.3	80.5	3.6	74	171.13	-8.4	66.4	4.2	122	175.03	-6.4	71.2	3.6	170	175.62	-8.1	67.7	4.1
27	66.51	-7.5	80.2	4.0	75	171.21	-9.0	66.4	4.3	123	175.11	-6.7	69.4	3.7	171	175.70	-9.4	66.6	4.4
28	66.59	-9.0	80.3	4.3	76	171.29	-9.4	67.2	4.4	124	175.19	-5.7	69.3	3.4	172	175.78	-6.8	67.9	3.8
29	66.68	-7.6	81.9	4.0	77	171.38	-9.6	64.8	4.4	125	175.27	-5.9	68.4	3.5	173	175.86	-7.7	68.3	4.0
30	66.76	-6.7	81.8	3.7	78	171.46	-8.3	67.1	4.2	126	175.36	-9.7	69.3	4.5	174	175.95	-10.2	66.2	4.6
31	66.84	-6.2	85.9	3.6	79	171.54	-6.5	68.0	3.7	127	175.44	-10.5	69.7	4.6	175	176.03	-9.5	66.4	4.4
32	66.92	-6.2	88.3	3.6	80	171.62	-7.3	66.1	3.9	128	175.52	-5.9	69.3	3.5	176	176.11	-9.4	66.1	4.4
33	67.00	-7.4	91.5	3.9	81	171.70	-8.2	66.8	4.1	129	172.29	-6.8	67.0	3.8	177	176.19	-11.4	66.6	4.8
34	67.08	-7.9	92.4	4.1	82	171.78	-6.9	67.1	3.8	130	172.37	-7.4	67.2	3.9	178	176.27	-10.7	67.4	4.6
35	67.16	-7.8	96.1	4.0	83	171.86	-9.9	67.3	4.5	131	172.45	-9.4	67.6	4.4	179	176.35	-27.3	68.2	6.9
36	67.24	-7.9	93.6	4.1	84	171.94	-17.4	65.9	5.4	132	172.53	-7.2	68.0	3.9	180	176.43	-27.5	68.3	9.0
37	67.32	-7.6	92.5	4.0	85	172.03	-8.4	66.7	4.2	133	172.62	-7.3	67.2	3.9	181	176.51	-26.8	67.7	8.7
38	67.41	-7.4	92.0	3.9	86	172.11	-9.7	67.0	4.5	134	172.70	-7.0	70.8	3.8	182	176.60	-25.8	66.6	7.7
39	67.49	-6.7	91.8	3.7	87	172.19	-8.6	66.5	4.2	135	172.78	-5.3	85.1	3.3	183	176.68	-27.6	68.5	8.5
40	67.57	-7.3	91.2	3.9	88	172.27	-7.3	66.1	3.9	136	172.86	-5.2	87.2	3.2	184	176.76	-28.3	69.1	7.5
41	67.65	-7.6	91.0	4.0	89	172.35	-7.0	66.8	3.8	137	172.94	-5.6	77.6	3.4	185	176.84	-27.9	68.8	7.5
42	67.73	-6.6	91.2	3.7	90	172.43	-9.8	66.9	4.5	138	173.02	-6.4	68.2	3.7	186	176.92	-28.4	69.2	8.3
43	67.81	-6.3	91.0	3.6	91	172.51	-7.1	67.9	3.9	139	173.10	-6.7	66.9	3.7	187	177.00	-30.2	71.1	10.6
44	67.89	-6.6	91.5	3.7	92	172.59	-7.5	66.7	4.0	140	173.18	-7.1	66.8	3.9	188	177.08	-33.2	74.0	12.4
45	67.97	-7.0	91.4	3.8	93	172.68	-7.1	68.4	3.9	141	173.27	-7.2	66.3	3.9	189	177.16	-34.4	75.3	12.5
46	68.06	-7.3	92.1	3.9	94	172.76	-5.4	82.9	3.3	142	173.35	-7.1	66.9	3.9	190	177.25	-35.0	75.9	12.1
47	68.14	-7.1	92.0	3.9	95	172.84	-5.2	87.6	3.2	143	173.43	-6.3	65.9	3.6	191	177.33	-34.8	75.7	11.2
48	68.22	-6.3	93.7	3.6	96	172.92	-5.4	80.8	3.3	144	173.51	-6.7	65.1	3.7	192	177.41	-35.2	76.0	10.5

FIGURE 4-17. (C) Mean Band Level Spectra with Minus and Plus Variance for 60 Hydrophones, 24 Ensembles in Three Filter Bands (U)

CONFIDENTIAL

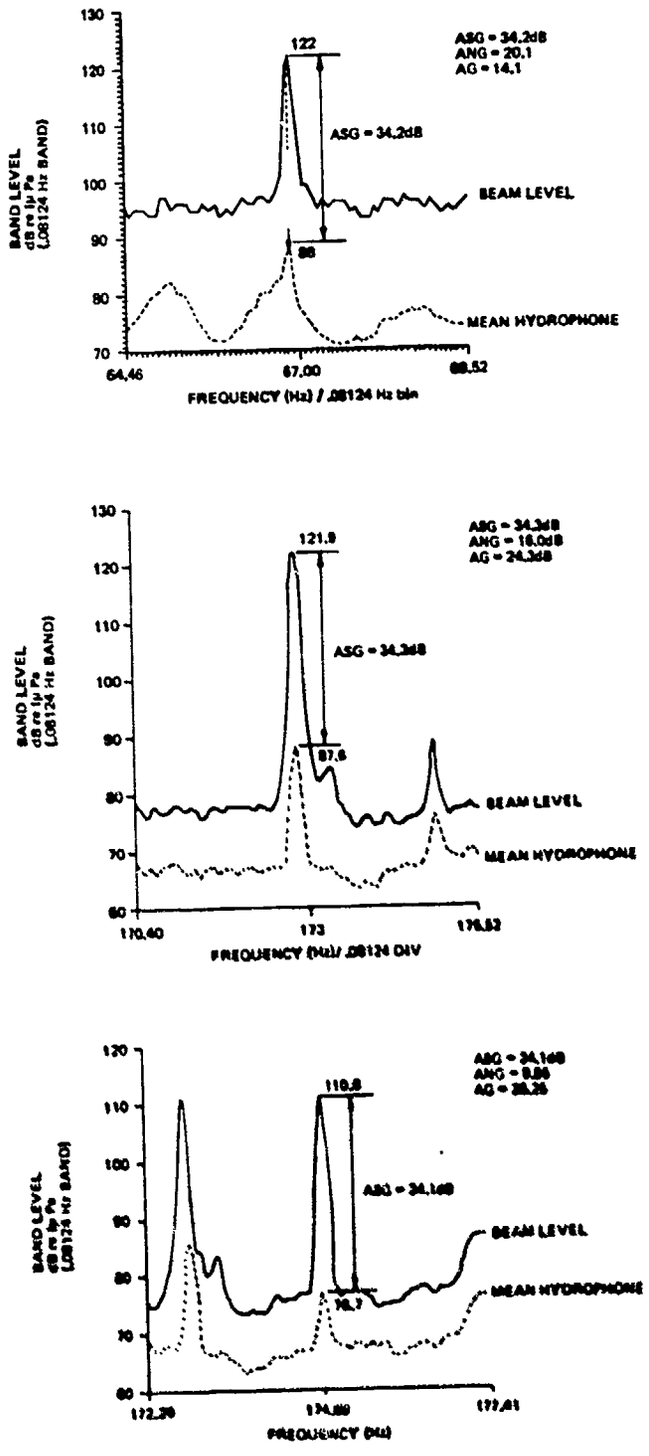

Figure 4-18. (C) Beam and Hydrophone Band Levels (U)

determined by applying the single hydrophone group calibration factor to the measure of the voltage level at the output of the beam forming process. The data on the signal level and noise levels are listed in the following Table.

	HYDROPHONE (dB)	BEAM (dB)
Mean Band Noise Level	75.8	-
Mean Band Level (less bins with signal)	75.5	95.61
Mean Noise Level Bin (25, 26, 27, 28)	79	-
Mean Noise Level Bin 34-39	73	-
Signal Level	88	122.2

(C) The beam noise level in the 64.40 to 69.52 level is well defined for the region not containing the signal. The hydrophone spectra are not as easily defined. We made several estimates of the noise level which are shown in the above table. This table shows that, without the signal peaks, the mean band level is 75.8 dB. In the neighborhood of the signal, the average over four noise bins on one side was 79 dB and over seven bins on the other side was 75 dB. The mean level between these two estimates is 75.5 dB. These numbers indicate that in the 67.0 Hz case we have an array signal gain (ASG) of 34.2 dB, an array noise gain (ANG) of 20 dB and an array gain (AG) of 14 dB.

(C) Figure 4-18b shows the beam and mean hydrophone level spectra in the filter II region, 170.40 Hz to 175.52 Hz. Beam number 36 is the beam of maximum response to the 177.84 Hz source as shown in Figure 4-18c. As before, we determined the mean hydrophone noise level by several different techniques:

Mean Hydrophone Band Level	58.7 dB
Mean Hydrophone Band Level - less peaks	66.7 dB
Noise Bin Average (Right Hand Side)	67.4 dB
Noise Bin Average (Left Hand Side)	67.5 dB

(C) The beam noise level, neglecting the two spectral peaks, is 75.8 dB. In this instance, ASG = 34 dB, ANG = 10 dB, and AG = 24 dB. This value of AG exceeds the 10 Log(n) value for a sinusoidal signal in an incoherent noise background.

(C) Figure 4-18c illustrates the data in filter III covering the frequency region 172.29 to 177.41 Hz. Here the mean hydrophone noise level (without the two signal peaks) is 67 dB and the beam noise is 75.8 dB. This results in an ASG of 34.1 dB, ANG = 8.8 dB, and an AG = 25.3 dB. Again, another high value of array gain is obtained. This will be discussed later in this section. The key result in this section is that the array signal gains were 34.2, 34.3, and 34.1 dB compared to a 20log(n) value of 36 dB. We note further that noise values were insensitive to the averaging technique when spectral peaks were ignored and the average was taken over the band.

4.2.2 Measured Spatial Characteristics

(C) Spectral characteristics of the array were determined by spatial and time averaging of the output of the individual hydrophones of the array to produce the mean hydrophone spectrum. When this mean hydrophone spectrum was used with the mean beam spectrum, the array signal and noise gains were realized. Spatial averaging was expedient and necessary for the determination of the gains. The question of the spatial variation arises. Figure 4-19 shows the band level versus hydrophone number (running fore to aft) along the length of the aperture. The hydrophone group spacing is 4.75 m. We show data for the source frequencies of 66.92 Hz, 172.92 Hz and 174.89 Hz. Each of these illumination ploys is shown for five .08124 Hz frequency bins. One bin is chosen at the source frequency and four represent noise bins. Also shown on these graphs are the positions of faulty hydrophone groups. These five groups are the sharp drops on each of the plots.

(C) The plot of the 66.92 Hz illumination shows a rather uniform signal plus noise level with a slightly decreasing noise level as one proceeds from the front to rear of the array. The noise is also shown to decrease at the lower frequency bins.

(C) The plot of the 172.84 Hz data shows a rather uniform noise level from the fore to aft hydrophone but a signal plus noise level which has a pronounced dip near the middle of the array. This plot represents 12 time ensembles averaged to yield a number of degrees of freedom equal to 24. We routinely examined our data for this type of structure. During this time period, we observed no major effect due to the number of time averages. We compared the first 12 ensembles, 2nd 12 ensembles and 24 ensembles averages and no major differences were observed. We did observe a shift in the relative shape of the illumination function and these plots are presented in a separate volume data appendix. During this period of time the source-receiver separation changed between 0.47 nmi for 12 ensembles and .94 nmi for 24 ensembles. This characteristic shape of the illumination function is most probably due to a multipath structure in the media.

(This page is unclassified.)

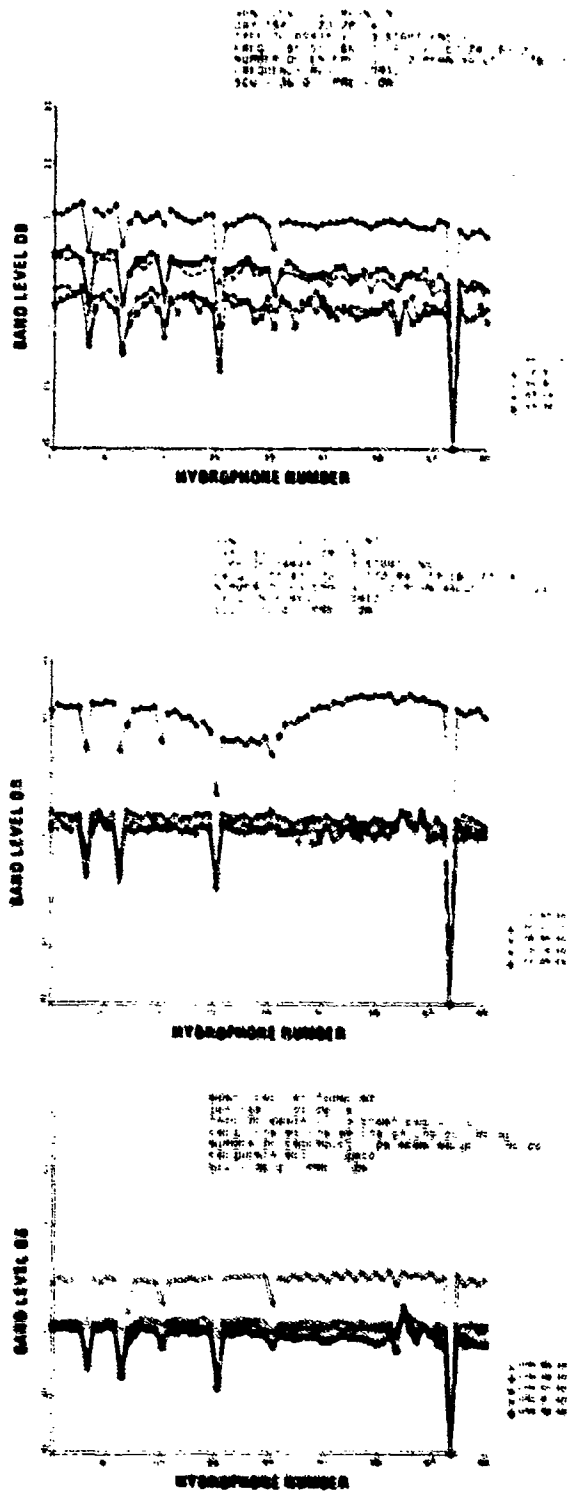

Figure 4-19. (U) Illumination Plots for the 67 Hz, 173 Hz and 175 Hz Signal (U)

(C) The 174.89 Hz case shows a rather uniform illumination with a periodic scalloping near the aft end of the array. During this period of time, the array had an upward tilt of approximately 6^{o} over the aperture. Also observe that there is a decrease in noise levels from the fore hydrophone group to the aft hydrophone group.

(C) These three lines are from two sources. The 66.92 and 172.84 Hz source lines are from the towed source (400 m depth) while the 174.89 Hz source is from the moored Webb Source (100.00 nm source receiver range, 988 meter depth). We would expect a different arrival structure based on these range distances and due to the fact that the sources are at different depths. We conclude that these effects as a function of operation are due to the arrival structure of the sound.

(C) Figure 4-21 and 4-22 show the magnitude square coherence and signal to noise ratio versus aperture length for the 172.84 Hz line and 174.89 Hz line shown in figure 4-20.

(C) The MSC for the high signal to noise ratio case of the 172.9 Hz line shows a smooth fore-aft variation. The minimum in the MSC Curve is consistent with the minimum in the S/N curve and S + N curve. The lowest value of S/N ratio is 14 dB. The case of the 174.81 Hz curve shows a more interesting picture. Although the S + N versus aperture plot is uniform, we see that the MSC plot is erratic at the forward end of the array. We observe that the signal to noise ratio is less than 10 dB as shown in Figure 4-22. When the signal to noise ration increases towards the aft portion of the array due to the decrease in noise levels, we observe that this MSC curve overlaps the previous case except for the dip near hydrophone 56. We conclude that we have a measure of the MSC of the signal for S/N > 10 dB; but that noise from the tow ship interferes with the determination at S/N $\leq$ 10 dB. This is consistent with and reinforces our discussion of the beam response function and array noise gain. We are measuring the properties of a signal in the directive coherent field of the ship. The high S/N case gives a clean measure of signal coherence to a distance of 300 meters for the case of bottom limited propagation.

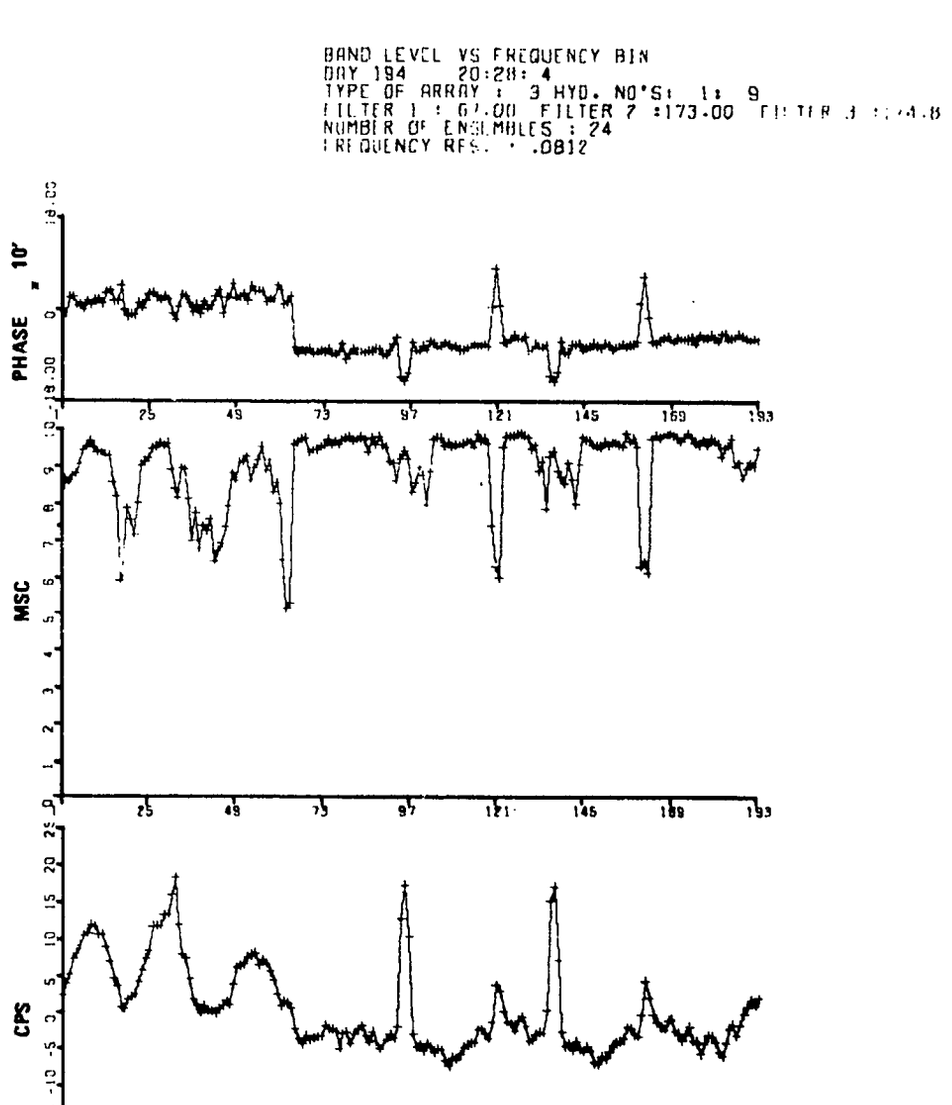

Figure 4-20. (U) MSC, Phase and Crosspower Versus Frequency (U)

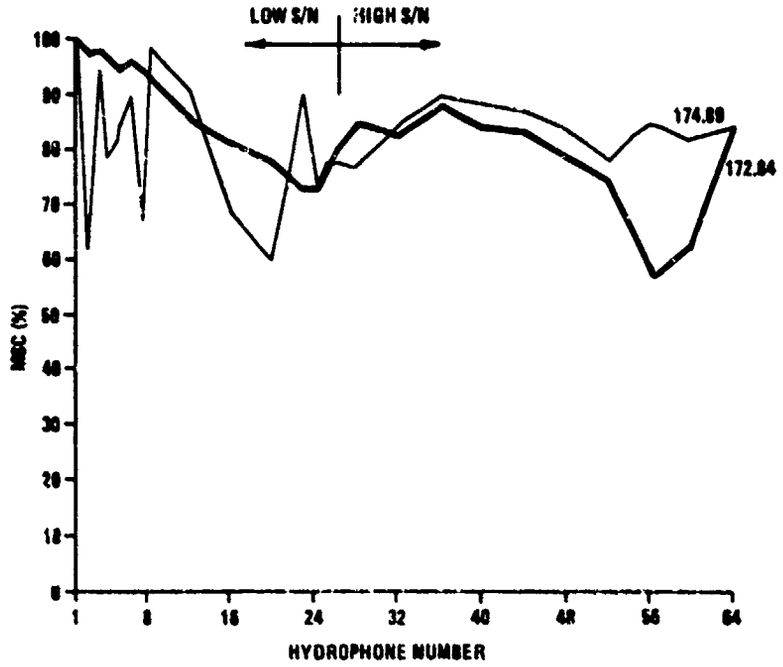

Figure 4-21. (U) MSC Versus Hydrophone Number (U)

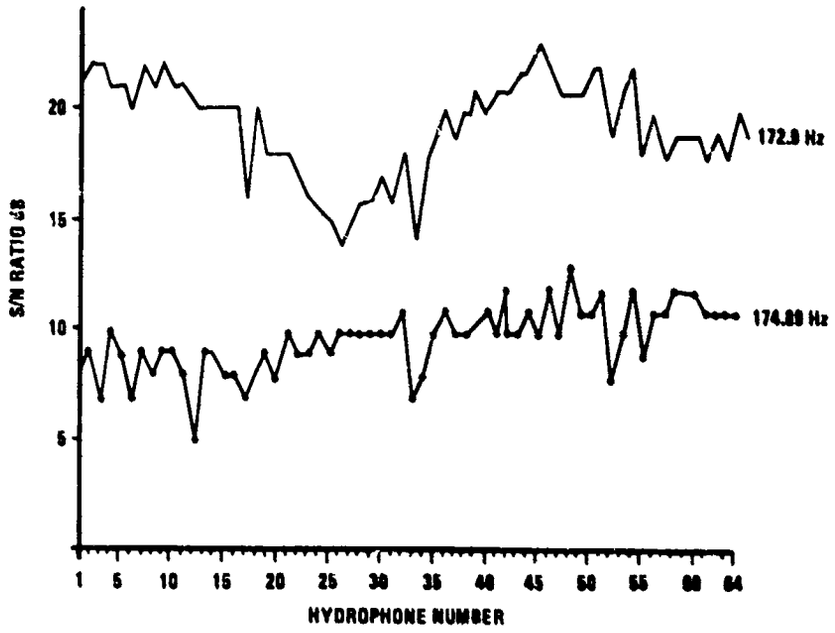

Figure 4-22. (U) S/N Versus Hydrophone Number (U)

4.3 Fluctuations (U)

(U) This section of the report presents data on short term and long term variations in the output level of the hydrophone groups and in the array signal gain.

(U) Short term fluctuations are defined here as the statistical distribution of band levels in a 12 to 25 minute period. As indicated in Table 4-1, during these time intervals, variations in the range between two ship and receiver ship averaged about .75 nm.

(U) For the purposes of this report, long term fluctuations are defined as the variation of mean band level with time over the period of hours without regard to transmission loss trends.

4.3.1 Short Term Fluctuations. (U)

(U) Data obtained in this experiment were routinely processed to determine the mean band level and the variance of the distribution of data about this mean. The standard deviations for the spectral analysis were determined by the mean squared pressure level and the sum of the squared errors around this mean squared pressure. This is the reason for the illustration of a + deviation. The example for the time period centered around Day 194:20:28:04 discussed in previous sections shall be discussed as to the characterization of these variances. The table shows the + deviation for this case with

$$-\Delta = 10 \log ((I_0 - \sigma)/I_0)$$
$$+\Delta = 10 \log ((I_0 + \sigma)/I_0)$$

where I_0 is the mean intensity, σ is the standard deviation and Δ is the logrithmic deviation.

f	(S+N)	N	<S/N>
	-Δ/+Δ	-Δ/-Δ	
67 Hz	-6.2/3.6	-9/4	12 dB
172.92 Hz	-5.2/3.2	-8.6/4.2	21 dB
174.89 Hz	-6.2/3.6	-8.5/4.0	10 dB

The +Δ are comparable to the estimate of the standard deviations determined by 'dB' averaging.

(U) The question arises as to the source of these variances in the data. In the section on calibration it was determined that these fluctuations in the acquired and processed data could not be due to the measurement system. Examination of the spatial illumination plots for signals and noise shows that spatial variations in the signal do occur and that the noise in general decreases from the fore to aft hydrophone groups in the array. Each hydrophone group shows signal and noise standard deviations comparable to those listed in the above table.

(U) The distribution of errors around the mean of each individual hydrophone group are shown in Figure 4-23 for the differential distribution (probability density) and for the integral distribution (cumulative distribution) in Figure 4-24. These figures show the cases for the first and last 24 hydrophone groups of the array.

(U) All differential distributions show a skew and asymmetry with respect to the abcissa.

(U) The cumulative distributions are shown in Figure 4-24. These distributions were compared to standard statistical distributions. The 67 Hz data for the forward 24 hydrophone groups was found to the Rayleigh distributed with a mean of -8.15 dB and a variance of 18 dB. Both the 173 and 175 Hz data distributions showed an approximate Gaussian distribution with a mean of -0.5 dB and a variance of approximately 9 dB. The nature of the distribution of the fluctuations in underwater acoustic signals has been treated by Urick, Dyer, and Whalen (Ref. 17, 18 and 19). Basically these data represent the case of a sine wave plus a narrowband Gaussian process inputed to a quadratic detector with post detection summation. The individual samples of the output of this system are statistically independent and for this case the distribution would be a non-central χ^2 density function. This distribution is characterized by a noncentral parameter which is proportional to the ratio of signal noise power at the input to the measurement system. Thus the input to the LAMBDA measurement system in the analysed case of a multipath sinusoidal signal in a narrowband Gaussian noise background should

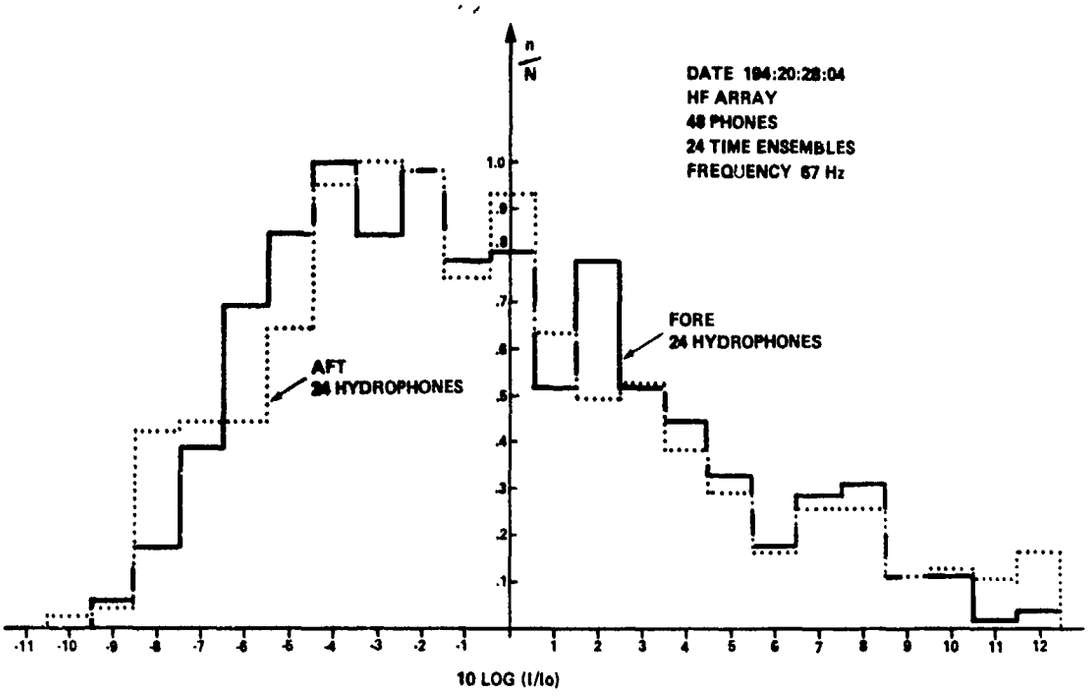

Figure 4-23a. (U) Probability Density Distribution for 48 Hydrophones at a Frequency of 172.92 Hz for the LAMBDA III, HF Array (U)

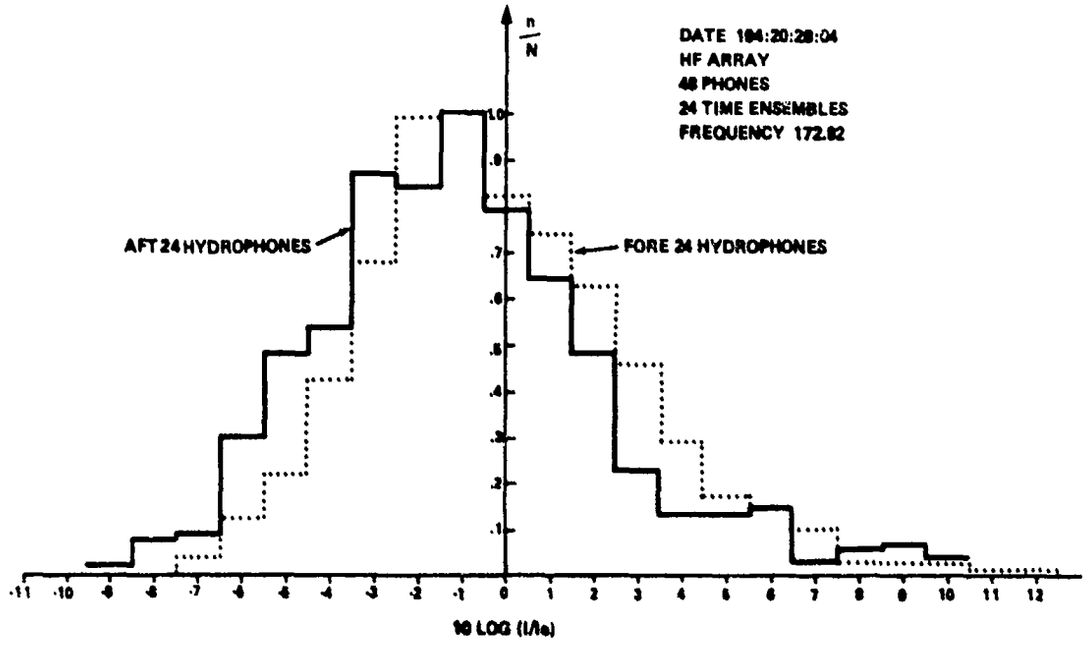

Figure 4-23b. (U) Probability Density Distribution for 48 Hydrophones at a Frequency of 172.92 Hz for the LAMBDA III, HF Array (U)

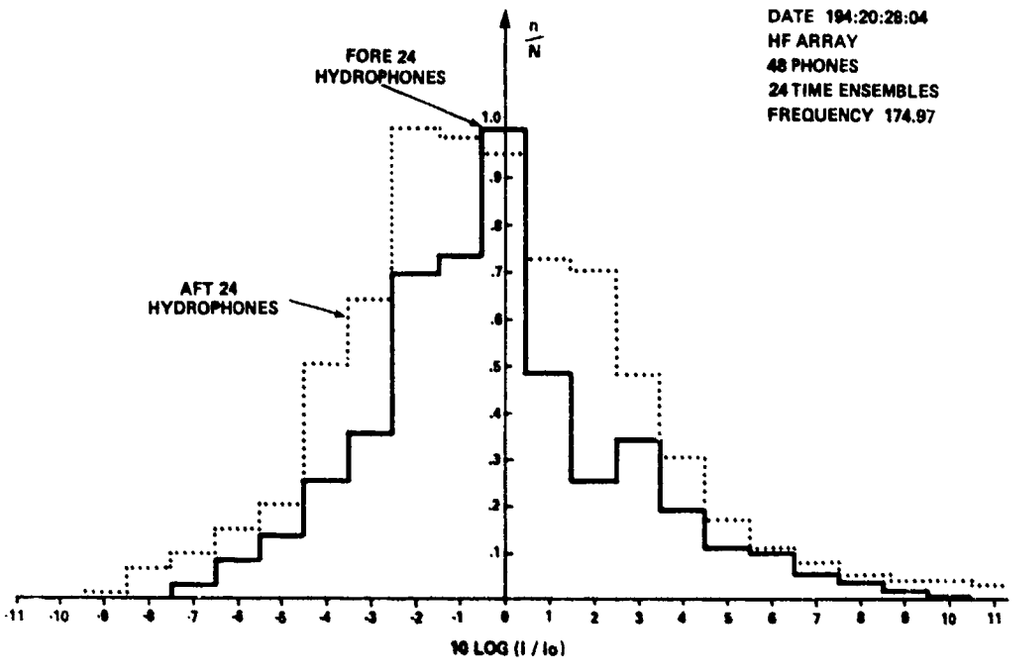

Figure 4-23c. (U) Probability Density Distribution for 48 Hydrophones at 172.97 Hz for the LAMBDA III, HF Array (U)

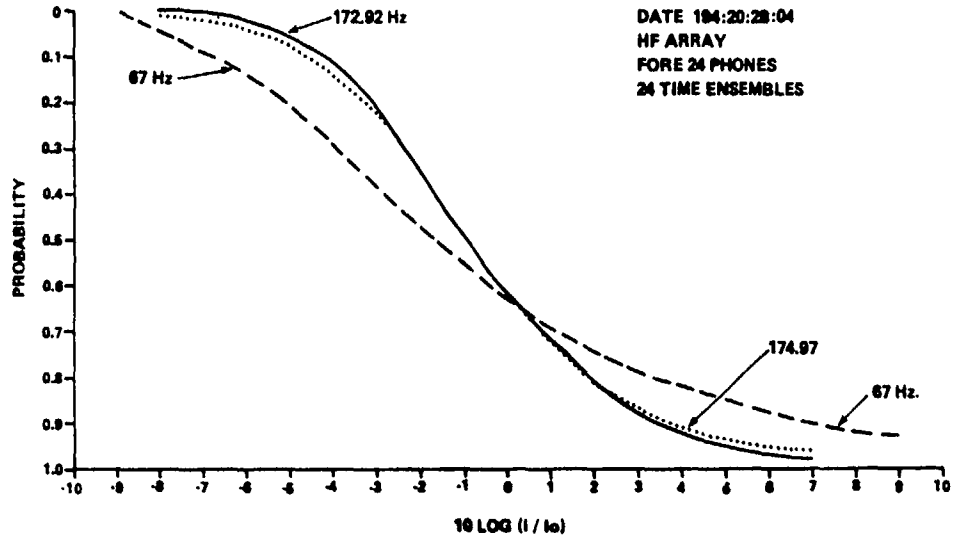

Figure 4-24a. (U) Cumulative Probability Distribution for 194:20:28:04, The LAMBDA III, HF Array, Aft 24 Hydrophones (U)

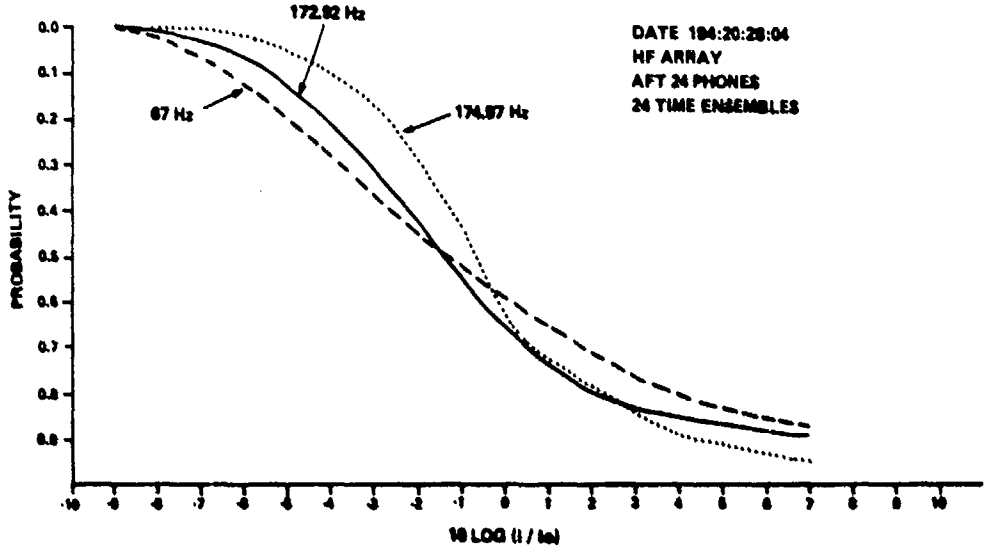

Figure 4-24b. (U) Cumulative Probability Distribution for 194:20:28:04, The LAMBDA III, HF Array, Aft 24 Hydrophones (U)

produce a non-central χ^2 distribution which is a function of the input signal-to-noise ratio. The noise case alone would produce a χ^2 distribution (Whalen Ref. 19). These are compared to the envelope of a narrowband Gaussian noise which is Rayleigh distributed and the envelope of a signal in narrowband noise which is Rician distributed.

(U) Although a detailed characterization of these distributions is beyond the scope of this report, the data presented here do not significantly deviate from results of other investigators (Urick and Dyer).

4.3.2 Long-term Fluctuations

(C) The time series of measured transmission loss over the approx. 24 hour period during the leg E-F is shown in Figure 4-25. To obtain these plots the transmission loss was estimated from the difference between the received signal level and the source level. The received signal level is the measured signal in a .08 Hz band averaged in space over 60 to 64 hydrophones and in time, coherently, for 12.5 second and incoherently over 24 ensembles spaced at about one minute intervals. The towed source had an average range rate of 3.2 knots, while the moored source experienced a range rate of less than 0.2 knots due to the motion of the array during the data-taking period. There is thus a range interval of 71.6 nm in the towed source data and a 4 nm interval in the moored source data. The data are shown only for the interval along the leg where the signal-to-noise is greater than 10 dB in the analysis band.

(C) The fluctuations for the two higher frequencies are similar, especially if the trend in the "towed" data is discounted. The computed variance and standard deviation of the values for each time series is (without removing trends).

Freq. (Hz)	Source	Variance	STD Deviation
67	Towed	3.4 dB	1.8 dB
173	Towed	10.4 dB	3.2 dB
174.9	Moored	4.9 dB	2.2 dB

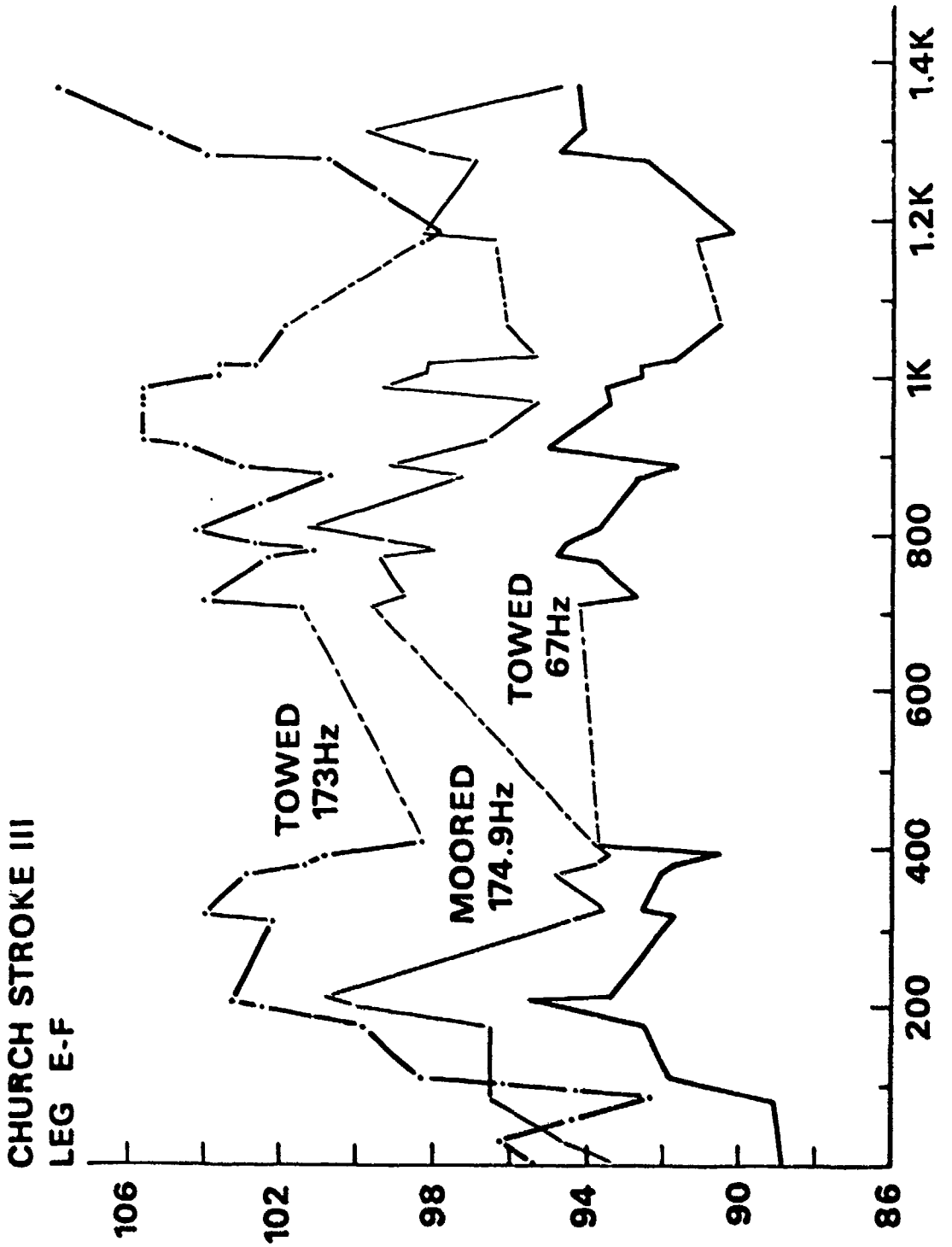

Figure 4-25. (U) Time Series for Signal Loss: Leg E-F (U)

To emphasize the similarity, a "moving" correlation coefficient was computed between the 173 Hz (towed) and the 174.9 Hz (moored) data. The window selected was 200 minutes, i.e., all TL values within that window were converted to power, multiplied, summed and normalized to the product of the auto power in each time series. The result is plotted in Figure 4-26 for the top two curves in Figure 4-25. In interpreting this curve it should be kept in mind that the towed source was relatively shallow (100 m), while the moored source was near the minimum of the sound velocity profile (988 m). Also, the moored source was placed about 5 nm from the point of the track E-F where the bottom slope began. Thus, the towed source range equals the moored source range at about 905 minutes elapsed time and then exceeds it from that point on as the source moves over the slope.

(U) The time intervals of high correlation seen between the towed and moored source received signal fluctuations may be explained by the following qualitative analysis.

(U) The hypothesis is that the two signals will have the same fluctuations when the two sources are on the same ray path (eigenray) to the receiver. To test this hypothesis, consider the ray trace curve of Figure 4-27 for the receiver depth of 400 m. If both sources are on the same ray, which is in this case the limiting ray, then both signals reach the receiver. If the moored source is placed on the ray at 988 m depth and the towed source is moved through the ray diagram at a constant depth of 400 m the towed source will cut across the shallow rays from the moored source at certain range separations. These separations are roughly at ¼, ½, 1¼, 1½, etc., times the cycle distance of the limiting ray. These range intervals are indicated by the horizontal bars in Figure 4-29 marked "Limiting Ray." For comparison a similar estimate of the required range separation was made from the ray trace curves (NORDA MPP) shown in Figure 4-28. These range intervals are also shown at the top of Figure 4-29.

(U) The points of data on Figure 4-29 are the plotted range separation versus time between the two sources. The two time scales are for elapsed

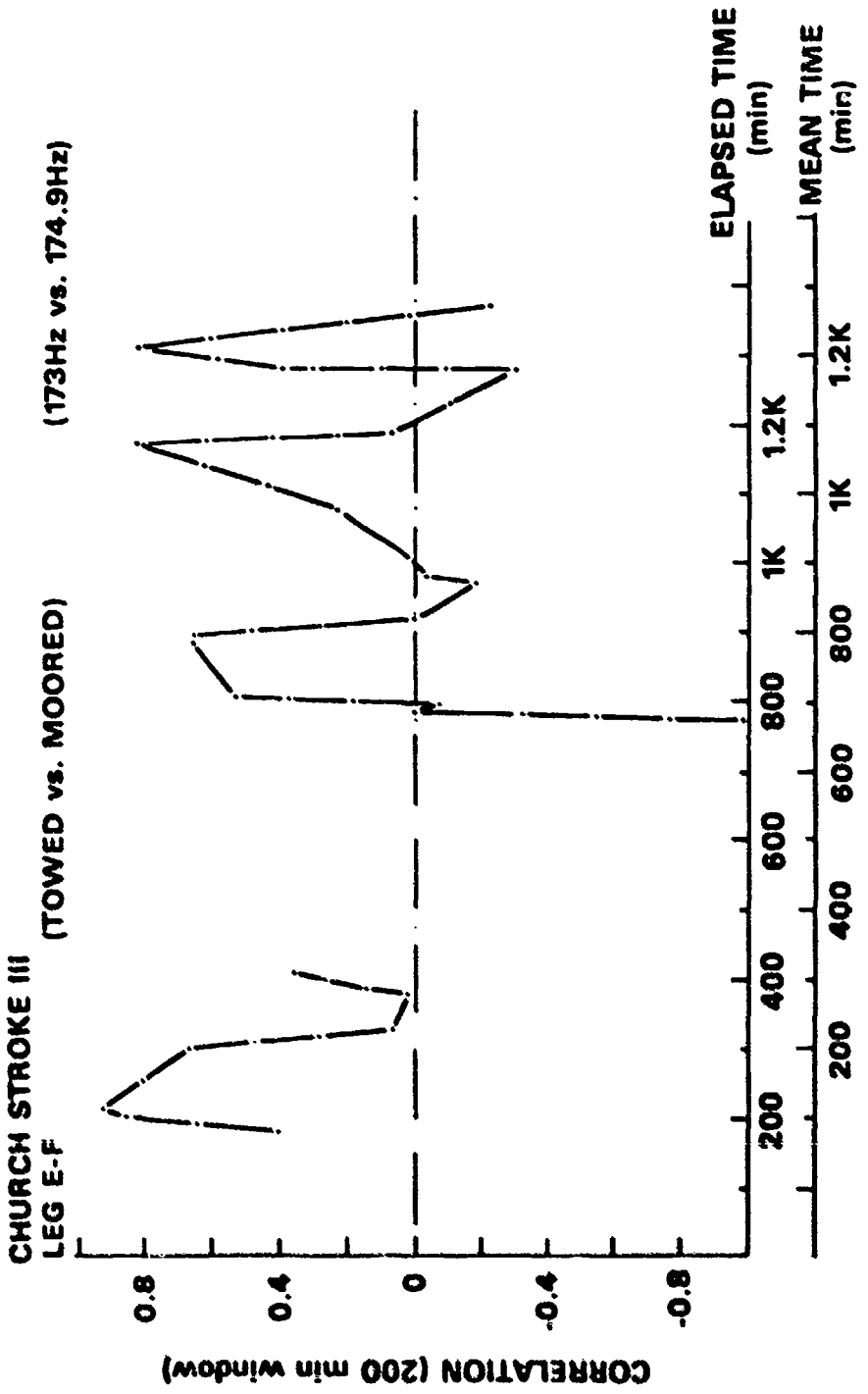

Figure 4-26. (U) "Windowed" Correlation for Time Series of Fig. 4-25 (200 Min. Window) (U)

UNCLASSIFIED

Figure 4-27. (U) Ranges and Depths for Sources and Receivers (U)

UNCLASSIFIED

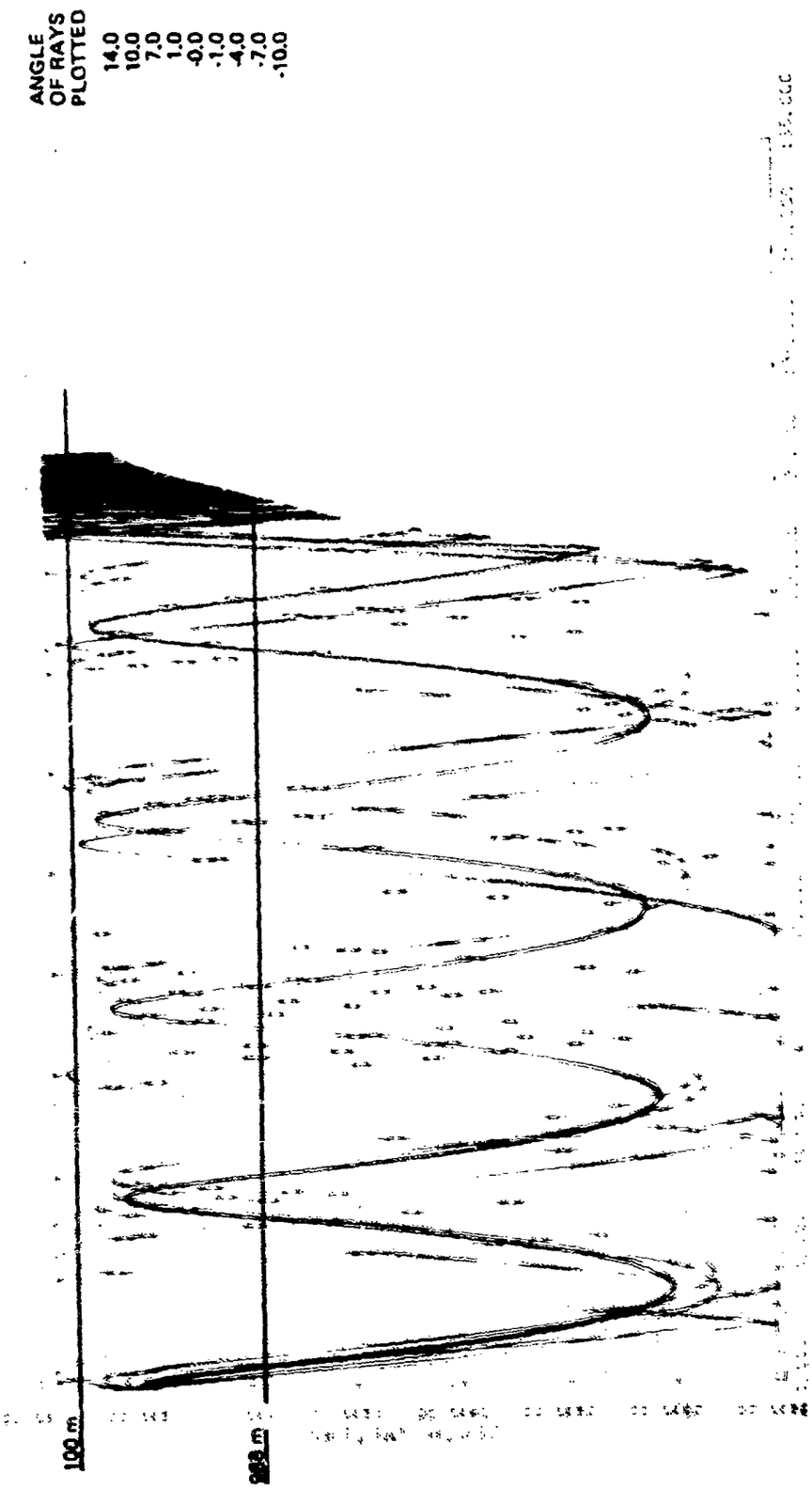

Figure 4-22. (U) Ray Trace for Leg E-F (400m Receiver Depth) (U)

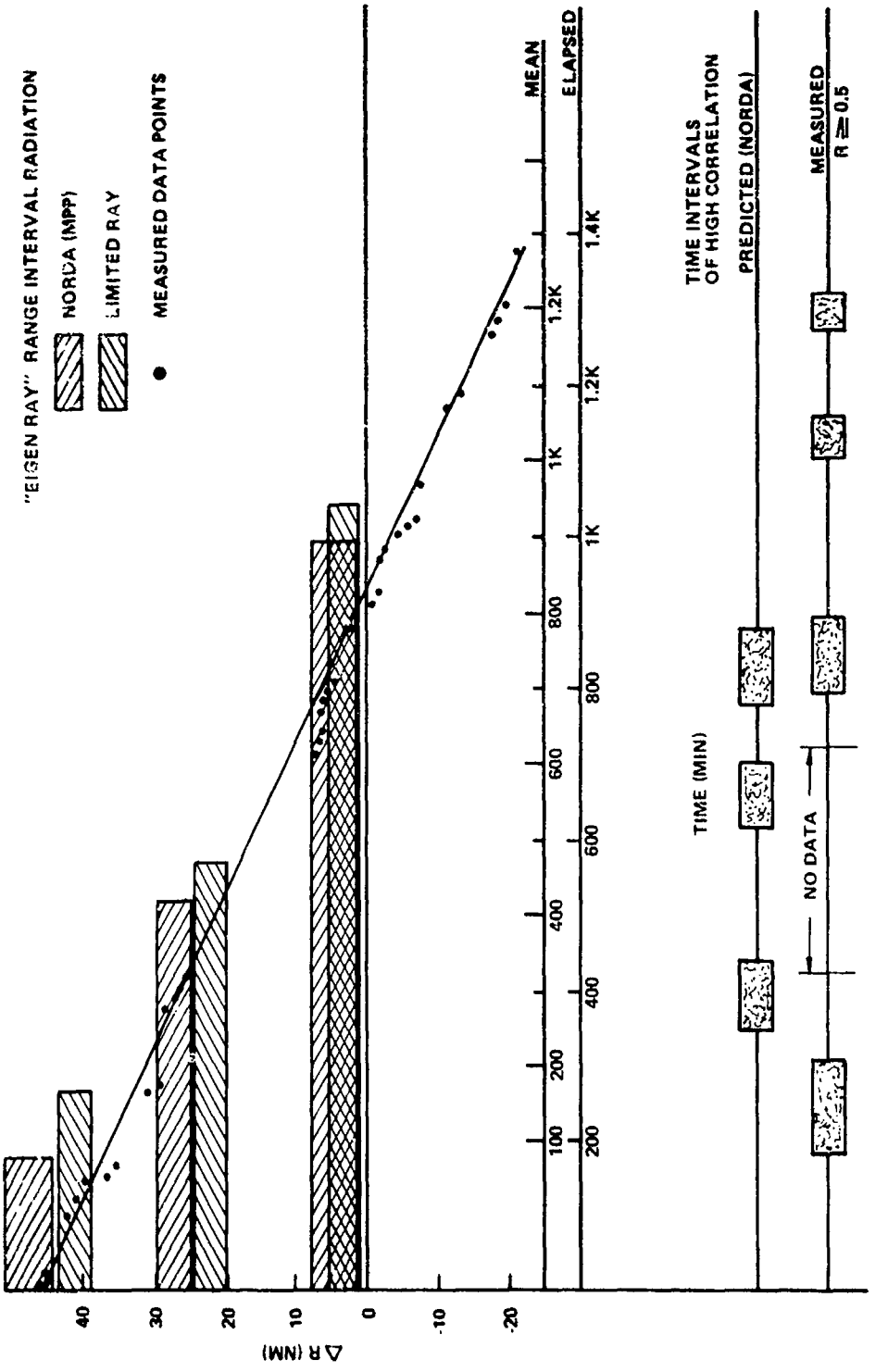

Figure 4-29. (U) Time Interval Comparisons for High Correlations Between Towed and Moored Source Signals (U)

time and mean time (elapsed time minus 100 minutes) for the correlation window. The time intervals where the range separation is right for high correlation between the two source signals is "blocked out" in the lower portion of Figure 4-29. Finally the time intervals of high measured correlation ($R > 0.5$) taken from Figure 4-26 are shown in the bottom time scale of Figure 4-29. There are two time intervals where the measured and predicted time intervals overlap, centered at 200 and 700 minutes mean time. Thus the hypothesis holds in these cases.

(U) It is concluded that if two sources are close in frequency ($\Delta f < 2$ Hz) the fluctuations of signals transmitted over similar paths can be highly correlated. There are two correlation peaks at ranges where the towed source range is greater than the moored source range and the towed source is over the slope. These could be due to some coincidence of eigenrays, but the analysis has not been done. This would require a complete eigenray analysis which could be accomplished but has not been attempted here.

4.3.3 Array Gain Fluctuations

(U) Previous sections have discussed the fluctuations of individual hydrophones and the importance of signal gain in the assessment of the performance of the array. During this experiment estimates of array signal gain, array noise gain, and array gain were performed with a computer program developed by R. Hecht of USI. The determination of array noise gain was based on selected noise bins on either side of the signal level. Figures 4-30 and 4-31 show examples of the output for each of these programs. This program was run for each group of 24 time ensembles.

(U) These figures show the time history for the signal and noise level average values for consecutive samples on the hydrophone; the consecutive estimates of ANG, ASG, and AG; the cumulative probability distribution for ANG, ASG, and AG; and finally a tabular summary. Figure 4-32 shows a summary of this ASG data for 173 Hz and 175 Hz signal. We see that two distributions are apparent--Class I and Class II. We refer to Class I distribution as those which are straight lines (close to Gaussian)

CONFIDENTIAL

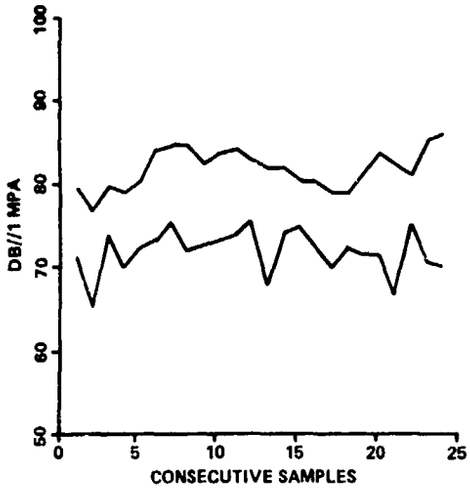

AVERAGE SIGNAL AND ADJACENT BAND NOISE LEVELS FOR THE ARRAY ELEMENTS

PROCESSED 65 15 59 8 222 1979
FREQUENCY 66.92 BEARING 96.39

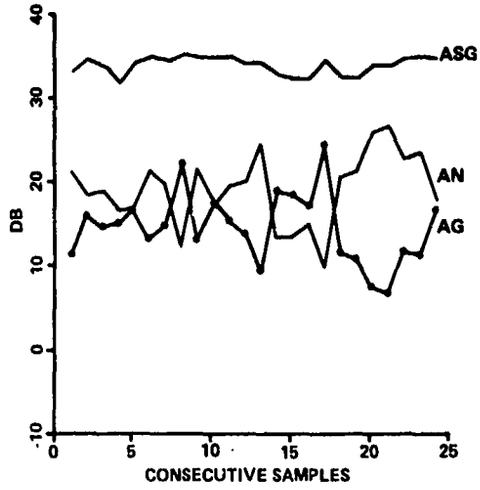

SIGNAL GAIN, ARRAY GAIN, AND NOISE GAIN FOR EACH SAMPLE

ACQUIRED 194 20 26 4
HF ARRAY

TAPIII HEADER INFORMATION

DATE 13 JULY 1979 REAL TIME 194 20 28 4 RECORD TIME 194 20 28 4
ARRAY TYPE 3 SOUND VELOCITY 1489.0000 SHADING TABLE 1

	FILTER1	FILTER2	FILTER3
FREQUENCY	67.000	173.000	174.890
WINDOW	2	2	2

BANDWIDTH .081224 TYPE RECORD 3
TYPE AVERAGING 1 AVERAGING TIME 0.000

	ELEMENT		BEAM				
	SIGNAL	NOISE	SIGNAL	NOISE	SIGNAL GAIN	NOISE GAIN	ARRAY GAIN
1	79.8	71.4	112.9	92.9	33.1	21.5	11.6
2	77.1	65.7	111.9	84.2	34.7	19.5	16.2
3	80.0	74.1	113.9	93.2	33.9	19.1	14.9
4	79.2	70.2	111.0	86.8	31.8	16.6	15.2
5	80.6	72.6	114.9	89.8	34.3	17.2	17.1
6	84.3	73.4	119.3	95.0	35.0	21.5	13.4
7	84.9	75.5	119.4	95.1	34.5	19.6	14.9
8	84.8	72.1	120.0	94.7	35.2	12.6	22.6
9	82.7	72.5	117.6	94.1	34.9	21.6	13.3
10	83.9	73.3	119.0	90.6	35.1	17.2	17.8
11	84.3	74.0	119.4	93.5	35.1	19.5	15.6
12	83.1	75.8	117.5	96.1	34.4	20.2	14.2
13	82.1	68.0	116.4	92.6	34.3	24.6	9.6
14	82.1	74.4	115.0	88.0	32.9	13.6	19.3
15	80.6	75.1	113.0	88.8	32.4	13.7	18.7
16	80.4	72.8	112.9	87.9	32.5	15.1	17.4
17	79.1	70.1	113.7	80.0	34.6	9.9	24.7
18	79.0	72.4	111.7	93.3	32.8	20.9	11.8
19	81.8	71.6	114.3	93.0	32.5	21.4	11.0
20	83.8	71.8	117.7	98.0	33.9	26.2	7.7
21	82.5	66.9	116.2	93.7	33.8	26.8	7.0
22	81.1	75.2	116.0	96.2	34.9	23.0	11.9
23	85.4	70.7	120.4	94.3	35.1	23.6	11.4
24	86.8	70.0	120.8	88.0	34.8	18.0	16.8
AVG	82.0	72.1	1[illegible]	91.3	34.8	19.3	14.8

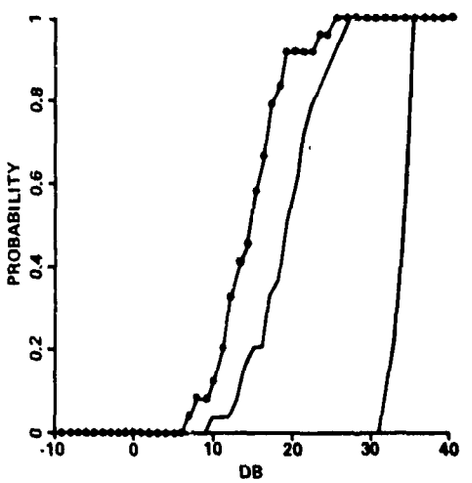

CUMULATIVE PROBABILITIES OF SIGNAL, ARRAY, AND NOISE GAIN

Figure 4-30. (C) Array Performance Statistics for 66.92 Hz (U)

CONFIDENTIAL

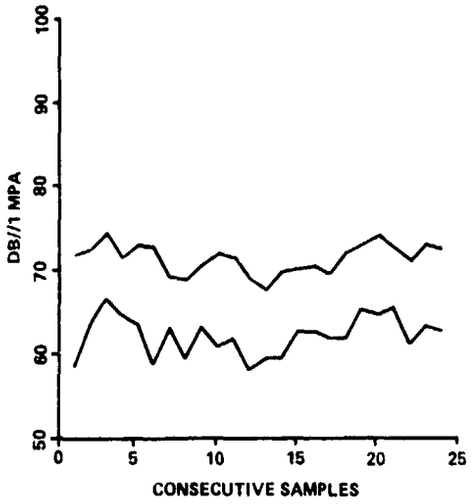

AVERAGE SIGNAL AND ADJACENT BAND NOISE LEVELS FOR THE ARRAY ELEMENTS

PROCESSED 96 48 19 7 222 1979
FREQUENCY 172.94 BEARING 97.16

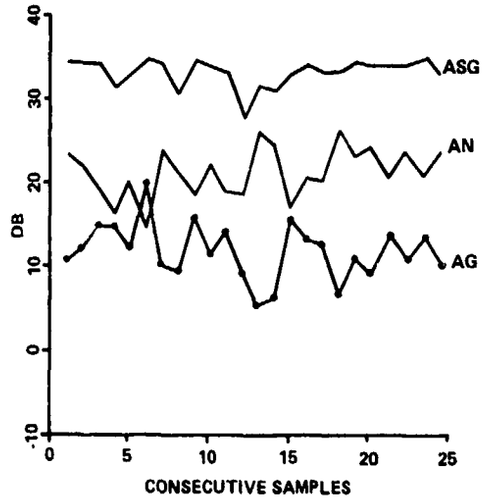

SIGNAL GAIN, ARRAY GAIN, AND NOISE GAIN FOR EACH SAMPLE

ACQUIRED 194 20 28 4
HF ARRAY

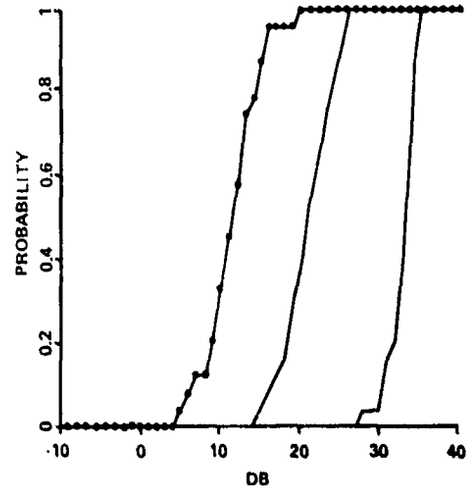

CUMULATIVE PROBABILITIES OF SIGNAL, ARRAY, AND NOISE GAIN

TAPIII HEADER INFORMATION

DATE 13 JULY 1979 REAL TIME 194 20 28 4 RECORD TIME 194 20 28 4
ARRAY TYPE 3 SOUND VELOCITY 1489.0000 SHADING TABLE 1

	FILTER1	FILTER2	FILTER3
FREQUENCY	67.000	173.000	174.890
WINDOW	2	2	2

BANDWIDTH .081224 TYPE RECORD 3
TYPE AVERAGING 1 AVERAGING TIME 0.000

	ELEMENT		BEAM				
	SIGNAL	NOISE	SIGNAL	NOISE	SIGNAL GAIN	NOISE GAIN	ARRAY GAIN
1	71.8	58.4	106.2	81.9	34.4	23.5	10.9
2	72.5	63.2	106.9	85.4	34.3	22.2	12.2
3	74.6	66.5	108.6	85.7	34.1	19.2	15.0
4	71.4	64.9	102.7	81.3	31.3	16.4	14.8
5	73.0	63.7	106.8	84.2	32.8	20.5	12.4
6	72.8	58.8	107.7	73.4	34.9	14.6	20.3
7	69.2	63.1	103.3	87.0	34.1	23.9	10.2
8	68.8	59.5	99.5	80.7	30.7	21.3	9.5
9	70.7	63.3	105.3	81.9	34.6	18.7	15.9
10	72.1	61.0	105.8	83.2	33.8	22.3	11.5
11	71.7	62.0	104.9	81.0	33.1	19.0	14.1
12	69.0	58.3	96.8	76.6	27.8	18.5	9.3
13	67.7	58.7	99.2	85.9	31.5	26.1	5.4
14	70.7	59.6	101.1	84.3	31.1	24.7	6.4
15	70.2	62.8	103.4	80.2	33.2	17.4	15.8
16	70.0	62.6	104.9	83.6	34.3	20.8	13.4
17	69.5	61.8	102.7	82.2	33.2	20.4	12.9
18	72.2	61.7	105.4	88.2	33.3	26.4	6.8
19	73.2	65.4	107.7	88.6	34.5	23.3	11.2
20	74.2	64.8	108.4	89.5	34.2	24.6	9.5
21	72.8	65.8	106.9	86.4	34.0	20.6	13.4
22	71.0	61.4	105.4	85.0	34.4	23.6	10.9
23	73.1	63.4	107.5	84.3	34.4	20.9	13.4
24	72.4	62.8	106.5	85.8	33.1	23.0	10.1
AVG	71.4	62.3	104.7	83.6	33.2	21.3	11.8

Figure 4-31. (C) Array Performance Statistics for 172.94 Hz (U)

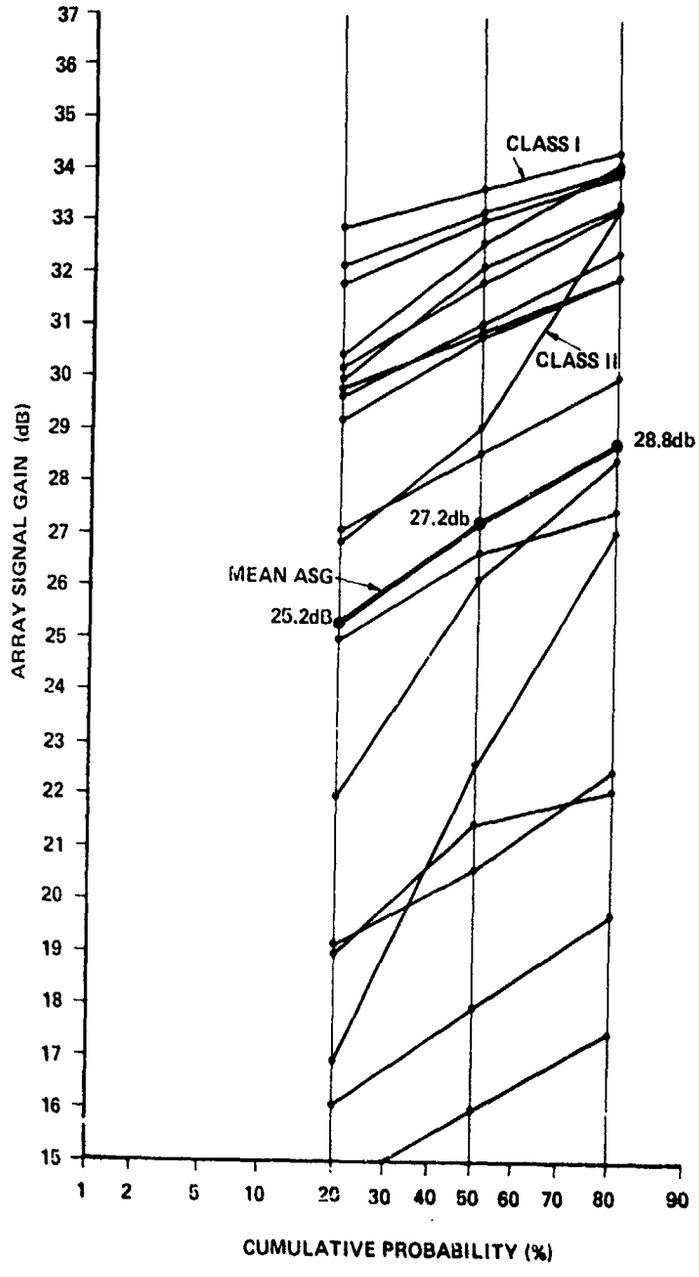

Figure 4-32. (C) Cumulative Probability for Array Signal Gain for the 173 Hz and 175 Hz Data (U)

with median levels of ASG between 16 and 34 dB with a central distribution with a median level of AG of 27.2 dB with a 20% point of 25.2 dB and an 80% point of 28.8 dB. Class II data points are those distributions with sharp inflection points and an obvious asymmetrical behavior. Examination of the sequential time data for these points shows that the ASG is rapidly varying and is most likely influenced by multipath effects. All data shown in Figure 4-32 represent selected points with respectable signal-to-noise ratios on individual hydrophones. Further investigation with the TAP III system was desirable to clarify the nature of these statistical distributions.

(C) Figure 4-33a shows the 173 Hz AG, ASG, ANG data versus the source receiver separation range. Also shown on this plot is the range dependent bathymetry. For this particular case in Figure 4-33b, we have the following summary of median, 10 percentile and 90 percentile values.

	ANG	ASG	AG
10%	6.6dB	27.4dB	12.6dB
50%	10dB	31.2dB	19.6dB
90%	15.8dB	33.4dB	24.8dB

(C) These data represent the statistical performance of the LAMBDA high frequency array in a bottom limited multipath environment. These commulative probability distributions are based on the distribution of twenty-two half hour intervals composed of 24 ensembles of .08124Hz bandwidth and 12.5 sec integration time.

(C) During the same period of time the moored source was observed. The ASG, ANG, and AG data are shown in Figure 4-34a versus the time of observation and the cummulative probability distributions are shown in Figure 4-34b. Also shown at the bottom of Figure 4-34a is the range variation with time. This case represents a summary of the array performance at a relatively constant range from a source in a bottom limited environment. For this case the median, 10 percentile and 90 percentile values are shown in the following table.

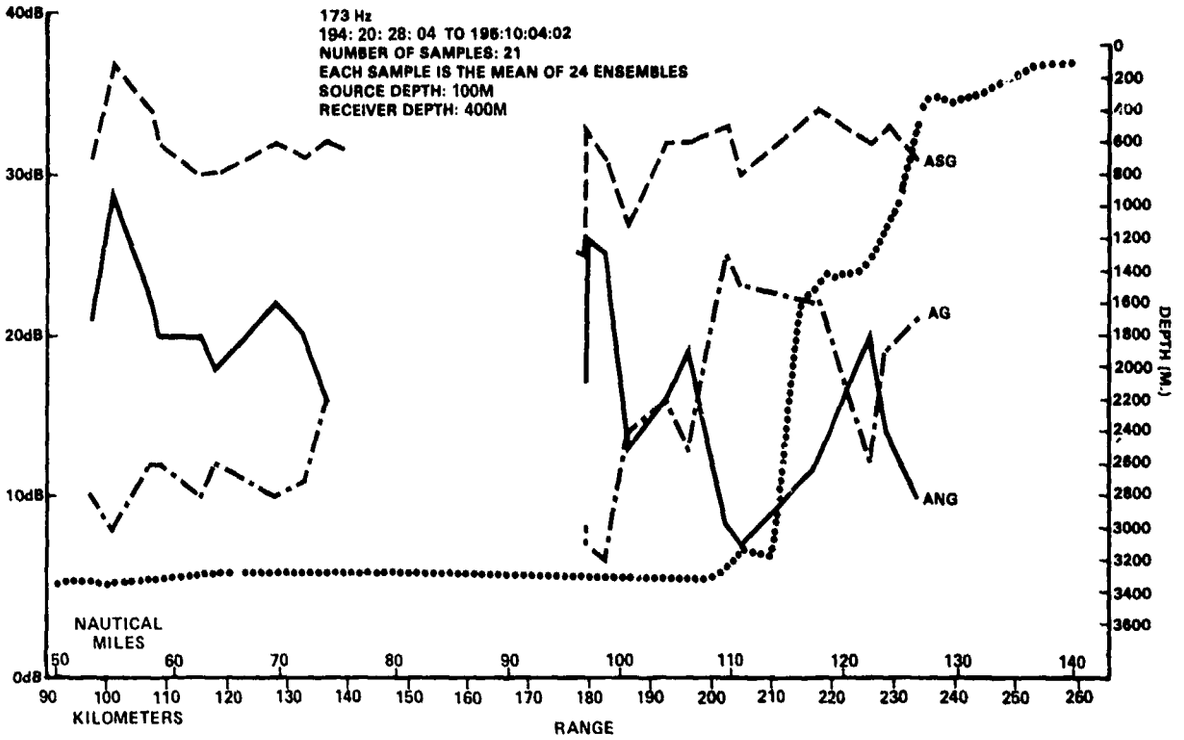

FIGURE 4-33a - (C) TOWED SOURCE, ANG, ASG, AG VERSUS RANGE (U)

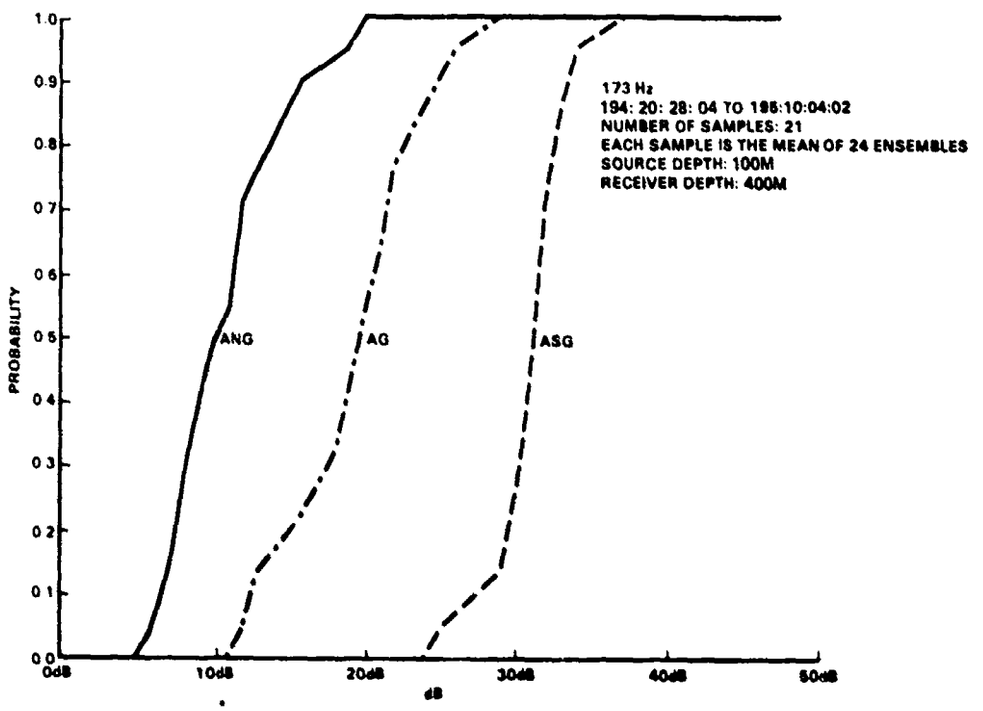

FIGURE 4-33b - (C) TOWED SOURCE, ANG, ASG, AG CUMULATIVE PROBABILITY DISTRIBUTIONS (U)

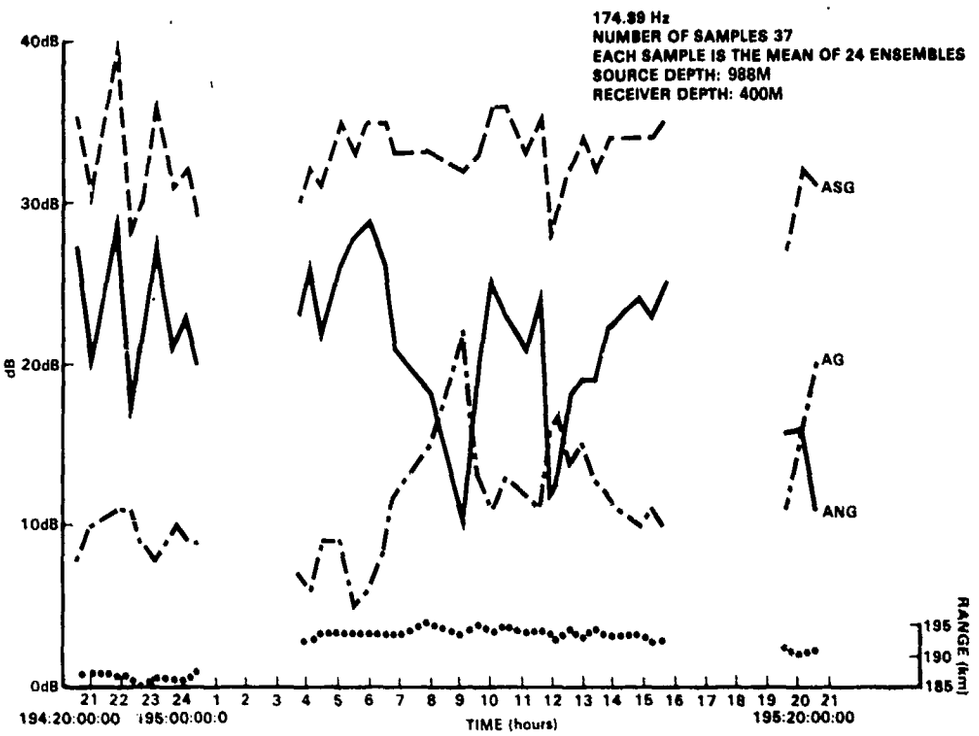

FIGURE 4-34a - (C) MOORED SOURCE, ANG, ASG, AG VERSUS TIME (U)

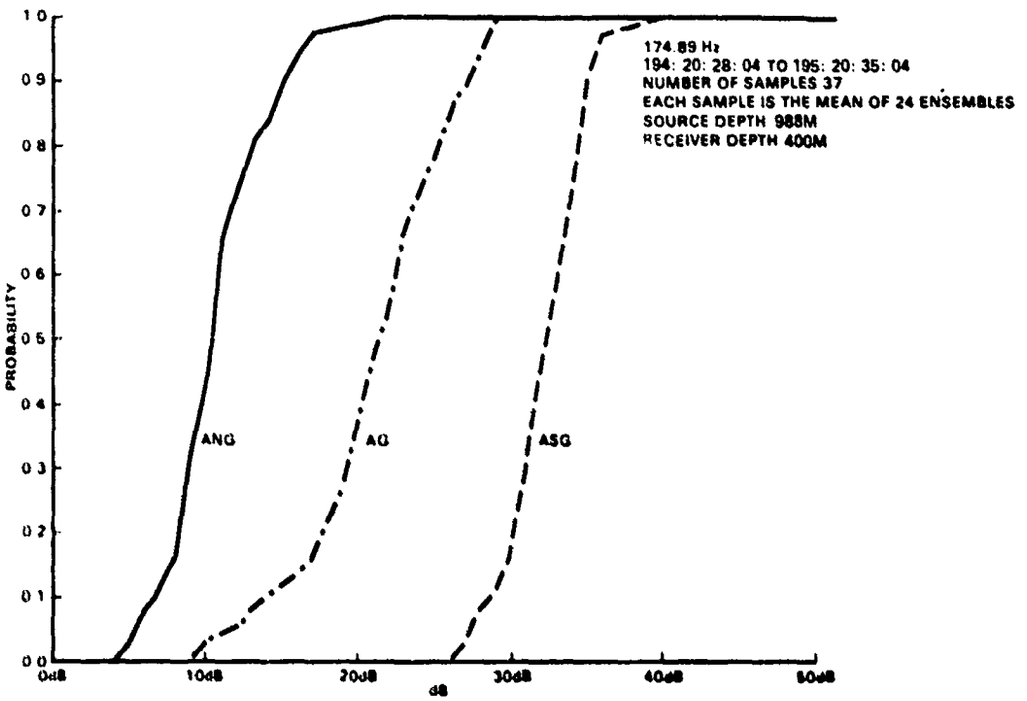

FIGURE 4-34b (C) MOORED SOURCE, ANG, ASG, AG CUMULATIVE PROBABILITY DISTRIBUTIONS (U)

	ANG	ASG	AG
10	6.7dB	28.6dB	14dB
50	10.3dB	32.3dB	21.4dB
90	15.2dB	35dB	27.2dB

These cummulative probability distributions consist of 37 one-half hour samples with each one-half hour sample consisting of twenty-four ensembles with a bandwidth of .08124Hz and an intergration time of 12.5 secs.

(C) In summary the array signal gain was observed to have a median value of 31.2dB for the 173Hz source and 32.3dB for the moored source during the course of the experiment. Rapid fluctuation in the data were observed as a function of time and range. These were most probably due to multipath effects. A comparison of the ASG data in Figures 4-33b and 4-34b show no major differences in the statistical distribution.

5. SUMMARY OF MEASUREMENTS AND EXPERIMENTAL RESULTS

(U) The CHURCH STROKE III Cruise 1 Exercise was conducted in July 1979 in the Entrance to the Gulf of Mexico including the western portions of the Florida Channel, the northern end of the Yucatan Channel, portions of the Tortugas Terrace and the East Yucatan Channel, the Catoche Tongue and the Eastern region of the Gulf of Mexico.

(U) The exercise was conducted by the Long Range Acoustic Propagation Project (LRAPP) of the Naval Oceanographic Research and Development Activity.

(U) Acoustic and supporting environmental data were acquired in order to provide information for the acoustic assessment of the region.

(U) The major assets employed during the exercise were the LAMBDA III Measurement System installed on R/V INDIAN SEAL, the HX-231F Sound Projector towed by the USNS DESTEIGEUR and the Webb Sound Source moored at the center of the exercise area. Both ships participating in the exercise were equipped with specialized navigational and environmental measurement systems supplementing and supporting the major roles of the ships in the meeting of exercise objectives.

(U) All acoustic systems used during the exercise were calibrated.

(U) The HX-231F Sound Projector was calibrated by the Naval Ocean Systems Center at Lake Pend Oreille using established procedures. The HX-231F Sound Projector emitted CW signals of 67 Hz and 173 Hz with source levels of 179.3 dB// 1μPa at 1 meter and 183.4 dB// 1μPa at 1 meter respectively. The error of the calibration is ± 0.4 dB. (Ref. 20)

(U) The Webb Sound Source was calibrated by the Underwater Sound Reference Division of the Naval Research Laboratory before deployment, and operated at 174.89 Hz with a source level of 171.0 dB// 1μPa at 1 meter.

(U) The hydrophones of the receiver, the LAMBDA III Measurement System were rigorously calibrated at different steps of the manufacture of the array. The individual hydrophone elements were carefully selected by a binning technique described in Ref 6. This selection ensured reliable and consistent sensitivities. Thirty-seven of the Benthos manufactured AQ-1 hydrophones were tested by the Underwater Sound Reference Division of the Naval Research Laboratory in its facilities at Orlando, Florida. All individual hydrophone elements, groups and array modules were calibrated by the CAVAC method developed by NOSC.

(U) These calibrations were verified by at-sea measurements using the Lloyd-Mirror calibration method described in Section 2.1.5 of this report.

(U) Electronic calibration of the LAMBDA III System was accomplished by several methods as described in Section 2.1.5 and in Reference 10 and Appendicies 1 and 2 of this report. The results of these calibrations were consistent with the results of the built-in calibration tests of the NOSC Ambient Noise Directionality Program and the tests conducted using calibrated tonal signals.

(U) Nonacoustic support data were obtained during the exercise such as ship speed, heading, wind speed, array heading and array depth data.

(U) Thirty-two sound velocity profiles were measured along the Exercise Baseline by the USNS DESTEIGEUR providing the data base for the isovelocity contours presented in Figure 3-4 and the sound velocity profiles presented in Figure 3-5. The tow measurements were corrected, analyzed and the refined information provided by NORDA Code 321.

(U) Weather information was collected throughout the Exercise. The general sea-state condition was calm to moderate and wind speed was variable -=20knts. Durations of higher wind speeds were not long enough to allow the full development of the sea.

(U) Bathymetric information was obtained along the track of the tow ship by using a Precission Depth Recorder. The tow data was later corrected for the appropriate sound velocity. The depth information presented in the report is based on the corrected values.

(U) Navigation data for both the R/V INDIAN SEAL and the USNS DESTEIGEUR were obtained by a Satellite Navigational System and later rectified by NORDA 320. All range and location information were derived from the rectified navigational data. It is estimated that the maximum uncertainty in location is ± 0.3 nm, in range ± 1 nm.

(U) Current measurements were not obtained during the exercise. The isovelocity contours however give a good indication about the behavior of the Loop Current of the Gulf of Mexico.

(U) The quality of the obtained information is judged excellent. Acoustic data on which the results presented in this report are based were acquired under well defined conditions dealt with rigorously calibrated systems.

the frequency levels are reliable, and the positions, and ranges are known to adequate accuracy. Bathythermal and bathymetric conditions are known to the extent required for the objectives of the measurements and their analysis.

5.1 SUMMARY OF THE MEASUREMENTS

(U) The acquired acoustic data was obtained and processed onboard the R/V INDIAN SEAL and analyzed on shore.

(U) The following parameters were produced by the onboard processing for transmission loss determination:

- Hydrophone Spectra for selected time periods by the Spectral Dynamics 301 Spectrum Analyzer.
- Average Hydrophone Spectra for selected 12 or 24 data resembles.
- Received Signal Levels as function of hydrophone number and frequency for a selected number of data ensembles.
- Coherence for selected data sets.
- Hydrophone level as function of time for selected number of data ensembles.

(U) All of the above mentioned data was processed for the signal frequencies (67 Hz, 173 Hz, 175 Hz). Some of the parameters covered the full 4 Hz wide frequency bands centered at the signal frequencies, some of the parameters were processed only for a few (up to 5) frequencies.

(U) Measurements used in the transmission loss analysis were obtained for four major time periods corresponding to the four legs of the track traveled by the USNS DESTEIGEUR towing the sound projector at 100 m depth. Data gaps occured due to equipment failure, maneuvers of the R/V INDIAN SEAL, calibration etc. The receiver operated in the vicinity of Site E. The source followed tracks connecting Sites F and E, E and G, G and E, E and F. (See Figure 3-3) Transmission loss data was obtained for:

- Leg F-E between 23 and 56 nm from Site E in the basin between the Florida escarpment and the East Yucatan Shelf. The receiver was at a nominal depth of 800 m.

- Leg E-F between 56 and 131 nm from Site E in the basin between the Florida Excarpment and the East Yucatan Shelf and up on the slope to the Florida Shelf. The receiver depth was at a nominal depth of 400 m.
- Leg E-G between 48 and 96 nm from the receiver located 22 nm northeast from Site E in the Catoche Tongue up on the East Yucatan Slope. The receiver was at a nominal 800 m depth.
- Leg G-E between 55 to 180 nm from Site E downslope on the East Yucatan Slope toward the Catoche Tongue. The receiver was at a nominal depth of 400 m.

(U) The data acquired at 67 and 173 Hz and at ranges to 108 nm for Leg E-F represents transmission loss characteristics at deep but bottom limited propagation conditions. The data at greater ranges exhibits the effects of the slope. Both types of propagation are dominated by bottom interference.

(U) It was established that transmission loss at 67 Hz can be defined by an empirical cylindrical spreading loss formula with a bottom loss value of 0.5 dB/bounce for glazing angles between 5-16^0 where most of the propagating acoustic energy is concentrated.

(U) The transmission loss at 173 Hz can be determined by the same empirical cylindrical spreading loss formula but with a bottom loss value of 1.5 dB/bounce for this frequency. Absorption loss is negligible at the measured ranges.

(U) The "Slope Effect" becomes observable when the source is still in deep water over the beginning of the slope. This effect exhibits itself in the measured data by the change of trend in the transmission loss values as function of range. The "Slope Effect" is defined as the dB difference between the transmission loss values measured over the slope and the transmission loss values derived from the empirical curves at the range where the measured minimum occurs over the slope.

(U) This effect is 3 dB for 67 Hz assuming a bottom loss of 0.5 dB/bounce bottom loss and is 6 dB for the 173 Hz data with bottom loss of 1.5 dB/bounce.

(U) Data are presented for Legs E-G and G-E; however, these measurements were acquired only over the slope. Transmission loss values were not determined for deep water propagation conditions and the lack of this information prevented the establishment of the effect of the slope for these legs.

(U) Limited measurements were made for Leg F-E. All measurements were obtained in deep water, off the slope, and therefore the determination of the "Slope Effect" was not possible. Missing measurements are not recoverable from the records of tow data. Equipment malfunction, ship operations, calibration procedures were the primary reasons for not being able to obtain the necessary information for analysis.

(U) Signal coherence information was analyzed for selected data segments of the approximately 300 m long High Frequency array. It was found that signal coherence is a function of signal to noise ratio in the presence of the directive coherent noise field of the tow ship. The measured signal coherence is a clear representation of bottom limited propagation conditions. The magnitude square coherence varied between 60 and 100% as function of distance.

(U) The following parameters were obtained for the analysis of array performance:

- Beam and Hydrophone Spectra for selected 12 or 24 data ensembles
- Received Signal Levels as function of hydrophone number and frequency providing acoustic illumination characteristics of the array for averages of selected numbers of data ensembles.
- Coherence Information on selected data sets.
- Array Signal Gain, Array Noise Gain Estimates using standard signal to noise determination techniques
- Bearing of Signal Beam for bearing accuracy estimates.

All of the above data was processed for the signal frequencies (67 Hz, 173 Hz and 175 Hz). Measurements for array performance analysis were obtained in parallel with transmission loss measurements and selected parameters were routinely processed for array performance characteristics determination. Selected data segments were processed for detailed analysis.

(U) The data acquired for transmission loss and array performance analysis were selectively processed and analyzed to determine signal fluctuation characteristics.

5.2 Discussion of Transmission Loss Data (U)

(U) Sound transmission in the Gulf of Mexico is bottom limited for shallow sources and receivers. Under these conditions sound propagation is described by sound transmission theory Ref. 21 (Officer, page 97-101). In this case, sound energy is propagated at all angles between the limiting and critical rays. At ranges greater than the cycle distance of the limiting ray all rays in this sector contribute to sound intensity. The contribution is not equal for all rays, for two reasons; all other rays have a shorter cycle distance than the limiting ray and strike the bottom at a higher grazing angle. If there were no bottom loss all rays would contribute equally resulting in a cylindrical spreading loss. However, it is known from Mitchell (Ref. 4) that the bottom loss is finite at low grazing angles (in the order of 0.5 to 1.0 dB at 67 Hz per reflection in the measurement area) and increases with grazing angle and frequency.

(U) This behavior tends to reduce the relative intensity of the higher angle rays especially at higher frequencies, with the result that the sound energy tends to concentrate at angles near the limiting ray. This effect is more noticeable at the high frequencies in regions where the bottom loss is low to moderate. Complicating the picture of bottom loss is the penetration of sound into the sub layer of the bottom. Mitchell (Ref. 4) discusses the refraction of the sound in the sub-bottom layer and points out that, at low frequencies, the concept of a point bottom loss value is not valid. The reason is that sound rays penetrate the bottom, enter the thick sedimentary layers and are refracted. These rays re-enter the water at a greater range but at the same angle as the reflected ray. The ray has split into two parts, one part being specularly reflected and the other refracted and returned to the water. The combination produces the arrival at the measurement point. The bottom loss "per bounce" is the loss suffered by the combined rays. For our purposes we have followed this description and estimated the loss per bounce from the empirical fit to the data.

(U) Our case considers shallow receivers (400-800m) and sources (100-1000m) only. With this source-receiver geometry, sound transmission loss under the

conditions of bottom limited propagation over a uniform flat bottom will result in transmission loss minima at definite range intervals. The strength, extent and spacing of these minima depend upon frequency and bottom loss values. At higher frequencies (up to 200Hz) we would expect sharper peaks in the TL versus range curves tending to concentrate in range toward the range cycles of the limiting ray. At lower frequencies, these peaks will be spread out in range as the rays of higher grazing angle contribute more to the intensity. The behavior of TL as a function of range may be described (Ref.22) by an initial spherical spreading to some reference range with a transition to cylindrical spreading (if the bottom loss is not too high) plus a mean loss per bounce reckoned on the average number of bounces of rays between the limiting and critical rays, $\bar{N}$, and an average bottom loss per bounce, B. The exact value of TL at the first peak depends upon the number of rays concentrating in that region and the spacing of the rays in a ray tracing diagram at that range. If the ray density becomes high enough, intensity estimates made by single ray counting become difficult and thus wave theory must be used. If neither the bottom properties nor the sound velocity profile change between successive TL minima, the value of minimum TL will be dependent only upon cylindrical spreading and bottom loss. This is because the region of energy concentration is spreading on a cylindrical surface of separation Δh according to

$$TL = 10 \log R\Delta h/\Delta\theta + \bar{N} \cdot B$$

where θ is the initial angular spread on the rays contributing to the TL at range, R. Although Δh depends upon range, it approaches a minimum at definite range intervals and is a constant for successive cycles. This leaves only bottom loss and the influence of 10 log R to effect the transmission minima.

(U) For this reason the TL data are assumed to take the following form

$$TL = A_B + 10 \log R + \bar{N}(R) \cdot B.$$

For the data presented in this report $\bar{N}(R)$ has been determined from ray trace diagrams. Then the value of A_B is taken to be the measured TL at the first

TL minimum in the data modified by the value of $\bar{N} \cdot B$ to that range. For greater ranges, curves of TL with B as the parameter are determined and the best "eye ball" fit to the experimental data is determined. These values are

0.5 to 1 dB/bounce at 67Hz
1.5 to 2 dB/bounce at 173Hz

The experimental values of bottom loss are consistent with the curves presented by Mitchell in the pre-exercise estimates based on the two-path "geoacoustic" model. The data indicate that a low to medium bottom loss describes the region of the experiment and explains the "good" sound transmission experienced in this experiment.

(U) The value for limiting ray grazing angle is slightly higher than the 8^0 value indicated in the pre-exercise estimates. Based on the measured cycle distance at high frequencies, a value of 9.24^0 was determined which yields a cycle distance of 18.6 nm.

(U) With the "best" value determined for bottom loss as a function of frequency and grazing angle, the FACT transmission loss model (Fast Asymptotic Coherent Transmission Loss Model, (Ref 23) was run for a constant sound speed profile and flat uniform bottom with coherent summation. This widely used model is a Navy Interim Standard Model and employs ray tracing and summation of the rays that reach a given receiving point (including those that strike the bottom with some loss). These rays are phase summed according to the assumptions on the coherence between rays.

(U) Using the ARL curves (Figure 3-8) with the bottom loss description as "low loss" and "medium loss," TL versus range curves were computed for the two lower source frequencies, 67 and 173 Hz. These curves are shown overplotted on the experimental data for leg E-F on Figures 5-1 and 5-2. Also shown is the empirical data fit determined in Chapter 4.

(U) Comparing the experimental data with the FACT computations at 67 Hz, the following is noted:

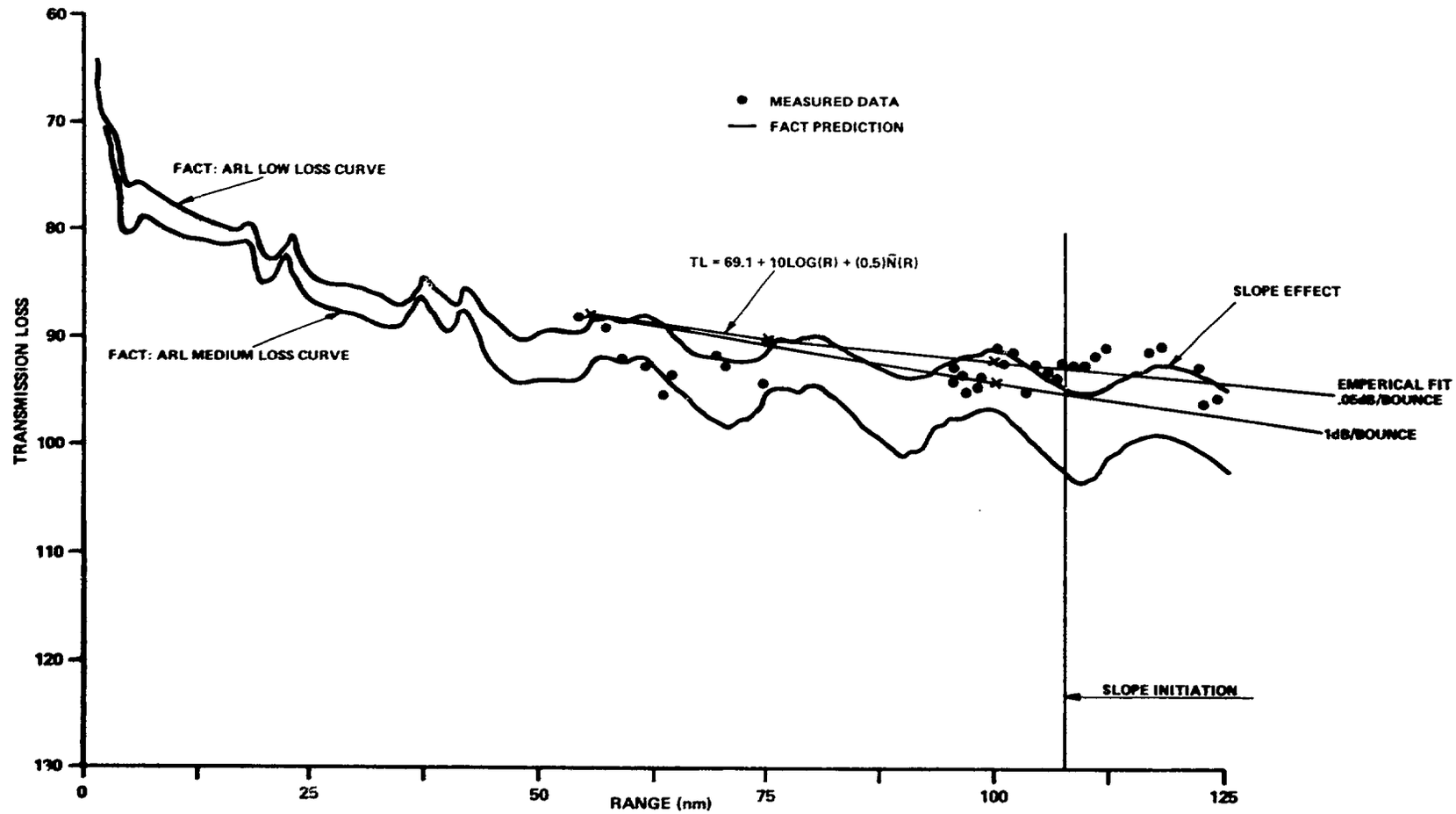

Figure 5-1. (U) Comparison of FACT Predicted and Measured Transmission Loss Values at 67 Hz as Function of Range for Leg E-F (U)

UNCLASSIFIED

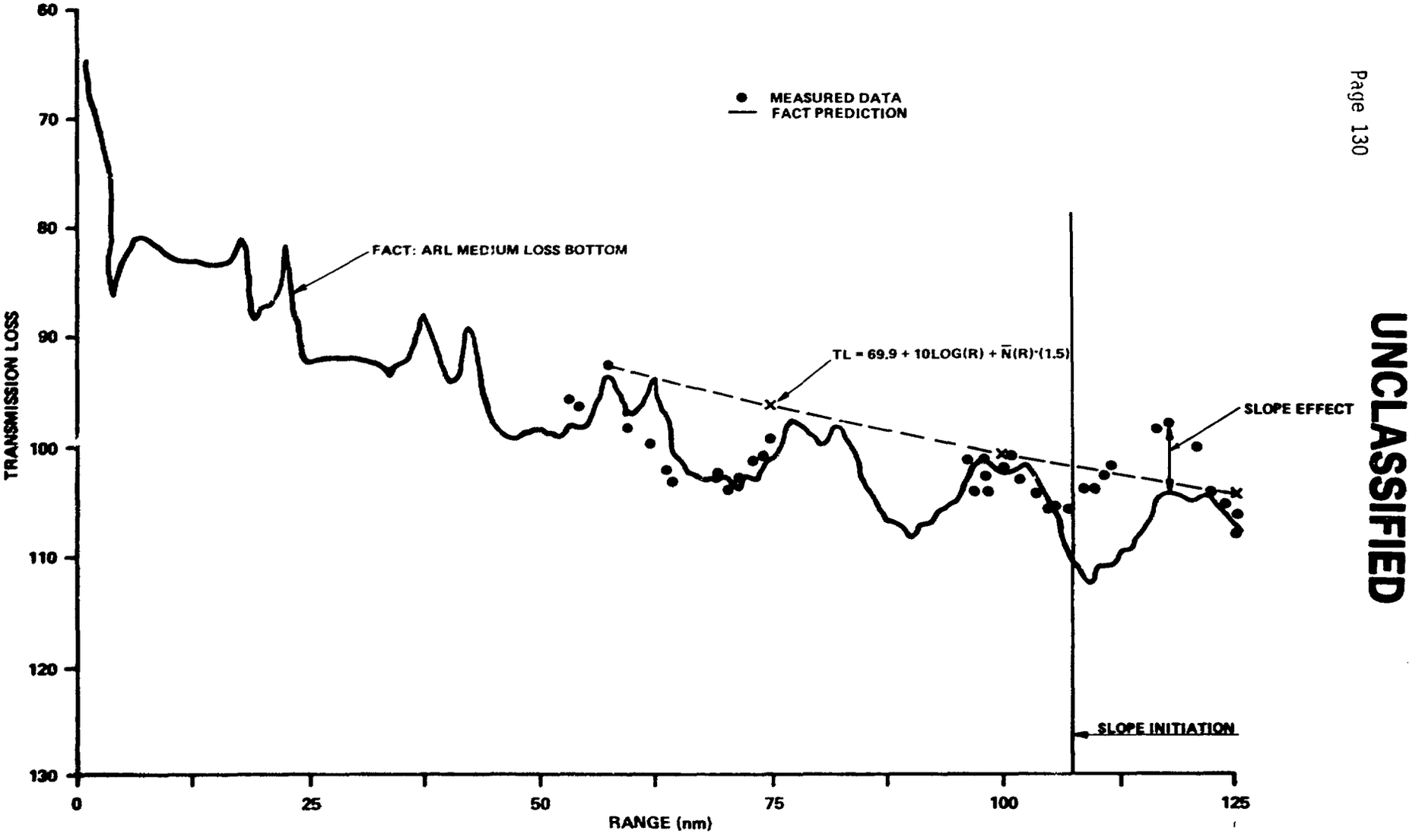

UNCLASSIFIED

Figure 5-2. (U) Comparison of FACT Predicted and Measured Transmission Loss Values at 173 Hz as Function of Range for Leg E-F (U)

(1) Between 50nm and 75nm, the points of minimum TL agree well with the 0.5dB/bounce curve and the "low loss" bottom described by ARL.

(2) Between 96 to 108nm, the FACT minimum and the data agree well and also follow the empirical curve for 0.5dB. All of the data lie in the region between the ARL "low" loss and "medium" loss curves and fit well to the region between the 0.5dB and 1.0dB per bottom bounce empirical curves.

(3) At 108nm, the range at which the bottom begins to slope up toward the Florida shelf, a change occurs in trend of the TL experimental data. This is called the "slope effect" and is measured for our purposes by the deviation of the measured TL data from the "best" fit or computed TL. At the minimum value of TL occurring at 118nm range the slope effect is 2-4dB relative to the FACT computations and ∿ 3dB relative to the empirical curves.

(U) The major point of the 67Hz data is that there is excellent agreement with the FACT model in the region of flat bottom before the slope is reached.

(U) The 173Hz data show similar behavior as seen in Figure 5-2, where the FACT model and empirical fit are overplotted on the experimental data. The following points are noted in the comparison:

(1) TL minima meet the empirical curve with 1.5dB/bounce bottom loss.

(2) The range and values of TL minima agree well with the FACT computations using the ARL "medium" loss bottom out to the range of slope initiation, 108nm.

(3) The slope effect begins in the deep water portion of the slope and reaches a maximum value at 118nm of 6dB relative to either the FACT computations or the empirical data fit.

(U) At 173Hz, the agreement between experimental data and FACT computations is excellent in the region of flat bottom if the ARL "medium" bottom loss values are used.

(U) In summary, we have found that the calibrated data set is in excellent agreement with the FACT model with the low to medium loss bottom characteristics of Mitchell (Ref 4). These data provide a basis for detailed TL studies exploring the further effects of bottom loss, slope enhancement, fluctuations and environmental effects such as the influence of the loop current.

5.3 DISCUSSION OF ARRAY PERFORMANCE RESULTS

(C) It was found that in a multipath environment the primary descriptor for the performance of a towed array is Array Signal Gain. The examination of Array Noise Gain revealed that it is dominated by the directional noise field of the tow ship. This condition is most likely characteristic of other towed arrays also.

(C) Array Signal Gain was determined by comparing the measured beam level in the signal beam with the signal level averaged through the 64 hydrophones. Array Noise Gain was determined by using several techniques. (See Section 4.2.1) Noise values were insensitive to the averaging technique when spectral peaks were ignored and the average was taken over the TAP III filter band (5.2 Hz wide).

(U) The analysis-based on extensive data-produced the following key results:

- o Half-power Beam Width is approximately $1.71^{\circ} \pm 0.35^{\circ}$
- o Side lobe levels near the Signal Beam are -9 dB for the first side lobe and -17 dB for the second side lobe. The remaining side lobes have levels between -20 dB and -27.5 dB.
- o Beam Width and Side Lobe levels are comparable to expected values for a line array of 64 median hydrophone locations with 6 inoperative hydrophones.
- o Array Signal Gain was estimated to be between 31 and 32 dB. Theoretical Array Signal Gain for line array of 64 hydrophones is 36.1 dB. The cummulative probability of Array Signal Gain estimates are:

	173 Hr.	175 Hr.
90%	33.4	35
50%	31.2	32.3
10%	27.4	28.6

- o Array Noise Gain, the median values were estimated to be 10 dB. The cummulative probability for these estimates are:

	173 Hr.	175 Hr.
90%	15.8	15.2
50%	10	10.3
10%	6.6	6.7

- o The results of the analysis suggest that the statistical distribution of Array Signal Gain is a Log Normal Distribution when the multipath environments were not changing rapidly.
- o Bearing accuracy was determined to be -1.6° to -4.7°. These errors can be the results of many causes, the most obvious being array tilt and array motion.

(This page is unclassified.)

6.0 CONCLUSIONS AND RECOMMENDATIONS

6.1 CONCLUSIONS

1. (U) Transmission loss data was acquired in the entrance to the Gulf of Mexico with a calibrated measurement system using tonal signals emitted by calibrated sound projectors. Supporting environmental information such as bathymetry and sound velocity profiles along the measurement tracks, and ship locations in the measurement area were also obtained.

   (U) The signal and support data sets represent a complete collection of information necessary to determine sound transmission characteristics in bottom limited and slope affected conditions. Signal data were acquired at 67 Hz and 173 Hz at source/receiver depths of 100/400 and 100/800 meters.

2. (U) The transmission loss results, interpreted as a function of range, are consistent with ARL expectations for bottom limited propagation encountering medium to low bottom loss conditions. When the influence of the slope was absent the measured transmission loss values fall in a region representing transmission loss determined by cylindrical spreading law. Furthermore, agreement with the FACT Model, the Navy's standard model, was also apparent for this condition when the ARL medium to low bottom loss curves were employed.

3. (U) The degree and location of initial effect of slope enhancement were determined by the range where the measured transmission loss values began to decrease with respect to the increasing trend established by ray analysis. This ray analysis shows similar trends up to this range as the measurements and the FACT model. Slope enhancement effect for a towed source proceeding from deep water towards the slope was observed by a change in the TL data trend when the source reached the bottom of the slope.

4. (U) Short term fluctuation data and their related statistics were acquired, processed and analyzed for approximately 12 and 24 minute time periods. Standard deviations determined from power averaging were found to be between 3 and 5 dB in the band of the signal. These observations are consistent with the results obtained by Urick and Dyer for bottom limited propagation.

PRECEDING PAGE BLANK-NOT FILMED

5. (U) Long term fluctuations of the 23 and 24 minute mean values taken for an approx. 24 hour period were found to be correlated with multipath structure due to changes in range between the sources and receiver. When the moored and towed sources had similar path structures their fluctuations were correlated.

6. (C) Beam response patterns indicated that the directional noise field was due to the array tow ship, the R/V INDIAN SEAL coherence analysis showed that this directional noise field was partially coherent. Array noise gain estimates reflected this coherence. Beam response curves for the high signal to noise ratio data were found to yield a near broad side beam width of 1.71° and mean side lobe level of 27.5 dB.

7. (C) Array signal gain ranged from 15 dB to 34 dB. The distributions of array singal gains were found to lie in two groups. One group with 60% of the data within 3 dB of the median value and another group with a wide and rapid variations. The array signal gain was found to depend on the multipath structure and; consequently, the statistics of these distributions are also decided by changes in the structure. It is concluded that array signal gain is the major parameter to be considered in the assessment of array performance under this type of bottom limited correlation.

8. (U) Coherence data were obtained over the aperature length of 300 meters. When the signal to noise ratio was high (S/N > 15 dB) a true measure of the coherence was observed.

9. (C) Array tilts of 4 to 12 degrees were observed. This tilt of the array was found to produce bearing errors between 1.5 to 5° depending the degree of tilt. A negative bias in the errors was attributed to upward tilt of the array.

10. (C) Array data consisting of spectral properties of the hydrophone groups and beams were necessary to determine the array performance, spatial variations, and to interpret the coherence data. The complete set of data enabled an analysis of a sinusoidal signal in a coherent noise background with multipath effects. In a multipath environment towed array performance is affected by array signal gain and its fluctuations. This is partially due to the relative variation of the source and receiver positions, and also the fluctuations in the medium along the transmission path.

6.2 RECOMMENDATIONS

1. (U) Measurements performed to characterize the performance of an array should be taken such that amplitude and phase information is preserved. At a minimum the following data should be obtained:

   a. Hydrophone average spectra and standard deviation.

   b. Beam spectra.

   c. Signal level and noise level versus aperture.

   d. Signal level and noise level versus beam number.

   e. Beam noise statistics.

2. (U) Coherence data are useful in interpreting array performance data. In the measurement of signal coherence on underwater acoustic signals with a towed array, only S/N > 15 dB data should be used to attribute the coherence to the signal.

3. (U) Signal structure studies of this kind should not be subjected to communications limitations imposed by simultaneously conducted fleet operations.

4. (U) Environmental data acquisition including knowledge of the bottom characteristic derived from core samples or measurements of bottom loss are necessary in transmission loss studies.

5. (U) Studies performed with towed arrays should have their absolute calibration factors verified at sea with a Lloyd mirror type calibration.

6. (U) Short term and long term fluctuation data obtained in this experiment should be further analyzed and compared to theoretical models.

7. (U) Slope enhancement effects observed in this experiment as well as other measurements should be the subject of more theoretical and experimental investigation. Explosive experiments which allow identification of individual paths should be performed. The data obtained in this report represents an unusual look at propagation of sound for a source proceeding from deep water to a shallow depth. Also the propagation of sound from a source moving up slope and down slope is also available.

8. (U) Data obtained in experiments such as these should be taken so that analysis on multiple signal processors is possible.

9. (U) The data in this experiment represent a rare case of absolute calibrated acoustic data under known bathymetric and environmental conditions. Close agreement with Navy Standard Models is also apparent. For these reasons a more comprehensive examination of the TL data would be warranted, especially since sound field coherence, signal statistics, and fine structure could be examined and additional TL versus range could be realized. A brief qualitative investigation of these effects has been presented in this regard. A finer examination with more sophisticated models is warranted to further qualify the slope effects.

10. (U) During this experiment a moored source was continuously transmitting data at a depth of 911 m and the array was at a depth of 400 m. The range separation between these two systems was not changing drastically. This data set represents a continuous measure of signal propagation and array performance in an interesting oceanographic area. These vital data should be analyzed in a continuous fashion.

7.0 REFERENCES

1. "Exercise Plan for CHURCH STROKE III" (U)
Long Range Acoustic Propagation Project Report NO.: S79-032
1 June 1979. (SECRET).

2. "Exercise Plan for CHURCH STROKE III; Annex A. Cruise 1." (U)
Long Range Acoustic Propagation Project Report No.: S79-032A
1 June 1979. (SECRET).

3. CINCLANTFLT, Norfolk, Va. 022304Z. July 1979.

4. "Gulf of Mexico and Caribbean Sea Data and Model Base Report" (U)
Long Range Acoustic Propagation Project Report No.: C79-027
July 1979. (CONFIDENTIAL).

5. "Quick Look Report for CHURCH STROKE III. Cruise 1" (U)
TRACOR, Inc. Document No.: T-79-RV-72S
13 September 1979. (SECRET).

6. Doolittle, R.D. "Hydrophone Evaluation for the LAMBDA III Array" (U)
Underwater Research Corp. Report No.: URC 79-10
June 1979. Contract No.: N00014-78-C-0129 (UNCLASSIFIED).

7. Rennie, Lawrence J. "The TAP III Beamforming System" Proceedings of IEEE OCEANS '79 Conference 17-19 September 1979, pp. 6-13.

8. "TAP III Final Report" (U). Bunker Ramo Report No.: U.0048-9C2
September 1979. (CONFIDENTIAL).

9. Madon, Rabinder N. "FIR Digital Filters in a Linear Array Processor"
Proceedings of IEEE OCEANS '79 Conference, September 1979, pp. 1-5.

9a. Blackman, R. B. and Tukey, J.W. "The Measurement of Power Spectra."
Dover Publications, Inc New York, N.Y. 1959.

10. Hecht, R. J.; Weinstein, M.S. "Quick Look Report, Oil Industry and Array Performance" (U) Underwater Systems Inc. Report No.: 720-1-80
30 November 1979. (CONFIDENTIAL).

11. Levine, Harold and Schwinger, William. On the theory of Diffraction by an Aperture in an Infinite Screen I. Physical Review October 15, 1948, Volume 74, Number 8, pp 958-974.

12. "Acoustic Source System as Installed on USNS DESTEIGUER" (U) Naval Undersea Center, Code 302, Internal Memo, July 1976. (UNCLASSIFIED).

13. Bucca, P.F. and Worsley, W.W. "The Environmental Variability during Phase I of the CHURCH STROKE III Exercise." NORDA Tech Note 29
(In preparation). (CONFIDENTIAL).

REFERENCES CON'T.

14. "Environmental-Acoustics Atlas of the Caribbean Sea and Gulf of Mexico. Vol. II Marine Environment". U.S. Naval Oceanographic Office Publication SP-189 II. August 1972. (UNCLASSIFIED).

15. Mitchell, S.K. "Pre-Exercise Estimates of Bottom Interaction in the Gulf of Mexico and the Caribbean Sea." Applied Research Laboratory, University of Texas. January 1979. (UNCLASSIFIED).

16. Browning, D.; Koenigs, P.; Laplante, R. "Attenuation Coefficients for the Caribbean Sea and the Gulf of Mexico"(U) Naval Underwater Systems Center Technical Memorandum No.: TA11-200-75. 10 July 1975. (UNCLASSIFIED).

17. R. J. Urick, "Models for Amplitude Fluctuations of Narrow-Band Signals and Noise in the Sea," J. Acoust. Soc. Am., 48, 759, (1970).

18. I. Dyer, "Statistics of Sound Propagation in the Ocean," J. Acoust, Soc. Am., 48, 337, (1970).

19. A. D. Whalen, Detection of Signals in Noise, (Academic Press, New York, 1971), pp. 87-122.

20. Percy, Joseph L., "A Quick Look at the Error Analysis of the April 1979 recalibration of the HX-231F", NOSC Memo: Serial 724/35-80, May 14, 1980, Unclassified.

21. C. B. Officer, "Introduction to the Theory of Sound Transmission," (McGraw-Hill, New York, 1958), pp. 97-101.

22. R. J. Urick, "Principles of Underwater Sound for Engineers," (McGraw-Hill, New York, 1967).

23. C. W. Spofford, "The FACT Model", Maury Center For Ocean Science, MC Report 109, November 1974.

8. DISTRIBUTION LIST (U)

ASSISTANT SECRETARY OF THE NAVY
(RESEARCH, ENG. AND SYSTEMS)
DEPARTMENT OF THE NAVY
WASHINGTON, DC 20350
ATTN: G. A. CANN 1

CHIEF OF NAVAL OPERATIONS
DEPARTMENT OF THE NAVY
WASHINGTON, DC 20350
ATTN: OP-02 1
OP-03 1
OP-05 1
OP-095 1
OP-096 1
OP-951 1
OP-952 1
OP-951F 1
OP-952D

HEADQUARTERS
NAVAL MATERIAL COMMAND
WASHINGTON, DC 20360
ATTN: CODE MAT-08T245 2

PROJECT MANAGER
ANTISUBMARINE WARFARE SYSTEM PROJ
DEPARTMENT OF THE NAVY
WASHINGTON, DC 20360
ATTN: PM-4 2

DIRECTOR
STRATEGIC SYSTEM PROJECTS OFFICE
DEPARTMENT OF THE NAVY
WASHINGTON, DC 20376
ATTN: PM-1 1

CHIEF OF NAVAL RESEARCH
800 NORTH QUINCY STREET
ARLINGTON, VA 22217
ATTN: CODE 100 1
CODE 102B 1
CODE 220 1
CODE 230 1
CODE 460 1
CODE 480 1

COMMANDER
NAVAL ELECTRONIC SYSTEMS COMMAND
NAVAL ELECTRONIC SYS COMMAND HDQS
WASHINGTON, DC 20360
ATTN: PME-124 1
PME-124TA 1
PME-124730 1
PME-124/40 1
PME-124/60 1
ELEX-320 1

COMMANDER 1
NAVAL SEA SYSTEMS COMMAND
NAVAL SEA SYSTEMS COMMAND HDQS
WASHINGTON, DC 20362
ATTN: NSEA-06H1 1

COMMANDER 1
NAVAL AIR SYSTEMS COMMAND
NAVAL AIR SYSTEMS COMMAND HDQS
WASHINGTON, DC 20361
ATTN: NAIR-370 1
PMA-264 1

DEPUTY UNDER SEC OF DEFENSE FOR 1
RESEARCH AND ENGINEERING
DEPARTMENT OF DEFENSE
WASHINGTON, DC 20301

DEFENSE ADV RESEARCH PROJ AGENCY
1400 WILSON BOULEVARD
ARLINGTON, VIRGINIA 22209
ATTN: DR. T. KOOIJ 1
CDR V. E. SIMMONS 1

COMMANDER 1
NAVAL OCEANOGRAPHY COMMAND
NSTL STATION, MS 39529

DIRECTOR OF NAVY LABORATORIES 1
RM 1062, CRYSTAL PLAZA BLDG 5
DEPARTMENT OF THE NAVY
WASHINGTON, DC 20360

DISTRIBUTION LIST (CONTINUED)

COMMANDER IN CHIEF, PAC FLEET 1
P. O. BOX 3
PEARL HARBOR, HI 96860
ATTN: CODE 3521 1

COMMANDER IN CHIEF 1
U. S. ATLANTIC FLEET
NORFOLK, VA 23511
ATTN: CODE 353 1

COMMANDER
THIRD FLEET
PEARL HARBOR, HI 96860
ATTN: CODE N-7 2

COMMANDER 1
SECOND FLEET
FPO NEW YORK, NY 09501

COMMANDER 1
SIXTH FLEET
FPO NEW YORK, NY 09501

COMMANDER SEVENTH FLEET 1
FPO SAN FRANCISCO, CA 96601
ATTN: CAPT J. T. TALBERT 1

COMMANDER FLEET AIR, MEDITERRANEAN 1
COMMANDER, ANTISUBMARINE WAR FORCE
U. S. SIXTH FLEET
FPO NEW YORK, NY 09521

COMMANDER 1
SUBMARINE FORCES
U. S. PACIFIC FLEET
PEARL HARBOR, HI 96860

COMMANDER 1
SUBMARINE DEVELOPMENT GROUP 12
BOX 70 NAV SUB BASE, N LONDON
GROTON, CT 06340

COMMANDER 1
SUBMARINE GROUP SEVEN
BOX 50
FPO SEATTLE, WA 98762
ATTN: CAPT J. HORISH 1

COMMANDER 1
OPERATIONAL TEST AND EVAL. FORCE
NAVAL BASE
NORFOLK, VA 23511
ATTN: CODE 42

COMMANDER 1
PATROL AND RECONNAISSANCE FORCE
SEVENTH FLEET
FPO SEATTLE, WA 98768
ATTN: CDR P. O'CONNOR 1

COMMANDER
U. S. NAVAL FORCES,
MARIANAS
FPO SAN FRANCISCO, CA 96630
ATTN: LCDR D. L. WETHERELL 1

COMMANDER PATROL WINGS 1
U. S. PACIFIC FLEET
NAVAL AIR STATION
MOFFETT FIELD, CA 94035

COMMANDER 2
OCEANOGRAPHIC SYSTEM, ATLANTIC
BOX 100
NORFOLK, VA 23511
ATTN: LT P. A. KUHN, N34
W. G. SCHREIBER

COMMANDER 2
OCEANOGRAPHIC SYSTEM, PACIFIC
BOX 1390
PEARL HARBOR, HI 96860
ATTN: LCDR W. F. JOHNSON
CODE N3

COMMANDER 1
PATROL WING TWO
FPO SAN FRANCISCO, CA 96601

OCEANOGRAPHIC DEVELOPMENT SQO 8 1
NAVAL AIR STATION
PATUXENT RIVER, MD 20670

DISTRIBUTION LIST (CONTINUED)

COMMANDING OFFICER CHESAPEAKE DIV 1
NAVAL FACILITIES ENG COMMAND
WASHINGTON NAVY YARD
WASHINGTON, DC 20374
ATTN: CODE FPO-1E4 1

ARPA RESEARCH CENTER
UNIT 1, BLDG 301A
NAS MOFFETT FIELD, CA 94035
ATTN: E. L. SMITH 1

DEFENSE DOCUMENTATION CENTER 1
CAMERON STATION
ALEXANDRIA, VA 22314

COMMANDING OFFICER
NAVAL RESEARCH LABORATORY
WASHINGTON, DC 20375
ATTN: CODE 8100 1
CODE 8160 1
CODE 2627 1

COMMANDING OFFICER 1
NAVAL RESEARCH LABORATORIES
P. O. BOX 8337
ORLANDO, FL 32806
ATTN: CODE 0277 1
CODE 8280 1
CODE 3289 1

COMMANDER 1
NAVAL OCEANOGRAPHIC OFFICE
NSTL STATION, MS 39529
ATTN: CODE 3000 1
CODE 3440 1
LIBRARY 1

COMMANDING OFFICER 1
NAVAL OCEAN RESEARCH & DEVELOPMENT
ACTIVITY
NSTL STATION, MS 39529
ATTN: CODE 110 1
CODE 125 1
CODE 115
CODE 300 1
CODE 320 1
CODE 340 1
CODE 560 1
CODE 520 FILE

NAVAL OCEAN RESEARCH & DEVEL. ACT
LIAISON OFFICE
800 NORTH QUINCY STREET
ARLINGTON, VA 22217
ATTN: CODE 130 1

OFFICER IN CHARGE 1
NEW LONDON LABORATORY
NAVAL UNDERWATER SYSTEMS CENTER
NEW LONDON, CT 06320
ATTN: CODE 31 1
CODE 312 1
CODE 542 1

COMMANDER 1
NAVAL OCEAN SYSTEMS CENTER
SAN DIEGO, CA 92152
ATTN: CODE 724 2
CODE 7243 1

COMMANDER
NAVAL AIR DEVELOPMENT CENTER
WARMINSTER, PA 18974
ATTN: CODE 303 1
CODE 3032 1

COMMANDING OFFICER 1
NAVAL COASTAL SYSTEMS LABORATORY
PANAMA CITY, FL 32407

OFFICER IN CHARGE 1
WHITE OAK LABORATORY
NAVAL SURFACE WEAPONS CENTER
SILVER SPRING, MD 20910

OFFICER IN CHARGE CARDEROCK LAB. 1
DAVID W. TAYLOR NAVAL SHIP RES &
DEVELOPMENT CENTER
BETHESDA, MD 20084

DIRECTOR 1
NAVAL OCEAN SURVEILLANCE INFO CENT
4301 SUITLAND ROAD
WASHINGTON, DC 20390

COMMANDING OFFICER 1
NAVAL INTELLIGENCE SUPPORT CENTER
4301 SUITLAND ROAD
WASHINGTON, DC 20390

DISTRIBUTION LIST (CONTINUED)

SUPERINTENDENT
NAVAL POSTGRADUATE SCHOOL
MONTEREY, CA 93940
ATTN: LIBRARY 1

COMMANDING OFFICER 1
NAVAL ENVIRONMENTAL PREDICTION
RESEARCH FACILITY
MONTEREY, CA 93940

CHIEF DEF. RES. EST. PACIFIC 1
FLEET MAIL OFFICE
CANADIAN FORCES BASE
VICTORIA, BC V0S1B0

CHIEF DEF. RES. EST. ATLANTIC 1
P. O. BOX 1012
DARTMOUTH, NOVA SCOTIA B2Y 3Z7

DIRECTOR OF NAVAL MATTERS 1
CENTER OF NAVAL ANALYSIS
ARLINGTON, VA 22209
ATTN: C. E. WOODS 1

UNIVERSITY OF CALIFORNIA 1
MARINE PHYSICAL LAB SAN DIEGO
P. O. BOX 6049
SAN DIEGO, CA 92106

UNIVERSITY OF HAWAII 1
HAWAII INSTITUTE OF GEOPHYSICS
2525 CORREA ROAD
HONOLULU, HI 96822

JOHN HOPKINS UNIVERSITY
APPLIED PHYSICS LABORATORY
JOHNS HOPKINS ROAD
LAUREL, MD 20810
ATTN: A. CHWASTYK 1
W. L. MAY 1
G. L. SMITH 1

PALISADES GEOPHYSICAL INST. INC. 1
131 ERIE STREET
P. O. BOX 396
BLAUVELT, NY 10913

UNIVERSITY OF TEXAS
APPLIED RESEARCH LABORATORIES
P. O. BOX 8029
AUSTIN, TX 78712
ATTN: G. E. ELLIS 1
DR. L. D. HAMPTON 1
DR. K. E. HAWKER 1

UNIVERSITY OF WASHINGTON 1
APPLIED PHYSICS LABORATORY
1013 NE FORTIETH STREET
SEATTLE, WA 98195

WOODS HOLE OCEANOGRAPHIC INST.
WOODS HOLE, MA 02543
ATTN: DR. E. E. HAYS 2

ANALYSIS AND TECHNOLOGY, INC.
ROUTE 2
NORTH STONINGTON, CT 06359
ATTN: S. ELAM 1

ARTHUR D. LITTLE, INC.
15 ACORN PARK
CAMBRIDGE, MA 02140
ATTN: DR. G. RAISBECK 1
W. G. SYKES 1

B-K DYNAMICS
15825 SHADY GROVE ROAD
ROCKVILLE, MD 20850
ATTN: P. G. BERNARD 1

BELL TELEPHONE LABORATORIES
1 WHIPPANY ROAD
WHIPPANY, NJ 07981
ATTN: DR. J. GOLDMAN 1
DR. L. F. FRETWELL

BOLT, BERANEK AND NEWMAN 1
1701 N. FORT MYER DRIVE
SUITE 1001
ARLINGTON, VA 22209

DISTRIBUTION LIST (CONTINUED)

BOLT, BERANEK AND NEWMAN 1
50 MOULTON ST.
CAMBRIDGE, MA 02138

BUNKER-RAMO
31717 LA TIENDA DRIVE
WESTLAKE VILLAGE, CA 91361
ATTN: F. K. FULLERTON 1

CLAUDE P. BRANCART & ASSOC., INC. 1
17150 BUTTE CREEK ROAD, SUITE 214
HOUSTON, TX 77090

DANIEL H. WAGNER ASSOCIATES 1
STATION SQUARE ONE
PAOLI, PA 19301

DAUBIN SYSTEMS CORP.
104 CRANDON BOULEVARD
SUITE 315
KEY BISCAYNE, FL 33149
ATTN: DR. S. C. DAUBIN 1

ENVO, INC.
800 FOLLIN LANE
VIENNA, VA 22180
ATTN: G. O'SULLIVAN 1

GENERAL ELECTRIC CORP.
FARRELL ROAD PLANT
SYRACUSE, NY 13201
ATTN: E. D. GREENBALGH 1

GENERAL ELECTRIC CORP.
REENTRY ENVIR. SYS. DIV.
3198 CHESTNUT STREET
PHILADELPHIA, PA 19101
ATTN: O. KLIMA 1
DR. E. L. MURPHY 1

GOULD, INC.
CHESAPEAKE INSTRUMENT DIV.
6711 BAYMEADOW DRIVE
GLEN BURNIE, MD 21061
ATTN: P. J. POLLOCK

LOCKHEED MISSILES AND SPACE
COMPANY, INC.
P. O. BOX 504
SUNNYVALE, CA 94088
ATTN: R. C. PARSONS 1

OCEAN DATA SYSTEMS, INC.
6000 EXECUTIVE BOULEVARD
ROCKVILLE, MD 20852
ATTN: G. V. JACOBS 1
DR. E. MORENOFF 1
J. H. LOCKLIN

OCEAN DATA SYSTEMS, INC. 1
2400 GARDEN ROAD
MONTEREY, CA 93940

OCEAN DATA SYSTEMS, INC. 1
3581 KENYON ST.
SAN DIEGO, CA 92110

OPERATIONS RESEARCH, INC.
1400 SPRING STREET
SILVER SPRING, MD 20910
ATTN: DR. J. I. BOWEN 1

PLANNING SYSTEMS INC.
7900 WESTPARK DRIVE
SUITE 600
McLEAN, VA 22101
ATTN: R. KLINKNER 1
DR. R. S. CAVANAUGH

PURVIS SYSTEMS, INC.
3420 KENYON ST., SUITE 130
SAN DIEGO, CA 92110
ATTN: T. J. FITZGERALD 1

RAYTHEON COMPANY
SUBMARINE SIGNAL DIVISION
P. O. BOX 360
PORTSMOUTH, RI 02871
ATTN: DR. B. A. BECKEN 1

SANDERS ASSOCIATES, INC.
95 CANAL STREET
NASHUA, NH 03060
ATTN: L. E. GAGNE 1
R. P. WHITE 1

SCIENCE APPLICATIONS INC. 1
SUITE 216
21133 VICTORY BLVD
CANOGA PARK, CA 91303
ATTN: DR. J. H. WILSON

DISTRIBUTION LIST (CONTINUED)

SCIENCE APPLICATIONS INC. 1
1200 PROSPECT ST
P. O. BOX 2351
LA JOLLA, CA 92038
ATTN: F. J. RYAN

SCIENCE APPLICATIONS, INC.
8400 WESTPARK DRIVE
McLEAN, VA 22101
ATTN: DR. J. S. HANNA 1
C. W. SPOFFORD 1

SUMMIT RESEARCH CORP. 1
1 WEST DEER PARK DRIVE
GAITHERSBURG, MD 20760

SUTRON CORP.
1925 N. LYNN STREET
SUITE 700
ARLINGTON, VA 22209
ATTN: C. H. DABNEY 1

TETRA TECH, INC.
1911 N. FORT MYER DRIVE
ARLINGTON, VA 22209
ATTN: JOHN PRESTON 1

TRACOR, INC.
1601 RESEARCH BOULEVARD
ROCKVILLE, MD 20850
ATTN: J. T. GOTTWALD 1
DR. A. F. WITTENBORN 1

TRW SYSTEMS GROUP
7600 COLSHIRE DRIVE
McLEAN, VA 22101
ATTN: R. T. BROWN 1
I. B. GEREBEN 1

UNDERWATER SYSTEMS, INC.
8121 GEORGIA AVENUE
SILVER SPRING, MD 20910
ATTN: DR. M. S. WEINSTEIN 1

WESTERN ELECTRIC COMPANY
P. O. BOX 20046
GREENSBOROUGH, NC 27420
ATTN: R. H. HARRIS 1

WESTINGHOUSE ELECTRIC COMPANY 1
P. O. BOX 1488
MAIL STOP 9R40
ANNAPOLIS, MD 21404

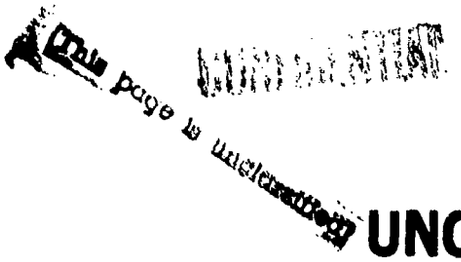

DEPARTMENT OF THE NAVY
OFFICE OF NAVAL RESEARCH
875 NORTH RANDOLPH STREET
SUITE 1425
ARLINGTON VA 22203-1995

IN REPLY REFER TO:

5510/1
Ser 321OA/011/06
31 Jan 06

MEMORANDUM FOR DISTRIBUTION LIST

Subj: DECLASSIFICATION OF LONG RANGE ACOUSTIC PROPAGATION PROJECT (LRAPP) DOCUMENTS

Ref: (a) SECNAVINST 5510.36

Encl: (1) List of DECLASSIFIED LRAPP Documents

1. In accordance with reference (a), a declassification review has been conducted on a number of classified LRAPP documents.

2. The LRAPP documents listed in enclosure (1) have been downgraded to UNCLASSIFIED and have been approved for public release. These documents should be remarked as follows:

   Classification changed to UNCLASSIFIED by authority of the Chief of Naval Operations (N772) letter N772A/6U875630, 20 January 2006.

   DISTRIBUTION STATEMENT A: Approved for Public Release; Distribution is unlimited.

3. Questions may be directed to the undersigned on (703) 696-4619, DSN 426-4619.

BRIAN LINK
By direction

Subj: DECLASSIFICATION OF LONG RANGE ACOUSTIC PROPAGATION PROJECT (LRAPP) DOCUMENTS

DISTRIBUTION LIST:

NAVOCEANO (Code N121LC – Jaime Ratliff)
NRL Washington (Code 5596.3 – Mary Templeman)
PEO LMW Det San Diego (PMS 181)
DTIC-OCQ (Larry Downing)
ARL, U of Texas
Blue Sea Corporation (Dr.Roy Gaul)
ONR 32B (CAPT Paul Stewart)
ONR 321OA (Dr. Ellen Livingston)
APL, U of Washington
APL, Johns Hopkins University
ARL, Penn State University
MPL of Scripps Institution of Oceanography
WHOI
NAVSEA
NAVAIR
NUWC
SAIC

Declassified LRAPP Documents

Report Number	Personal Author	Title	Publication Source (Originator)	Pub. Date	Current Availability	Class.
ARLTR7952	Focke, K. C., et al.	CHURCH STROKE 2 CRUISE 5 PAR/ACODAC ENVIRONMENTAL ACOUSTIC MEASUREMENTS AND ANALYSIS (U)	University of Texas, Applied Research Laboratories	791029	ADC025102; NS; AU; ND	C
Unavailable	Van Wyckhouse, R. J.	SYNBAPS. VOLUME I. DATA BASE SOURCES AND DATA PREPARATION	Naval Ocean R&D Activity	791201	ADC025193	C
NORDATN63	Brunson, B. A., et al.	ENVIRONMENTAL EFFECTS ON LOW FREQUENCY TRANSMISSION LOSS IN THE GULF OF MEXICO (U)	Naval Ocean R&D Activity	800901	ADC029543; ND	C
NORDATN80C	Gereben, I. B.	ACOUSTIC SIGNAL CHARACTERISTICS MEASURED WITH THE LAMBDA III DURING CHURCH STROKE III (U)	Naval Ocean R&D Activity	800915	ADC023527; NS; AU; ND	C
NOSCTR664	Gordon, D. F.	ARRAY SIMULATION AT THE BEARING STAKE SITES	Naval Ocean Systems Center	810401	ADC025992; NS; AU; ND	C
NOSCTR703	Gordon, D. F.	NORMAL MODE ANALYSIS OF PROPAGATION LOSS AT THE BEARING STAKE SITES (U)	Naval Ocean Systems Center	810801	ADC026872; NS; AU; ND	C
NOSCTR680	Neubert, J. A.	COHERENCE VARIABILITY OF ARRAYS DURING BEARING STAKE (U)	Naval Ocean Systems Center	810801	ADC028075; NS; ND	C
HSECO735	Luehrmann, W. H.	SQUARE DEAL R/V SEISMIC EXPLORER FIELD OPERATIONS REPORT (U)	Seismic Engineering Co.	731121	AD0530744; NS; ND	C; U
MPL-C-42/76	Morris, G. B.	CHURCH ANCHOR EXPLOSIVE SOURCE (SUS) PROPAGATION MEASUREMENTS FROM R/P FLIP (U)	Marine Physical Laboratory	760701	ADC010072; AU; ND	C; U
ARLTR7637	Mitchell, S. K., et al.	SQUARE DEAL EXPLOSIVE SOURCE (SUS) PROPAGATION MEASUREMENTS. (U)	University of Texas, Applied Research Laboratories	760719	ADC014196; NS; AU; ND	C; U
NORDAR23	Fenner, D. F.	SOUND SPEED STRUCTURE OF THE NORTHEAST ATLANTIC OCEAN IN SUMMER 1973 DURING THE	Naval Ocean R&D Activity	800301	ADC029546; NS; ND	C; U
NOOTR230	Bucca, P. J.	SOUND VELOCITY CONDITIONS DURING THE CHURCH ANCHOR EXERCISE (U)	Naval Oceanographic Office	751201	NS; AU; ND	C;U
ONR SP 2-69; MC PLAN-01	Unavailable	PARKA II EXPERIMENT UTILIZING SEA SPIDER, ONR SCIENTIFIC PLAN 2-69 (U)	Maury Center for Ocean Science	690626	ADB020846; ND	U
Unavailable	Unavailable	PARKA I EXPERIMENT	Maury Center for Ocean Science	691101	AD0506209	U
USRD CR 3105	Unavailable	SEA SPIDER TRANSPONDER TRANSDUCER	Naval Research Laboratory	700505	ND	U
MC PLAN 05; ONR Scientific Plan 1-71	Unavailable	ATLANTIC TEST BED MEASUREMENT PROGRAM (U)	Maury Center for Ocean Science	701020	ND	U
ACR-170 VOL.1	Hurdle, B. G.	PROJECT NEAT- A COLLABORATIVE LONG RANGE PROPAGATION EXPERIMENT IN THE NORTHEAST ATLANTIC, PART I (U)	Naval Research Laboratory	701118	ND	U
MC-003-VOL-2	Unavailable	THE PARKA I EXPERIMENT. APPENDICES- PACIFIC ACOUSTIC RESEARCH KANEOHE-ALASKA (U)	Maury Center for Ocean Science	710101	ND	U